

# **Experimental assessment of the wettability and surface free energy of homogeneous and heterogeneous porous media**

Von der Naturwissenschaftlichen Fakultät  
der Gottfried Wilhelm Leibniz Universität Hannover  
zur Erlangung des Grades eines  
DOKTORS DER NATURWISSENSCHAFTEN  
Dr. rer. nat.  
genehmigte Dissertation

von  
Magister en Ciencias Mención Silvicultura  
Juan Carlos Ramírez-Flores  
geboren am 26.02.1972 in Valdivia, Chile

2009

**Referent:** Prof. Dr. Jörg Bachmann

**Korreferent:** PD Dr. Horst Gerke

Tag der Promotion: 10. 06.2009

## Acknowledgements

I want to express my deep gratitude to my supervisor Prof. Dr. Jörg Bachmann, for his guidance and friendship through these years in the Institut für Bodenkunde of the Gottfried Wilhelm Leibniz Universität Hannover.

To our estimated friend of the Universidad Austral de Chile, Prof. Dr. Achim Ellies (1944-2004), for helping me in this great opportunity in my life and career. Love to his family.

Special thanks to all the great scientists I had the chance to meet, for helping me in shaping this work: Prof. Dr. Abraham Marmur, Prof. Dr. J. Bottcher, Prof. Dr. K. H. Hartge, Prof. Dr. W. R. Fischer and Prof. Dr. M. Th. Van Genuchten.

Many thanks to all my friends and colleagues of the Institut für Bodenkunde, for their support and helpful advice.

Deep gratitude to the Niedersachsen Foundation for financing the results of this research (NHDF N° 22002).

Many thanks to CONICYT (National Commission for Science and Technology), for its valuable support in the first years of my academic career in Chile.

To our friends in the beautiful and interesting Israel.

To Hannover and Herrenhausen, my second home after Valdivia, and the beautiful Hamburg and Berlin.

*To my dear family*



## Kurzfassung

Die Benetzbarkeit von Boden beeinflusst wichtige Eigenschaften wie Wasserverteilung und Wasserdynamik. Für die Bewertung der Benetzbarkeit sind verschiedene Methoden entwickelt worden. Weil unterschiedliche Methoden in der Regel verschiedene Ergebnisse liefern, ist z. B. die Messung des Kontaktwinkels (CA) von Böden immer noch Problematisch. Die vorliegende Dissertation vergleicht verschiedene experimentelle und theoretische Ansätze. Hierzu erfolgte ein Vergleich von Methoden für die Beurteilung der Hydrophobie von natürlichen Materialien und Modellböden. Es wurden die Kapillare Aufstiegsmethode (CRM, advancing CA), Wilhelmy Platten Methode (WPM, advancing und receding CA) und die Sessile Drop Methode (SDM, equilibrium CA) angewandt und mit den Ergebnissen zur Kapillarität der gleichen Materialien unter der Einwirkung der Schwerkraft in langen Säulen verglichen. Der nächste Abschnitt vergleicht die Bestimmung der Oberflächenenergien in Zisman-Plots. In dem folgenden Kapitel wird ein alternatives theoretisches Modell für den Kapillaraufstieg (Equivalent Capillary Modell) experimentell getestet. Schließlich wird die CRM angewendet um eine Bewertung der Benetzbarkeit natürlicher Böden unter Berücksichtigung der Bodenstruktur im Vergleich intakte Aggregate-zerkleinerte Aggregate vorzunehmen.

Der Vergleich der CA ergab, dass CRM eine kleinere Auflösung als WPM und SDM aufweist, besonders bei Materialien mit den kleinen Durchmessern (z. B. Schluff). Es wird angenommen, dass diese Unterschiede möglicherweise mit der Geometrie des Systems, d. h. mit der Abweichung der Partikel von einer idealen Kugelform, zusammenhängt. WPM (advancing und receding CA) haben grundsätzlich eine starke Abhängigkeit vom Messmodus (Eintauchengeschwindigkeit und -tiefe), wobei ihre gemittelten Kontaktwinkel (WPM-ECA, equilibrium CA) aber stabil sind. WPM-ECA und SDM zeigten eine bessere Übereinstimmung mit dem Gleichgewichtskontaktwinkel, der unter der Wirkung der Schwerkraft unabhängig in langen Säulen mittels der finalen kapillaren Aufstiegshöhe bestimmt wurde. Schlechter war die Übereinstimmung der Gleichgewichtskontaktwinkel aus den Säulenversuchen im Vergleich zu dynamischen Kontaktwinkeln, wie sie mittels CRM und WPM (advancing CA) gemessen wurden.

Der Vergleich basiert auf der Anwendung einer Equation of State (ES) zeigt dass die Fit-Parameter ( $\alpha$  and  $\beta$ ) im Prinzip konstant für alle Materialien (besonders  $\beta$ ) sind. Bei WPM-ACA, die ES zeigt einen engen Messbereich im Vergleich zur direkten Bestimmung des Kontaktwinkels. Weitere Forschung braucht man um die Eignung der anderen Methoden bei der ES zu testen.

Das Equivalent Capillary Modell, das eine alternative Auswertungsmethode zu der konventionellen CRM mit zwei Testflüssigkeiten darstellt, zeigte Einschränkungen, die ebenfalls zu überschätzen Kontaktwinkeln, auch für die hydrophilen Materialien, führen. Die Bewertung der natürlichen Boden mit der CRM zeigte gute Reproduzierbarkeit in dem gemessenen Spektrum der Benetzungshemmungen, vor allem auch für die Messung an natürlichen Bodenaggregaten, was mit WPM und SDM nicht möglich ist. Die Benetzbarkeit der Aggregate war nutzungsspezifisch. Es werden ähnliche Werte (im Vergleich mit homogenisierten Aggregaten) nur bei Waldböden gemessen; v.a. bei Ackerböden sind die CA von intakten Aggregaten kleiner als von homogenisiertem Material. Das zeigt, dass nicht nur Gesamtgehalte der organischen Substanz sondern auch deren mikroskopische Verteilung in strukturierten Böden von Bedeutung sind. Aus diesem Grund sollte die Charakterisierung der Benetzbarkeit nicht nur auf der Untersuchung homogenisierter Proben beruhen.

Zusammenfassend zeigen die Ergebnissen dieser Dissertation dass die Standardmethode zur Bestimmung von Kontaktwinkeln körniger Materialien, CRM, dann eine geeignete Methode zur Bestimmung der Benetzbarkeit des Bodens ist, wenn Aspekte wie Aggregation einbezogen werden sollen. Allerdings hat die CRM aber auch Probleme, die möglicherweise mit der notwendigen Definition von Pore-Geometriefaktoren zusammenhängen, die nicht immer konsistent bestimmt werden können. Die Ergebnissen zeigen auch dass WPM (WPM-ECA) und SDM geeignete Methoden für die Bestimmung der Benetzbarkeit von trockenen Bodenmaterialien sind, v.a. auch wenn sie mit unabhängigen Phänomenen wie dem maximalen kapillaren Aufstieg in Bodensäulen verglichen werden. Somit besteht die Möglichkeit, mit unabhängigen CA-Messungen Aussagen über die Kapillarität von Böden zu treffen.

Schlagwörter: Kontaktwinkel / Kapillarität / Lucas-Washburn Gleichung



## Abstract

Wettability of soil is a significant factor affecting properties like water distribution and erodibility. Different methods assessing wettability in terms of contact angle (CA) and surface free energies have been developed. However, due to different methods usually deliver different results, the assessment of the representative CA for soil materials is still a pending problem.

The present thesis compares different experimental and theoretical methods, in order to evaluate their potential for the quantification of soil wettability. Firstly, a comparison of methods assessing CAs was carried out for model materials with different degrees of water repellency. The Capillary Rise Method (CRM, dynamic-advancing CA), Wilhelmy Plate Method (WPM, dynamic-advancing and receding CA) and the Sessile Drop Method (SDM, equilibrium CA) were compared with the capillarity of the same materials in long columns under the impact of gravity. The next section of this thesis compared CRM and WPM for model materials with an alternative approach, based on the quantification of surface free energies in Zisman plots. By applying an equation of state, the surface free energies data were used to predict the CAs for each method. Next, a recent theoretical model for capillary rise (Equivalent Capillary model) is experimentally tested. It assumes that a capillary, representing the average properties of the system, is possible to be defined. Finally, CRM was tested in describing real natural soils, by comparing intact versus crushed aggregates.

The comparison of CAs showed that CRM has a restricted resolution range compared with WPM and SDM, with a significant overestimation of the CA, especially in materials with the smallest particle diameter. Although not completely proved, it is thought that this overestimation is related to the geometry of the system. WPM showed a monotonic relation with water repellency, with both advancing and receding CAs having strong dependency on the set-up parameters (immersion speed and depth), although their average (WPM-ECA, equilibrium CA) remains stable. WPM-ECA and SDM showed a better agreement with the equilibrium CA measured under the effect of gravity in long vertical soil columns than CRM and WPM considering only the dynamic-advancing CA (WPM-ACA). The comparison based on the application of an Equation of State (ES) showed that the fitting parameters of this model ( $\alpha$  and  $\beta$ ) can be considered constants for the different materials, although the parameter  $\alpha$  showed bigger scattering. For WPM-ACA, the ES showed a narrower range estimating CAs in comparison to direct assessment. Further research is needed in order to test the suitability of the other methods by the ES approach.

The Equivalent Capillary model showed limitations in fitting the entire capillary process evaluated in long-columns under the impact of gravity. However, reasonable fit between experimental data and the model is reached when only the initial linear section of the process is considered. The estimated dynamic- and intrinsic- CAs of the model appear as overestimated even for hydrophilic materials. These results suggest a lack of resolution of the wetting model, possibly due to factors like the not completely accurate characterization of the geometry factor. However, aspects like simplicity and reasonable fit should be considered as major advantage of this model for future application on real soil-systems. The evaluation of natural soils with CRM showed good and consistent levels of reproducibility. Different kind of manures had different CAs measured for intact aggregates but not by comparing the corresponding homogenized materials. This demonstrated that water repellency at the scale of aggregates is more affected by the distribution of organic matter rather than by the total amount of organic matter. For this reason, the description of wetting behavior with CRM should not be restricted to homogenized soil samples.

Overall, it was concluded that CRM is a suitable method for the evaluation of soil materials, in particular when effects of soil structure should be included into the analysis. However, CRM has limitations, like a significant overestimation of the CA for certain combinations of wettability and pore size. It was further proved that WPM (especially WPM-ECA) and SDM are suitable methods for the evaluation of soil samples and their capillarity in the entire range of hydrophobicity.

Keywords: Contact angle / capillarity / Lucas-Washburn equation





# Contents

<b>Acknowledgements.....</b>	<b>I</b>
<b>Kurzfassung.....</b>	<b>III</b>
<b>Abstract.....</b>	<b>V</b>
<b>List of Figures.....</b>	<b>X</b>
<b>List of Tables.....</b>	<b>XIII</b>
<b>List of Symbols and units.....</b>	<b>XIV</b>
<b>Abbreviations.....</b>	<b>XVI</b>
<b>1 Introduction.....</b>	<b>1</b>
<b>1.1 Background of the research.....</b>	<b>1</b>
<b>1.2 Objectives.....</b>	<b>3</b>
<b>1.3 Outline of the thesis.....</b>	<b>5</b>
<b>2 Contact angles and capillarity of heterogeneous porous media: a comparison of methods.....</b>	<b>6</b>
<b>2.1. Introduction.....</b>	<b>6</b>
<b>2.2. Methods.....</b>	<b>8</b>
<b>2.2.1. Capillary Rise Method.....</b>	<b>8</b>
<b>2.2.2. Wilhelmy Plate Method.....</b>	<b>9</b>
<b>2.2.3. Sessile Drop Method.....</b>	<b>10</b>
<b>2.2.4. Capillary rise under gravity impact.....</b>	<b>11</b>
<b>2.3. Materials and measurements.....</b>	<b>12</b>
<b>2.3.1. Materials.....</b>	<b>12</b>
<b>2.3.2. Measurement.....</b>	<b>14</b>
<b>2.3.2.1. Capillary Rise Method.....</b>	<b>14</b>
<b>2.3.2.2. Wilhelmy Plate Method.....</b>	<b>14</b>
<b>2.3.2.3. Sessile Drop Method.....</b>	<b>15</b>
<b>2.3.2.4. Capillary rise under gravity impact.....</b>	<b>15</b>
<b>2.4. Results and discussion.....</b>	<b>17</b>
<b>2.4.1. Capillary Rise Method.....</b>	<b>17</b>

2.4.2. Wilhelmy Plate Method.....	21
2.4.3. Sessile Drop Method.....	22
2.4.4. Capillary rise in long columns.....	22
2.5. Comparison of methods.....	23
2.6. Conclusions.....	27
<b>3 Prediction of contact angles from solid and liquid surface free energies of model porous materials.....</b>	<b>31</b>
3.1. Introduction.....	31
3.2. Theory.....	32
3.3. Methodology.....	34
3.3.1. Materials and treatments.....	34
3.3.2. Contact angle measurement.....	34
3.3.3. Assessment of the critical surface tension.....	35
3.3.4. Application of the equation of state.....	35
3.4. Results and discussion.....	36
3.4.1. Zisman plots and assessment of the critical surface tension.....	36
3.4.2. Equation of state approach.....	40
3.4.2.1. Estimation of the parameters $\Phi$ , $\alpha$ and $\beta$ .....	40
3.4.2.2. Prediction of contact angles.....	44
3.5. Conclusions.....	47
<b>4 Assessing contact angles in porous media by evaluating the kinetics of capillary rise and hydraulic properties.....</b>	<b>49</b>
4.1. Introduction.....	49
4.2. Theory.....	50
4.2.1. Equivalent Capillary model.....	50
4.2.2. Capillary pressure-saturation curves.....	54
4.3. Methodology.....	55
4.3.1. Materials and treatments.....	55
4.3.2. Evaluation of kinetics of capillary rise and fit to the Van Genuchten model.....	55

4.3.3. Evaluation of the C geometry factor and shape of the particles.....	55
<b>4.4. Results and discussion.....</b>	<b>56</b>
4.4.1. Equivalent Capillary model.....	56
4.4.1.1. Kinetics of capillary rise.....	56
4.4.1.2. Fit of the wetting model.....	58
4.4.1.3. Hydraulic properties, shape of the particles and C geometry factor....	63
4.4.2. Capillary pressure-saturation curves.....	65
4.4.3. Comparison of contact angles.....	67
<b>4.5. Conclusions.....</b>	<b>71</b>
<b>5 Comparing capillary rise contact angles of soil aggregates and homogenized soil.....</b>	<b>73</b>
5.1. Introduction.....	73
5.2. Methodology.....	75
5.2.1. Materials.....	75
5.2.2. Contact angle measurements.....	75
5.3. Results and discussion.....	82
5.4. Conclusions.....	87
<b>6 Final discussion and conclusions.....</b>	<b>90</b>
6.1. Experimental and theoretical assessment of wettability in model porous media.....	91
6.2. Evaluation of natural soils.....	96
6.3. Concluding remarks and perspectives.....	101
<b>References.....</b>	<b>104</b>
<b>Appendix</b>	
<b>Curriculum vitae</b>	
<b>Erklärung</b>	

## List of Figures

<b>Fig. 1</b>	Relation between $\theta^{\text{CRM}}$ and $\theta_{\text{A}}^{\text{WPM}}$ for a set of natural soil samples (source: Goebel, 2007).....	4
<b>Fig. 2</b>	Evaluation of $\theta_{\text{A}}^{\text{WPM}}$ (ACA), $\theta_{\text{R}}^{\text{WPM}}$ (RCA) and $\theta_{\text{E}}^{\text{WPM}}$ (ECA) for sand. A: Effect of the immersion speed (50% hydrophobic particles = $2.5 \cdot 10^{-4}$ mL g <sup>-1</sup> DCDMS. $\theta_{\text{A}}^{\text{WPM}} = 138.4^\circ$ , $\theta_{\text{R}}^{\text{WPM}} = 52.6^\circ$ , $\theta_{\text{E}}^{\text{WPM}} = 95.5^\circ$ ). B: Effect of the immersion depth (100% hydrophobic particles = $5.0 \cdot 10^{-4}$ mL g <sup>-1</sup> DCDMS. $\theta_{\text{A}}^{\text{WPM}} = 137.5^\circ$ , $\theta_{\text{R}}^{\text{WPM}} = 70.4^\circ$ , $\theta_{\text{E}}^{\text{WPM}} = 104.0^\circ$ ).....	16
<b>Fig. 3</b>	Wetting evaluation in segmented columns, examples for sand. A: Typical wetting front in homogeneous wettability (= $2.5 \cdot 10^{-5}$ mL g <sup>-1</sup> DCDMS). B: Typical wetting front in mixed wettability (20% hydrophobic particles = $1 \cdot 10^{-4}$ mL g <sup>-1</sup> DCDMS).....	18
<b>Fig. 4</b>	Comparison of $\theta^{\text{CRM}}$ , $\theta_{\text{A}}^{\text{WPM}}$ , $\theta_{\text{E}}^{\text{WPM}}$ , $\theta^{\text{SDM}}$ values and equilibrium CA estimated in segmented columns in samples with homogeneous wettability. A: Silt, B: Sand, C: GB 40-70 $\mu\text{m}$ , D: GB 150-250 $\mu\text{m}$ . Note the x-axis has different scales between treatments and materials.....	19
<b>Fig. 5</b>	Comparison of $\theta^{\text{CRM}}$ , $\theta_{\text{A}}^{\text{WPM}}$ , $\theta_{\text{E}}^{\text{WPM}}$ , $\theta^{\text{SDM}}$ values and equilibrium CA estimated in segmented columns in samples with mixed wettability (estimated DCDMS content in 100% hydrophobic particles = $2.0 \cdot 10^{-3}$ mL g <sup>-1</sup> in silt and = $5.0 \cdot 10^{-4}$ mL g <sup>-1</sup> DCDMS in sand and GB). A: Silt, B: Sand, C: GB 40-70 $\mu\text{m}$ , D: GB 150-250 $\mu\text{m}$ . Note the x-axis has different scales between treatments and materials.....	20
<b>Fig. 6</b>	Wetting evaluation in segmented columns, examples for sand. A: Initial dynamic of wetting in homogeneous wettability samples. RM: Reference material, 1: Sample = $2.5 \cdot 10^{-5}$ mL g <sup>-1</sup> DCDMS, 2: Sample = $5.5 \cdot 10^{-5}$ mL g <sup>-1</sup> DCDMS, 3: Sample = $1.0 \cdot 10^{-4}$ mL g <sup>-1</sup> DCDMS. B: Wetting retention curves of ethanol, ethanol-scaled curves and water (reference material). Note the different scales between graphics.....	24
<b>Fig. 7</b>	Relative deviation (RD, %) of the equilibrium contact angle ( $\theta_{\text{E}}$ ) and $\theta^{\text{CRM}}$ calculated in glass capillaries. Calculations for a penetration length of 10 mm with water as test liquid ( $\sigma_{\text{L}} = 73$ mN m <sup>-1</sup> and $\rho = 1000$ kg m <sup>-3</sup> ) (source: Lavi et al., 2008).....	25
<b>Fig. 8</b>	Measured relative deviation RD (%) of $\theta^{\text{CRM}}$ with respect to $\theta_{\text{E}}^{\text{CR}}$ for the material with mixed and homogeneous wettability. RD was calculated according to the expression $100 \cdot (\theta^{\text{CRM}} - \theta_{\text{E}}^{\text{CR}}) / \theta_{\text{E}}^{\text{CR}}$ .....	26
<b>Fig. 9</b>	Relation of the contact angles between the experimental methods CRM, SDM and WPM ( $\theta^{\text{CRM}}$ , $\theta^{\text{SDM}}$ and $\theta_{\text{E}}^{\text{WPM}}$ respectively) and the equilibrium contact angles measured in long segmented columns ( $\theta_{\text{E}}^{\text{CR}}$ ) for all model materials with increasing water repellency.....	28

<b>Fig. 10</b>	Examples of Zisman plots and linear regressions to estimate $\sigma_C$ in two samples of sand. A: 50% hydrophobic particles ( $2.5 \cdot 10^{-4}$ mL g <sup>-1</sup> DCDMS). B: 100% hydrophobic particles ( $5.0 \cdot 10^{-4}$ mL g <sup>-1</sup> DCDMS). 1: CRM data, 2: WPM data. The estimated $\sigma_C$ for each plot is also indicated.....	37
<b>Fig. 11</b>	Critical surface tension ( $\sigma_C$ ) as a function of the water repellency (% hydrophobic particles). A: Silt. B: Sand. C: GB 40-70 $\mu$ m. D: GB 150-250 $\mu$ m (100% hydrophobic particles are equivalent to $5.0 \cdot 10^{-4}$ mL g <sup>-1</sup> DCDMS for sand and GB, and to $2.0 \cdot 10^{-3}$ mL g <sup>-1</sup> DCDMS for silt.....	39
<b>Fig. 12</b>	Girifalco interaction parameter ( $\Phi$ ) as a function of the water repellency (% of hydrophobic particles) for sand.....	41
<b>Fig. 13</b>	Regression parameters $\alpha$ and $\beta$ as a function of the solid-vapor surface free energy ( $\sigma_{SV}$ ) for the three different experimental methods. Examples for sand.....	43
<b>Fig. 14</b>	Linear regressions between the directly measured CA versus the predicted CAs (ES approach). A: Silt and GB 40-70 $\mu$ m. B: Sand and GB 150-250 $\mu$ m.	45
<b>Fig. 15</b>	Comparison of measured and predicted contact angles (WPM-ACA) as a function of the water repellency (% hydrophobic particles). A: Sand. B: GB 150-250 $\mu$ m.....	46
<b>Fig. 16</b>	Wetting kinetics in segmented columns for sand and GB 150-250 $\mu$ m (reference materials, no addition of DCDMS). A: Complete measurement determined after one week. B: Rate of liquid uptake (g s <sup>-1</sup> ) (first three hours of the measurement).....	57
<b>Fig. 17</b>	Relation between the expression $-Bx - \ln(1 - Bx)$ versus time (t) for a complete measurement of the capillary process (about one week). Example for sand (wetable reference material).....	59
<b>Fig. 18</b>	Application of the Equivalent Capillary model on sand (reference material) and one MW sample (30% hydrophobic particles particles = $1.5 \cdot 10^{-4}$ mL g <sup>-1</sup> DCDMS) considering the first stages of capillary rise. A: Plots between the expression $-Bx - \ln(1 - Bx)$ versus time (t) and the corresponding linear regressions, used to estimate the fitting parameters A and B. B: Relation between the dimensionless expressions $(Bx)^3/At$ and $(At)$ .....	60
<b>Fig. 19</b>	Fit of the Equivalent Capillary model on sand (reference and MW 30 % hydrophobic particles = $1.5 \cdot 10^{-4}$ mL g <sup>-1</sup> DCDMS). The standard error (SE) is indicated in brackets.....	63
<b>Fig. 20</b>	Photographs of the particles of the model materials. A: Silt, B: Sand, C: GB 40-70 $\mu$ m, D: GB 150-250 $\mu$ m. Note the different scale of silt.....	64

<b>Fig. 21</b>	Capillary pressure-saturation curves fitted to the van Genuchten model. A: Silt, B: Sand, C: GB 40-70 $\mu\text{m}$ , D: GB 150-250 $\mu\text{m}$ . 1: Water uptake in reference material. 2: Ethanol scaled curve. 3: Water uptake in a MW sample (Silt = 60% hydrophobic particles, sand = 30%, GB 40-70 $\mu\text{m}$ = 15%, GB 150-250 $\mu\text{m}$ = 5%). The van Genuchten $\omega$ -parameter is indicated in brackets. Note the different scales of the y-axis.....	66
<b>Fig. 22</b>	Contact angles (CA) calculated for samples with homogeneous wettability ( $\theta_E$ : Equilibrium CA calculated from water retention curves; $\theta_D$ : Dynamic CA from Equivalent Capillary Model; $\theta_I$ : Intrinsic CA) A: Silt, B: Sand, C: GB 40-70 $\mu\text{m}$ , D: GB 150-250 $\mu\text{m}$ .....	68
<b>Fig. 23</b>	Contact angles (CA) calculated for samples with mixed wettability ( $\theta_E$ : Equilibrium CA calculated from water retention curves; $\theta_D$ : Dynamic CA from Equivalent Capillary Model; $\theta_I$ : Intrinsic CA) A: Silt, B: Sand, C: GB 40-70 $\mu\text{m}$ , D: GB 150-250 $\mu\text{m}$ .....	69
<b>Fig. 24</b>	Scheme of Capillary Rise Method (CRM) sample arrangement. A: Homogenized aggregates, B: Aggregate packings, C: Single aggregates. The testing fluid is on a lifting stage to establish contact with the sample.....	78
<b>Fig. 25</b>	Weight increase as a function of time for sand fraction 1-2 mm, $\theta^{\text{CRM}} = 61^\circ$ ..	81
<b>Fig. 26</b>	Weight increase (squared, $W^2 = f(t)$ ) as a function of time in single aggregates, for the sites Halle and Waldstein. The decrease in weight for Halle after 1.3 s (water) corresponds to the dispersion of the aggregate.....	83
<b>Fig. 27</b>	Water (1) and n-hexane (2) uptake curves $m = f(t^{0.5})$ for the wettable soil Halle $H_{\text{NPK}} 1$ and the almost non-wettable forest soil Waldstein $WS_{\text{Bh}}$ . A: Homogenized aggregates, B: Aggregates packings, C: Single aggregates. Also indicated are the domains for analyzing Slope I (homogenized aggregates, single aggregates) and Slope I/II (aggregate packings) by grey vertical lines. Note the different scales between the graphics.....	84
<b>Fig. 28</b>	Evaluation of wettability for a DCDMS-treated sample of silt. A: Water Drop Penetration Time. B: Capillary Rise Method. C: Wilhelmy Plate Method.....	94
<b>Fig. 29</b>	Intrinsic CA ( $\theta_I$ ) estimated from the dynamic CA ( $\theta_D$ ), according to the Equivalent Capillary Model, for different values of C. Example for silt (mixed wettability samples). The value of C is indicated in brackets.....	96
<b>Fig. 30</b>	Example for a set of natural soil samples, of the estimation of the intrinsic CA ( $\theta_I$ ) by correcting the dynamic CA measured with the Capillary Rise Method ( $\theta^{\text{CRM}}$ ) with the estimated C geometry factor, in comparison with the values estimated with the Wilhelmy Plate Method ( $\theta_A^{\text{WPM}}$ and $\theta_E^{\text{WPM}}$ approaches).....	100

## List of Tables

<b>Table 1</b>	Materials used for the experiments.....	12
<b>Table 2</b>	Regression parameters $\alpha$ and $\beta$ for each sample and experimental method, calculated by fitting the data of the Girifalco's interaction parameter ( $\Phi$ ) and solid-liquid surface free energy ( $\sigma_{SL}$ ) to the equation $\Phi = \beta - \alpha\sigma_{SL}$ .....	42
<b>Table 3</b>	Values of the fitting parameters $A$ and $B$ and the dimensionless expressions $(Bx)^3/At$ and $At$ for the reference (no addition of DCDMS) and the most hydrophobic materials (HW and MW samples).....	62
<b>Table 4</b>	Values of hydraulic conductivity ( $K_C$ ), permeability ( $\kappa$ ), Circularity ( $C_i$ ) and $C$ geometry factor estimated for reference materials.....	64
<b>Table 5</b>	Location and land-use data of the samples.....	76
<b>Table 6</b>	Data of particle-size distribution, total organic carbon content (SOC), and pH (all determined on bulk soil <2 mm diameter).....	77
<b>Table 7</b>	Bulk density $\rho_B$ ( $\text{g cm}^{-3}$ ) and standard deviation (SD) of sample tubes filled with aggregates packings and with homogenized aggregates.....	81
<b>Table 8</b>	Results of CRM measurements: contact angle ( $\theta^{\text{CRM}}$ ) and wetting coefficient ( $k$ ).....	86
<b>Table 9</b>	P-values for differences in mean wetting coefficient $k = \cos\theta$ obtained for homogenized aggregates, single aggregates and aggregate packings of the soils investigated.....	88
<b>Table 10</b>	Values of contact angle and equilibrium height of water ( $H_1$ ) of two natural soils evaluated in experiments with long segmented columns.....	101

## List of Symbols and units

### Latin Symbols

$g$	Acceleration due to gravity	$(L T^{-2})$
$h, x$	Height of the liquid front / Length of the capillary	$(L)$
$k$	Wetting coefficient	$(-)$
$k_0$	Shape-factor of solid particles and pore channels	$(-)$
$l$	Tortuosity	$(-)$
$r$	Radius	$(L)$
$r_{EQV}$	Equivalent radius	$(L)$
$t$	Time	$(T)$
$v$	Speed	$(L T^{-1})$
$C$	Pore geometry factor from Cozeny-Karman equation	$(-)$
$K_C$	Hidraulic conductivity	$(L T^{-1})$
$K$	Geometry factor from Lucas-Washburn equation	$(L^5)$
$S$	Specific surface area	$(L^2 M^{-1}) / L^{-1}$
$T$	Temperature	$(^{\circ}C)$
$V$	Volume	$(L^3)$
$W$	Weight	$(M)$



## Greek Symbols

$\varepsilon$	Porosity	(-)
$\eta$	Liquid viscosity	(L <sup>-1</sup> M <sup>-1</sup> T <sup>-1</sup> )
$\kappa$	Permeability	(L <sup>-2</sup> )
$\theta$	Contact angle	(°)
$\theta_D$	Dynamic contact angle	(°)
$\theta_E$	Equilibrium contact angle	(°)
$\theta_I$	Intrinsic contact angle	(°)
$\theta_{ACA}$	Advancing contact angle	(°)
$\theta^{CRM}$	Contact angle obtained with the capillary rise method	(°)
$\theta_{RCA}$	Receding contact angle	(°)
$\theta_E^{CR}$	Equilibrium contact angle obtained from long-segmented columns	(°)
$\theta^{SDM}$	Contact angle obtained with the sessile drop method	(°)
$\theta_A^{WPM}$	Advancing contact angle obtained with the Wilhelmy Plate Method	(°)
$\theta_E^{WPM}$	Equilibrium contact angle obtained with the Wilhelmy Plate Method	(°)
$\theta_R^{WPM}$	Receding contact angle obtained with the Wilhelmy Plate Method	(°)
$\rho$	Density of the liquid	(M L <sup>-3</sup> )
$\sigma$	Surface tension (surface free energy)	(M T <sup>-2</sup> )
$\sigma_C$	Critical surface tension	(M T <sup>-2</sup> )
$\sigma_{LV}$	Liquid-vapour surface tension	(M T <sup>-2</sup> )
$\sigma_{SL}$	Solid-liquid surface tension	(M T <sup>-2</sup> )
$\sigma_{SV}$	Solid-vapour surface tension	(M T <sup>-2</sup> )
$\Phi$	Solid-liquid interaction parameter	(-)
$\omega$	Scaling factor of the van Genuchten model	(L)
$\Psi$	Water potential	(L)

## Abbreviations

CA	Contact angle
CRM	Capillary Rise Method
DCDMS	Dichlorodimethylsilane
ES	Equation of state
GB	Glass beads
HW	Homogeneous wettability
ICE	Initial capillary rise-effect in Wilhelmy Plate Method
LW	Lucas-Washburn equation
MED	Molarity of an Ethanol Droplet Method
MW	Mixed wettability
PDMS	Polydimethylsiloxane
RD	Relative deviation between dynamic and equilibrium contact angle
SD	Standard deviation
SDM	Sessile drop Method
SE	Standard error
SOC	Organic carbon content
SOM	Soil organic matter
WDPT	Water Drop Penetration Time
WPM	Wilhelmy Plate Method
WPM-ACA	Wilhelmy Plate Method-Advancing contact angle approach
WPM-ECA	Wilhelmy Plate Method-Equilibrium contact angle approach
WRC	Water retention curve

# Chapter 1

## Introduction

### 1.1. Background of the research

Wetting behavior or wettability is defined as the ability of a fluid to wet a solid (El Ghzaoui, 1999). This process depends on the interaction between adhesion and cohesion forces, resulting in phenomena like incomplete wettability, liquid spreading on solid surfaces and liquid rise in capillaries (Craig, 1971; Shedid and Ghannam, 2004).

The wettability is usually characterized by the contact angle (CA). In that way, it can be considered as an indicator of the material (Letey et al., 1999; Woche et al., 2005). The CA results from the balance of surface free energies or surface tensions between solid, liquid and vapour interfaces, as originally defined by Thomas Young in 1805. Although this relation is often used in research for characterizing interfacial phenomena, its experimental verification is difficult. The (so-called) intrinsic contact angle defined by Young, which has traditionally also been known as the intrinsic or true CA, assumes ideal conditions, like a perfectly smooth solid surface and chemical homogeneity. However, such conditions are eventually never observed in real porous media like soils (Or and Tuller, 2005), which implies that deviations between the observed and the intrinsic CA can be expected (Marmur, 1993 and 2006). Another problem involved in describing wettability in terms of the Young equation components, is that the direct assessment of the solid free energy is normally not possible. In this context, Zisman (1964) developed an empirical approach to characterize the wettability of solid surfaces.

In soil science, wettability and particularly the assessment of water repellency are relevant topics of research, as they constitute essential factors affecting the vegetation and soil biota (Eynard et al., 2004). They are also significant factors in determining the occurrence of phenomena like surface runoff and erodibility (Doerr et al., 2000; Goebel et al., 2005). Water repellency is present at different scales in the soil profile, influencing the dynamics of aggregation and movement of nutrients (Dekker et al., 2005; Goebel et al., 2005). In this context, a well known effect of increasing water repellency is the reduction of the infiltration rate, affecting the water

distribution and the germination and crop yield (Bond, 1968; King, 1981). An increasing number of publications in this topic, especially during the last years (DeBano, 2000), have demonstrated that water repellency is a widespread phenomenon, being observed in different geographical zones and climates all over the world, depending on factors like land use, vegetation and soil type (King, 1981; Doerr et al., 2000; Ritsema and Dekker, 2000). Water repellency is induced by a significant number of highly hydrophobic organic materials present in soil (soil organic matter, SOM). Litter and fungal hyphae are among the most important sources of repellency (Doerr et al., 2000). It is also a recurrent phenomenon after exposing soil to high temperature (e.g. wildfires), and also in certain forest soils, especially in commercial stands of species likes *Eucalyptus globulus* Labill. and *Pinus spp.* (Crockford et al., 1991; Doerr et al., 2000; Keizer et al., 2005).

Different methods have been developed for the assessment of wettability, both quantitative (e.g. estimating the CA) and qualitative (e.g. defining ranges of water repellency) (Letey et al., 1999; Shedid and Ghannam, 2004). Standard methods for soil samples are the Water Drop Penetration Time (WDTP) and the Molarity of Ethanol Droplets (MED) (Letey, 1969; Watson and Letey, 1970; Doerr, 1998). The first method measures the time needed for a drop to infiltrate, allowing to correlate the hydrological implications of repellency and its persistency as a function of time. MED can be considered as an indirect assessment of the soil particle surface tension (Doerr, 1998). Normally, a value  $CA = 90^\circ$  is assumed as the limit to distinguish between hydrophilic (CA in the range  $0-90^\circ$ ) or hydrophobic ( $CA >90^\circ$ ) conditions. A number of methods to assess the CA have been adapted from different fields of research, like the Capillary Rise Method (CRM), a standard approach in pharmacology (Siebold et al., 2000). This method is based on the Lucas-Washburn equation (Washburn, 1921), which is also considered as a fundamental relation describing the kinetics of liquid uptake in porous media. More recently, the Sessile Drop Method (SDM) and the Wilhelmy Plate Method (WPM) have also been proposed for use in soil research (Bachmann et al., 2000 and 2003).

A major problem in describing wettability is the fact that the mentioned methods normally have limitations (e.g. MED should be only used in dry samples and CRM has a theoretical resolution range up to only  $90^\circ$ ) (Doerr, 1998; Bachmann et al., 2003). At the same time, factors like sampling method, reproducibility and time needed for measurement become critical factors when a large number of highly variable samples must be evaluated. According to Doerr (1998), in soil

research, contrary to other fields (e.g. textile engineering, petroleum industry, etc.), methods measuring water repellency are not yet completely standardized, and they mostly have been applied to homogeneous samples. This eventually can lead to erroneous conclusions, especially when highly heterogeneous soils are evaluated (e.g. loamy soils derived from volcanic ashes in southern Chile<sup>1</sup>) and/or more than one single method is applied simultaneously (Bachmann et al., 2001 and 2003). An example of this last aspect is shown in Fig. 1, a comparison of the methods already mentioned (CRM and WPM) applied to a set of soil samples (Goebel, 2007). In this case, it is observed how different the CAs can be. It leads to the question of which method is the correct one, or which one describes the samples more accurately, regarding e.g. the intrinsic contact angle of Young (1805). In this context, previous publications concluded that the CRM based on the standard Washburn's equation, eventually can lead to an overestimation of the CA (Siebold et al., 2000, Lavi et al., 2008). At the same time, although WPM is an approach having a number of advantages in relation to CRM (e.g. shorter time needed for measurement), it still needs to be completely tested to prove it as a reliable method for application in soil science (Bachmann et al., 2001 and 2003).

## 1.2. Objectives

From the considerations mentioned above, it is hypothesized that (i) CRM usually overestimates CAs in comparison with other experimental approaches due to different factors like the geometry of the porous-system, resulting in verifiable deviations from the equilibrium or intrinsic CA and that (ii) WPM (e.g. characterization of surface properties) can be used as a reliable and accurate method for the estimation of the CA of soil material.

The main objectives of this thesis are therefore

- *To describe and compare the results of different experimental methods assessing contact angles and surface free energies in model soil systems.*

The wettability of materials with defined properties (e.g. particle shape, amount and distribution of hydrophobic components) and increasing water repellency is tested.

---

<sup>1</sup> **Ellies, A.** 2004. Personal communication. Facultad de Ciencias Agrarias, Universidad Austral de Chile. Valdivia. Chile

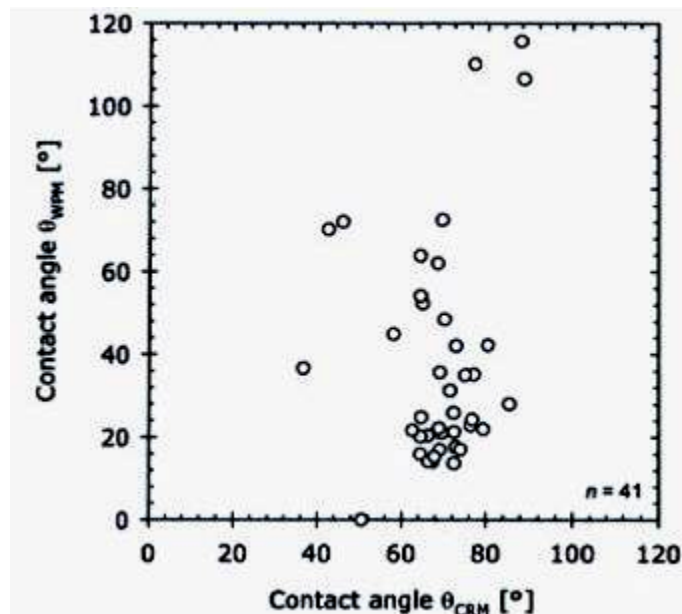


Fig. 1 Relation between  $\theta^{\text{CRM}}$  and  $\theta^{\text{WPM}}$  for a set of natural soil samples (source: Goebel, 2007).

- *To compare the results of the experimental methods with independent measurements carried out in similar materials.*

The wetting behavior of the same model materials are evaluated in a system with a different balance of forces regarding the laboratory methods (e.g. gravity). The significance of both kinds of systems is then compared.

- *To test the applicability of a new, generalized Lucas-Washburn model for the characterization of capillary rise in porous media.*

A recently proposed model, based on the incorporation of hydraulic properties derived from Darcy's law to the standard method for evaluation of capillary rise, is experimentally tested.

- *To carry out initial measurements in natural soil samples.*

A set of samples from sites with different soil-management and wettability is tested experimentally.

### 1.3. Outline of the thesis

The present thesis consists of a series of individual chapters, conceived to be published as scientific papers. Each chapter deals with a sub-topic of the research, with introduction, theory, discussion and conclusions. As the material, treatments and experimental methods of Chapters 2, 3 and 4 are similar, they are explained in detail only in Chapter 2, in order to avoid unnecessary repetition. At the same time, Chapter 5 is presented in its original published form.

Chapter 1 presents the problem and the objectives. Chapter 2<sup>2</sup> focuses on the comparison of different experimental methods assessing CA (CRM, WPM and SDM). In order to identify the capability of each method in describing wettability, the comparison is applied to a set of model materials (e.g. defined particle size and specific surface) with different degrees of water repellency. Chapter 3 focuses on comparing the two principal methods under test (CRM and WPM) with an alternative approach, based on the quantification of surface free energies with Zisman plots. Chapter 4 deals with the experimental validation of an alternative generalized Lucas-Washburn model (Marmur and Cohen, 1997; Marmur 2003), which is based on the combined evaluation of wetting kinetics and hydraulic properties, for characterization of capillary rise in porous media. This model assumes that an equivalent capillary, representing the average properties of the porous-system under test, can be defined. Chapter 5<sup>3</sup> tests the suitability of CRM to describe the wettability of real soil samples (i.e. samples with a range of particle-size distribution and wettability). In the final section, Chapter 6 presents a general discussion addressing the results and objectives of the present research and additional information, regarding especially the application of the experimental methods to natural soils.

---

<sup>2</sup> **Ramírez, J.C.; Bachmann, J.; Marmur, A.** 2009. On the determination of contact angles and capillarity of porous media (paper submitted to J. Hydrol.).

<sup>3</sup> **Ramírez, J.C.; Woche, S.; Bachmann, J.; Goebel, M.-O; Hallett, P.** 2008. Comparing capillary rise contact angles of soil aggregates and homogenized soil. Geoderma, doi: 10.1016/j.geoderma.2008.05.032.

## Chapter 2

# On the determination of contact angles and capillarity of porous media

### 2.1. Introduction

The quantification of the wetting properties of porous materials is a relevant research topic in many disciplines of science and technology, e.g production of waterproof materials, printing devices and oil extraction (Marmur and Cohen, 1997; Shahidzadeh et al., 2004). With respect to environmental sciences, wettability of the soil plays a significant role at different scales. Soils with extended water repellency tend to show a very specific time-dependent infiltration rate compared to wettable soils (Clothier, 2001), which has, in turn, significant implications on important processes like surface run-off, erodibility of the soil, or the formation of preferential flow pathways in the unsaturated zone (Goebel, 2007; Dekker and Ritsema, 1994; Doerr et al., 2000). On a much smaller microscopic scale, some studies indicate that sorption and transport of colloids like bacteria is also affected by the wetting properties of the solid particles under certain conditions (Schneider, 1997). However, in contrast to observations presented in many research papers, most standard textbooks of soil physics and subsurface hydrology still hypothesize complete wettability of the porous media, resulting in a wetting coefficient of  $\cos\theta = 1$ , where  $\theta$  is the contact angle (CA) of the medium. However, ignoring wettability effects might lead to misinterpretations of hydrological processes observed in the landscape as well as for processes in soil profiles or on the particle and aggregate scale.

The main objective of the present research is to test the capability of the methods to describe the wettability of porous media. One common laboratory method to quantify wettability of porous materials is the determination of the CA. As the routine measurement for powdered materials, the Capillary Rise Method ( $\theta^{\text{CRM}}$ ) has been proposed since decades, especially in chemistry and pharmacological research (Marmur & Cohen, 1997). This method is indirect and estimates the



CA through the initial rate of liquid penetration into a porous sample via a two-liquid analysis by employing the Lucas-Washburn equation (Siebold et al., 1997; Marmur & Cohen, 1997). Another option is the optical measurement of the CA formed by a liquid drop on the surface of a solid (Sessile Drop Method,  $\theta^{\text{SDM}}$ ). This CA reflects, according to the physical and chemical composition of the sample surface, more or less unstable CAs between the advancing or receding CA, but usually not exactly the energetically favorable equilibrium state, which is reflected by the Young CA. More recently, the Wilhelmy Plate Method ( $\theta^{\text{WPM}}$ ) was proposed and modified to measure the CA of soil particles attached to a plane surface (Bachmann et al., 2003). However, taking into account that water repellency and its effects have been reported in soils all over the world (Dekker and Ritsema, 1994), it is obvious that it becomes relevant to test and compare different approaches to evaluate their potential for the quantification of soil wetting properties and corresponding liquid dynamics with a defined level of accuracy and reproducibility. Time consumption is also an important factor since soils show generally a high variability of wettability, which requires, i.e. for many soil hydraulic investigations, the investigation of extended numbers of samples (Dekker and Ritsema, 1994). However, because different methods deliver often different results (Shahidzadeh et al., 2004), the assessment of the representative CA which is significant for the soil hydraulics is still a pending problem.

Thermodynamic equilibrium of a liquid on an ideal surface is characterized by a single CA. It has been known for a long time, that a wide range of stable apparent CA can be measured on real surfaces, which are usually rough and / or chemically heterogeneous which gives generally a range of quasi-static CA. This has the consequence, that the measurement of wetting properties of soil particles is not possible by direct methods (Marmur et al., 1986). As an example, equilibrium CA are, among many other factors, also a function of the drop volume (Brandon and Marmur, 1996), therefore there exist in general no unique CA for a given non-ideal natural system. The CA that corresponds to the absolute energy minimum, which should be used to derive quantitatively surface properties, is the stable state, the other states are metastable. Measurements of wettability with common methods are often associated with moving wetting fronts. In this respect, the term dynamic CA is used for a CA that depends on the velocity of the contact line. If the velocity is not zero, for the sake of measurement, but low, it would be termed quasi-static CA. Hence, the advancing and receding CAs are static, because they represent a metastable equilibrium, but still an equilibrium state. A wide range of stable apparent CA can be measured

on real surfaces. Multiple thermodynamic equilibrium states exist on rough / heterogeneous surfaces (metastable), hence hysteresis can be considered as multiplicity of equilibrium apparent CA. Hence, different physical backgrounds of the experimental CA determination must also be considered: force measurements (e.g. Wilhelmy Plate Method) are different than optical assessment or measurements of liquid penetration. However, there might be a meaningful relation between these different approaches, which is investigated in this study.

We focused on comparing the results of two different dynamic approaches ( $\theta^{\text{CRM}}$  and  $\theta^{\text{WPM}}$ ) and a further quasi-static method ( $\theta^{\text{SDM}}$ ). As a reference, the final capillary rise in long vertical columns under the impact of gravity ( $\theta_{\text{E}}^{\text{CR}}$ ) was also evaluated. All methods are applied to a set of porous materials (silt, sand and glass beads) with different degrees of water repellency, particle size and particle shape. Because soil is often a mixture of hydrophobic and hydrophilic particles (Becerra, 2006; Doerr et al., 2006), a second objective is to compare the wetting behavior between homogeneous (HW) and heterogeneous (mixed, MW) water repellency. These results should also allow to prove the consistency of CA determination techniques, including some recently published specific restrictions regarding the standard two-liquid Capillary Rise Method. We use in the present paper the term capillarity as a summarizing expression to account for the capillary rise in a porous medium which is affected by pore space topology as well as through interfacial properties.

## 2.2. Methods

### 2.2.1. Capillary Rise Method

The dynamic-advancing CA can be measured with the Capillary Rise Method ( $\theta^{\text{CRM}}$ ), during the initial liquid penetration into the medium, when the equilibrium state in a solid-liquid-vapor system has not yet been established (van Mourik et al., 2005). This method is in theory valid for CAs between 0 and 90°. The Lucas-Washburn equation for capillary penetration of liquids represents a standard approach to describe the kinetics of the wetting process in capillaries. The general equation is expressed as

$$x^2 = \frac{r\sigma \cos \theta}{2\eta} t \quad (1)$$

where  $x$  (m) represents the liquid-penetration length of the wetting-front,  $t$  (s) is the time,  $r$  (m) is the effective radius of the capillary (assuming them as straight and cylindrical),  $\sigma$  (mN m<sup>-1</sup>) and  $\eta$  (kg m<sup>-1</sup> s<sup>-1</sup>) are the surface tension and viscosity of the test liquid, respectively, and  $\theta$  is the CA between the liquid and the capillary wall. According to Marmur (2003), Eq. (1) is suitable for evaluation of short samples, where the effect of gravitation can in theory be neglected. Generally, the variation of the sample weight ( $W$ ) is easier to measure as the optical evaluation of the height of the wetting front. In this case, a modified Lucas-Washburn equation is applied,

$$W^2 = K \frac{\rho^2 \sigma \cos \theta}{2\eta} t \quad (2)$$

where  $K$  (m<sup>5</sup>) is a constant related to the geometry of the test material (e.g. porosity, pore radius, tortuosity and continuity of the pores) and  $\rho$  (kg m<sup>-3</sup>) is the density of the test liquid. The model can be applied by using a sensitive microbalance (Jackson et al., 2004). A clear disadvantage by using (1) and (2) arises because the products  $r \cdot \cos\theta$  and  $K \cdot \cos\theta$  are not possible to separate, usually making it necessary to use additionally a reference liquid (with assumed  $\theta = 0^\circ$ ) to estimate  $r$  and  $K$ . The CA is evaluated by applying Eqs. (1) or (2) (Siebold et al., 1997; Bachmann et al., 2003; Marmur, 2003). Chibowski and Perea-Carpio (2002) reported a number of reasons leading to inaccuracies associated with this method: as mentioned,  $\theta^{\text{CRM}}$  involves the necessity of a completely wettable reference liquid during the dynamic process of liquid penetration, which is actually very difficult if not impossible to prove. Further, low reproducibility of necessarily similar packing conditions of such complex systems could also lead to poor reproducibility (Siebold et al., 1997). Siebold et al. (2000) observed that  $\theta^{\text{CRM}}$  could be rather higher than the expected value for an almost completely wettable material, which has been theoretically verified by Czachor (2006).

### 2.2.2. Wilhelmy Plate Method

Bachmann et al. (2003) modified and suggested the Wilhelmy Plate Method ( $\theta^{\text{WPM}}$ ) for applications in soil science. This method is in principle applicable between 0 and 180°. The sample is attached to a glass slide by an adhesive tape (around 10 cm<sup>2</sup> of surface) on all sides of

the slide. In theory, the tape is completely covered with a monolayer of particles. This sample is immersed and withdrawn into a test liquid with constant velocity, usually deionized water. Acting forces ( $F_T$ ) associated with the immersed slide are described by the equation

$$F_T = W - F_B + F_W = W - V\rho g + l_w \sigma_{LV} \cos \theta \quad (3)$$

where  $W$  (kg) is the weight of the slide (or plate),  $F_B$  the buoyancy force,  $F_W$  the wetting force acting at the three phase boundary,  $V$  ( $m^3$ ) is the volume of the fraction of the slide immersed,  $g$  corresponds to the gravitational acceleration ( $9.81 \text{ m s}^{-2}$ ),  $l_w$  (m) is the wetted length, approximated by the circumference of the glass slide, and  $\sigma_{LV}$  ( $\text{mN m}^{-1}$ ) is the surface tension of the liquid. Finally, the CA is evaluated with the expression ( $w$  has been set to zero):

$$\cos \theta = \frac{F_T + V\rho g}{l_w \sigma_{LV}} \quad (4)$$

A single measurement involves the evaluation of  $F_T$  with time. Eq. (4) can be solved during immersion (advancing CA,  $\theta_A^{\text{WPM}}$ ) as well as during lifting (receding CA,  $\theta_R^{\text{WPM}}$ ). The main advantage of this method is low time demand, while the disadvantages are limitations in handling large particles or soil aggregates (for further details we refer to Bachmann et al., 2003).

### 2.2.3. Sessile Drop Method

Theoretically, the equilibrium contact angle ( $\theta_E$ ) on an ideal surface can be described by the Young equation (Young, 1805; Good, 1993):

$$\sigma_{LV} \cos \theta_E = \sigma_{SV} - \sigma_{SL} \quad (5)$$

where L, S and V represent the liquid, solid and vapor phases, respectively. Experimentally,  $\theta_E$  usually can be measured on very clean, smooth and planar surfaces. According to this equation, the thermodynamic equilibrium of the surface tensions between the components results in a measurable CA ( $\theta_E$  is between 0 and  $180^\circ$ ). Although, in practice, it is usually not possible to

measure directly the value of  $\theta_E$  on real surfaces, different approaches allow to get approximations, e. g. with the Sessile Drop Method ( $\theta^{SDM}$ ) (Adamson, 1990). This method was modified by Bachmann et al. (2000) for soil particles. The sample preparation is similar as for  $\theta^{WPM}$ . Yang (1995) stated by considering the first law of thermodynamics, that  $\theta_E$  will not have a defined value in a three-phases system submitted to a wetting-dewetting process, merely, it will be located over a range of angles, defined by the envelopes described by the advancing CA and receding CA. This consideration stated originally for  $\theta^{SDM}$  can also be applied to  $\theta^{WPM}$ , where the average of  $\theta_A^{WPM}$  and  $\theta_R^{WPM}$  with the expression  $\cos\theta_E^{WPM} = (\cos\theta_A^{WPM} + \cos\theta_R^{WPM})/2$  will apparently correspond better to  $\theta_E$  than the individual advancing or receding CA.

#### 2.2.4. Capillary rise under gravity impact

Experiments done to evaluate  $\theta_E$  were carried out by Arye et al. (2007) with long soil columns by measuring final moisture profiles and determining the maximal height of capillary rise, i.e. the stage, where capillary and gravitational forces are similar but opposed, resulting in an assumed equilibrium state. The value of this equilibrium CA in long columns ( $\theta_E^{CR}$ ) can be assessed by scaling the final height (H) in relation with a reference liquid (zero CA assumption), usually ethanol, by the expression

$$\frac{H_{EQ0}}{H_{EQ1}} = \frac{\rho_1 \sigma_0}{\rho_0 \sigma_1} \frac{1}{\cos\theta_{EQ1}} \quad (6)$$

where subscripts 0 and 1 refer for ethanol ( $\sigma_0= 22.4 \text{ mN m}^{-1}$ ;  $\rho_0= 0.789 \text{ g cm}^{-3}$ , at 20°C) and water ( $\sigma_0= 73.1 \text{ mN m}^{-1}$ ;  $\rho_0= 0.9982 \text{ g cm}^{-3}$ , at 20°C) respectively. This method is applicable without any modifications for CAs between 0 and 90°.

As capillary rise evaluations have been carried out in samples very different in size, the dimensionless Bond number ( $B_N$ ) allows a comparison of the size-dependent relative importance of gravitational to capillary forces. One form of the equation is (Shahidzadeh et al., 2003 and 2004):

$$B_N = \frac{\rho g L}{2\sigma/r_X} \quad (7)$$

where  $L$  is the length of the test system. If  $B_N < 1$ , capillary forces dominate the system, if  $B_N > 1$ , gravitational forces have also to be considered. An estimation of  $B_N$  for our systems (glass tubes and long columns), considering  $L$  as the filling height and  $r$  being calculated from the expression  $2r = d/3$  ( $d$ : diameter of the particles) (Shahidzadeh et al., 2004), rendered  $\sim 0.1$  for the Capillary Rise Method and  $> 3$  for the long columns. For comparison, Shahidzadeh et al. (2004) worked with  $B_N$  in the range 3.0-3.7, in glass columns (diameter: 3 cm, length: 34 cm) filled with sand and glass beads for drainage behavior evaluation.

## 2.3. Materials and measurements

### 2.3.1. Materials

Four different porous materials were used: two natural materials, sand (Location: Duingen. Lower Saxony, Germany) and silt (Location: Asel. Lower Saxony, Germany). Additionally, glass beads (GB) (Swarco Vestglas GmbH, Recklinghausen, Germany) of two different grain-size distributions (40-70 and 150-250  $\mu\text{m}$ ) were used (Table 1). The particles of the materials are comparable in diameter (i.e. silt with GB 40-70  $\mu\text{m}$  and sand with GB 150-250  $\mu\text{m}$ ), but they were significantly different in shape, surface roughness and specific surface area.

**Table 1:** Materials used for the experiments

Material	Diameter ( $\mu\text{m}$ )	Specific surface Area (S) ( $\text{m}^2 \text{g}^{-1}$ )	Bulk density ( $\text{g cm}^{-3}$ )		Porosity (%)		Description
			1	2	1	2	
Silt	20 - 63	1.98	1.11	1.13	58.16	57.26	Platy, very rough
Sand	63 - 200	0.15	1.59	1.53	40.23	40.81	Sphere-like, rough, irregular
GB	40 - 70	0.07	1.42	1.41	43.01	43.01	Perfect sphere, no internal porosity
	150 - 250	0.04	1.54	1.52	38.56	38.99	Perfect sphere, no internal porosity

S: Estimated with the BET  $\text{N}_2$  Method (Quantasorb system).

1: Average of 20 samples packed in glass tubes (sample length: 2 cm; diameter: 0.8 cm).

2: Estimated from material packed in segmented Plexiglas<sup>®</sup> columns (length: 60 cm; diameter 1.6 cm). Average of 10 samples (5 for silt).

The degree of water repellency was modified by pre-treatment of the samples with heat (400°C for both GB materials and 800°C for silt and sand) in order to remove organic impurities, and then hydrophobized through the addition of increasing amounts of Dichlorodimethylsilane (DCDMS) (Merck Laboratories, Darmstadt, Germany).

At first, a set of materials with homogeneous wettability (HW), i.e. all particles have approximately the same degree of water repellency, was prepared. At room conditions, a DCDMS/n-hexane solution (DCDMS concentration: 0.5%) was added in different amounts to the air-dry hydrophilic materials (500g). The DCDMS added to dry soil ranged between  $5.5 \cdot 10^{-6}$  and  $1.0 \cdot 10^{-2}$  ml g<sup>-1</sup>. After one hour, deionized water was added until complete saturation. The mixture was then stirred, surplus water was removed in order to remove the HCl created by the silanization process. The samples were finally dried at 105° for 48 hours. After contact with water, DCDMS (Si(CH<sub>3</sub>)Cl<sub>2</sub>) reacts with water on the particle surface to Polydimethylsiloxane, (PDMS, Si(CH<sub>3</sub>)<sub>2</sub>O)<sub>n</sub>, which gives finally the stable hydrophobic coating (Binks et al., 2006; Goebel, 2007). A second set of materials with mixed wettability (MW) was prepared by mixing hydrophilic and hydrophobic grains with different mass ratios. The amount of hydrophobic particles ranged between 1.5 to 60.0% of the total mass of the sample. The water repellent components of the mixtures were hydrophobized in a glass desiccator: 1 kg of material was exposed to the vapor of 5 ml (10 ml for silt) of DCDMS for three days. The evaporation technique was used for the hydrophobic fraction because it leads in case of mixed wettability materials to a more stable hydrophilic fraction in contact with the treated fraction compared with direct DCDMS application. The treated fractions were then immersed in water and dried twice at 105 °C before mixing. For silt it was necessary to add again 10 ml of CMS directly to the hydrophobic fraction to ensure a permanent hydrophobicity. To reduce possible migration of PDMS to untreated grains (Science Lab, 2005), this fraction was also dried twice at 105 °C. It should be noted that for MW the DCDMS concentration per unit mass cannot be evaluated exactly with the same accuracy as for the HW materials due to probable adsorption of DCDMS on the inner glass surfaces of the desiccator. However, this error should be rated as low, since the total surface area of the particles was at least two magnitudes larger which suggests a low loss rate of DCDMS due to adsorption on the desiccator.

### 2.3.2. Measurements

The experimental procedures followed Bachmann et al. (2000, 2003) and Goebel et al. (2004). For  $\theta^{\text{CRM}}$  and  $\theta^{\text{WPM}}$ , a digital tensiometer (DCAT 11, DATA PHYSICS, Filderstadt, Germany; Resolution  $10^{-5}$ g; frequency of data sampling  $10\text{-}30\text{ s}^{-1}$ ) was used. Air humidity in the laboratory during measurements was 50-65%. The temperature of liquids was kept constant around  $20\pm 0.5$  °C. Fresh deionized water was used and replaced after each measurement. For  $\theta^{\text{SDM}}$ , CAs were evaluated with a goniometer (Contact Angle System OCA, DATA PHYSICS).

#### 2.3.2.1. Capillary Rise Method

Glass tubes of 0.8 cm diameter and 6 cm length were used, which were closed with filter paper at the bottom, fixed with a plastic ring. The tubes were filled with 1g for silt and GB 40-70  $\mu\text{m}$  and with 2g sand and GB 150-250  $\mu\text{m}$ . These weights correspond to an average filling height of  $1.4\pm 0.1$  cm for silt and GB 40-70  $\mu\text{m}$ , and  $2.1\pm 0.2$  cm for sand and GB 150-250  $\mu\text{m}$ . Before each measurement, the samples were gently compacted by the weight of a 50g plastic stick, which was placed in the vertical tube for 10 s. The fitting range to evaluate the liquid penetration rate from the  $W^2 = f(t)$  curves was 1-3 s for n-hexane and ethanol and 3-5 s for water, respectively. Three measurements in water and two in n-hexane were carried out.

#### 2.3.2.2. Wilhelmy Plate Method

A double-side adhesive tape (TESA, Hamburg, Germany) attached to microscopic glass slides (ELKA, Sondheim, Germany) was used. The fitting range of the  $F_T = f(t)$  curve was adjusted to 3.0-4.8 cm immersion depth for  $\theta_A^{\text{WPM}}$  and 0-1.0 cm for  $\theta_R^{\text{WPM}}$  (Bachmann et al., 2003). An immersion depth of 5 mm and speed of  $0.2\text{ mm s}^{-1}$  were used for both modes. Five replications were carried out. The effect of immersion depth (range: 1-10 mm) and velocity of immersion in both  $\theta_A^{\text{WPM}}$  and  $\theta_R^{\text{WPM}}$  (range:  $0.01\text{-}10\text{ mm s}^{-1}$ ), was analyzed previously to find ideal parameter settings regarding measurement time and stability of  $\theta_E^{\text{WPM}}$ .

The influence of immersion speed and immersion depth on the CAs is significant (Figs. 2A and 2B, respectively). Depending on the set-up, different  $\theta_A^{\text{WPM}}$  and  $\theta_R^{\text{WPM}}$  are measured, whereas the mean  $\theta_E^{\text{WPM}}$  is rather stable. The  $\theta_A^{\text{WPM}}$  of the hydrophobic sand (Fig. 2A) decreased from



132.4° (velocity: 0.01 mm s<sup>-1</sup>) to 76.6° (10 mm s<sup>-1</sup>), while  $\theta_R^{\text{WPM}}$  increased from 35.8° to 84.6° (10 mm s<sup>-1</sup>), whereas  $\theta_E^{\text{WPM}}$  maintained a relatively stable value between 86.1° (0.01 mm s<sup>-1</sup>) and 80.5° (10 mm s<sup>-1</sup>). In general, stable values are observed in the range <0.1-0.2 mm s<sup>-1</sup>. These values agree with Bachmann et al. (2006), who found a similar threshold value. Regarding the immersion depth (Fig. 1B), which was measured with the standard set-up of our experiments (0.2 mm s<sup>-1</sup>), it is observed that  $\theta_E^{\text{WPM}}$  tends to remain stable, ranging between 98° with 1 mm immersion depth and 104° with 10 mm ( $\theta_A^{\text{WPM}} = 180^\circ$ ,  $\theta_R^{\text{WPM}} = 60.4^\circ$ ). These results indicate that an immersion depth of at least 6 mm should be maintained in order to measure quasi-stable CAs. For smaller depths in combination with extreme hydrophobic surfaces, the shape of the meniscus at the surface during the immersion process is still developing.

### 2.3.2.3. Sessile drop method

The capability of the method to measure reproducible CAs on a flat monolayer of grains like soil particles was already analyzed by Bachmann et al. (2000). For each sample, 6 drops of deionized water were placed onto a horizontal positioned WPM-sample. This allowed 12 readings by measuring the tangent at the three-phase boundary on both sides of the droplets. Drop diameter ranged between 3.0 and 3.5 mm, considerably larger than average diameter of the particles, minimizing the effect of the particle-size on the measured contact angle.

### 2.3.2.4. Capillary rise under gravity conditions

Segmented Plexiglas columns (length of one segment: 1.0 cm; inner diameter: 1.6 cm) were filled with the different test materials. They were hand-packed and gently compacted along the column in 5 cm increments, until reaching a height of around 60 cm for sand and GBs and 150 cm for silt. Hand-packing of the columns and the separating of segments after the experiment produced a variable bulk density between segments, with the highest deviation for sand. In general, the standard deviation (SD) for bulk density calculated for all segments of a column was <0.1 g cm<sup>-3</sup> for silt and GB 40-70 μm, and <0.06 g cm<sup>-3</sup> for sand and GB 150-250 μm. From top to bottom no significant trend for bulk density was observed.

The bottoms of the columns were closed with pierced rubber-plugs covered with silk sheets to prevent loss of material while allowing free penetration of liquid into the column. The first segment was submerged into the liquid which was in a polyethylene bottle, containing 160g of

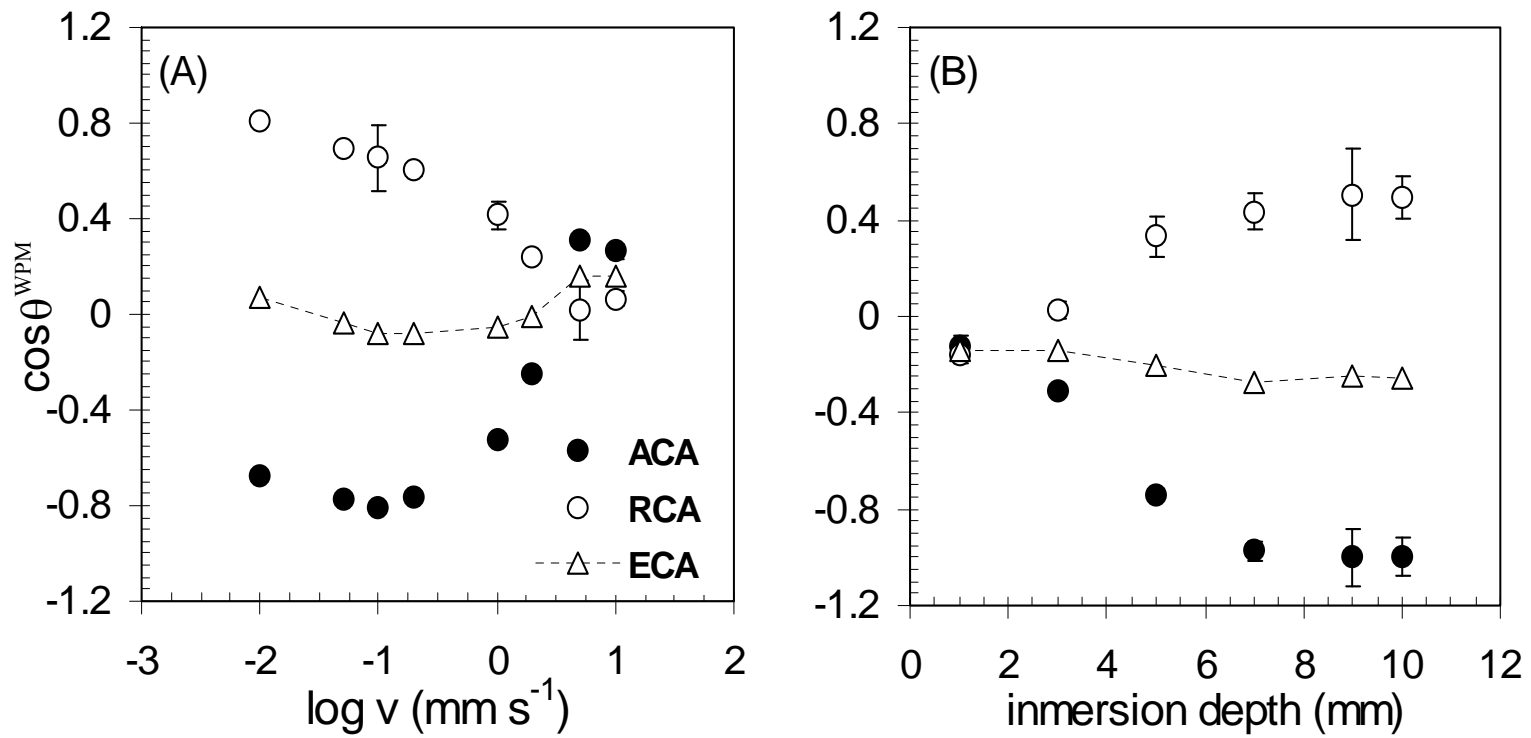


**Fig. 2** Evaluation of  $\theta_{\text{A}}^{\text{WPM}}$  (ACA),  $\theta_{\text{R}}^{\text{WPM}}$  (RCA) and  $\theta_{\text{E}}^{\text{WPM}}$  (ECA) for sand. A: Effect of the immersion speed (50% hydrophobic particles =  $2.5 \cdot 10^{-4}$  mL  $\text{g}^{-1}$  DCDMS.  $\theta_{\text{A}}^{\text{WPM}} = 138.4^\circ$ ,  $\theta_{\text{R}}^{\text{WPM}} = 52.6^\circ$ ,  $\theta_{\text{E}}^{\text{WPM}} = 95.5^\circ$ ). B: Effect of the immersion depth (100% hydrophobic particles =  $5.0 \cdot 10^{-4}$  mL  $\text{g}^{-1}$  DCDMS.  $\theta_{\text{A}}^{\text{WPM}} = 137.5^\circ$ ,  $\theta_{\text{R}}^{\text{WPM}} = 70.4^\circ$ ,  $\theta_{\text{E}}^{\text{WPM}} = 104.0^\circ$ ).

deionized water. The adsorbed water was determined via mass loss of the water reservoir with a balance (Mettler PM200, Switzerland. Precision:  $1.0 \cdot 10^{-3}$  g). Weight was measured at different time intervals: each 1-2 s the first 5 minutes, 30-60 s until 30 minutes, 60 min the first 12 hours and later once per day. The columns were all evaluated in duplicate. The measurements continued until the equilibrium between capillary and gravitational forces was observed, which was checked by controlling the weight of the reservoir bottle and by comparison with a reference system (a bottle filled with water). When the liquid uptake was equal or in some cases lower than the loss of water due to evaporation of the reference system (loss due to vapour diffusion through Plexiglas walls), the measurement was considered as terminated. For the corresponding measurements with the reference liquid (ethanol), PVC columns were also prepared in duplicate. Ethanol was chosen instead of n-hexane as reference liquid, because of its lower volatilization. After the experiment, each column segment was individually weighted and dried at 105 °C for 48 hours. For each segment, the gravimetric liquid content was determined to characterize the vertical water content distribution profile. The bulk density per segment and column was also determined and used to fit the bulk density data along the column. These linear regression parameters were used instead of segment-specific bulk densities to account for the small fluctuations in mass of the soil associated with non-ideal segmentation of the column, which affects the dry mass per volume, but not the gravimetric water contents. The bulk density data from the linear regression were used to calculate the volumetric water content as a function of height.

The characteristics of the wetting front during the capillary rise is different for HW and MW. For the HW columns it is expected to observe a more uniform wetting front compared to MW, where the liquid will tend to rise through hydrophilic pathways (Steenhuis et al., 2005). Fig. 3 shows examples of the wetting fronts for HW (Fig. 3A) and MW samples (Fig. 3B), confirming the different wetting conditions caused by the preparation techniques.

## **2.4. Results and discussion**

### **2.4.1. Capillary Rise Method**

Figures 4 and 5 show the results of the entire study. The average SD for replicate measurements made with the CRM was low, i.e. 2.7° for HW and 1.9° for MW materials, with no obvious differences between the four model soils. Results obtained from the CRM gave  $\theta^{\text{CRM}}$  values that

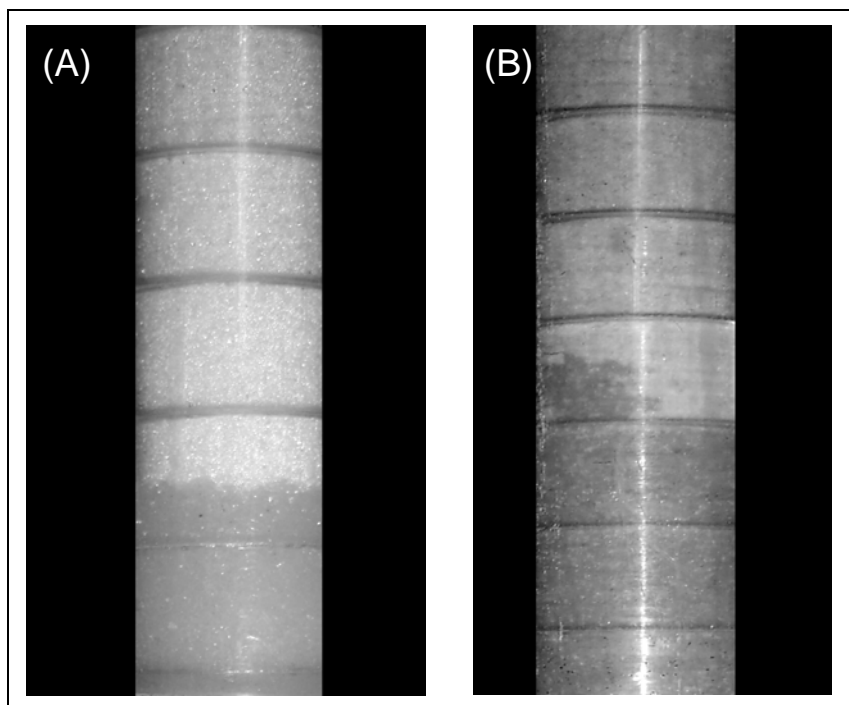


**Fig. 3** Wetting evaluation in segmented columns, examples for sand. A: Typical wetting front in homogeneous wettability ( $= 2.5 \cdot 10^{-5} \text{ mL g}^{-1} \text{ DCDMS}$ ). B: Typical wetting front in mixed wettability (20% hydrophobic particles  $= 1 \cdot 10^{-4} \text{ mL g}^{-1} \text{ DCDMS}$ ).

show in most cases a clear relation between increasing CA and increasing hydrophobicity, no matter if the samples had a HW or MW characteristics. This indicates a stable reproducibility of the CRM data. In all cases, the relation  $\theta^{\text{CRM}}$  versus hydrophobicity shows a curvilinear slope, except silt with HW. In the less water repellent domain ( $CA < 50^\circ$ ),  $\theta^{\text{CRM}}$  angles are generally larger than for  $\theta^{\text{WPM}}$  and  $\theta^{\text{SDM}}$ , especially for HW samples. For the unregular-shaped and smaller silt particles, these differences are larger, followed by the smaller GB fraction 40-70  $\mu\text{m}$ . Despite the fact that CRM allows the measurement of CAs only between  $0^\circ$  and  $90^\circ$ , there appears to be an overestimation of the CA by using the standard two-liquids approach in comparison with  $\theta^{\text{WPM}}$  and  $\theta^{\text{SDM}}$ , especially for samples with a relatively low degree of water repellency. These results agreed well with corresponding observations of dynamic CAs, measured with CRM for powdered materials in comparison with the static or equilibrium CAs measured for glass capillaries (Siebold et al., 2000; Lavi et al., 2008) or on ideal smooth glass plates (Morrow, 1976; Chibowski and Perea-Carpio, 2002). Another point of view is that these results indicate that  $\theta^{\text{CRM}}$  has obviously a considerable smaller range of CAs for the tested materials as the theoretical limits ( $0$ - $90^\circ$ ). This is surprising since we treated accordingly to obtain

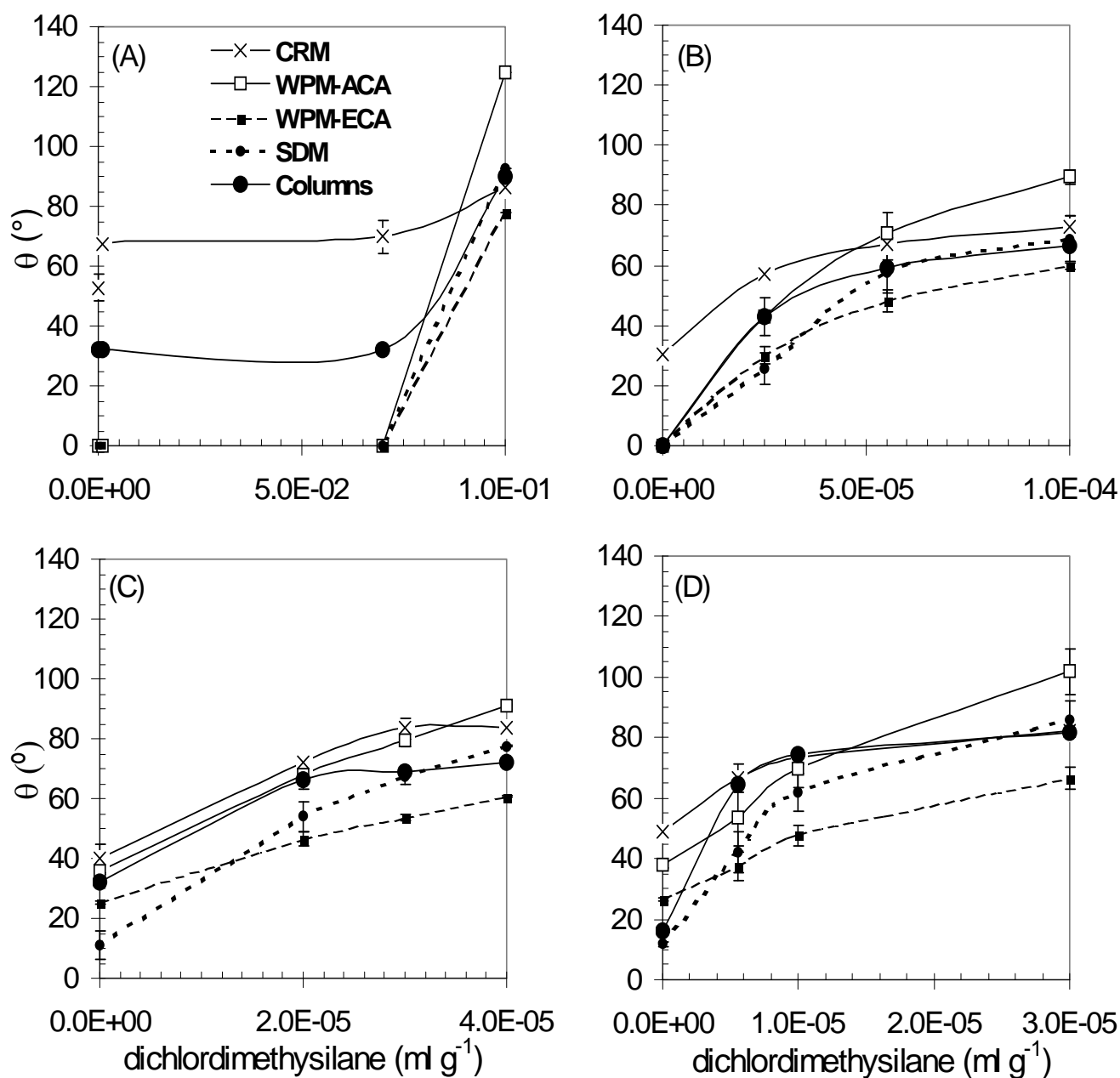


**Fig. 4** Comparison of  $\theta^{\text{CRM}}$  (CRM),  $\theta_{\text{A}}^{\text{WPM}}$  (WPM-ACA),  $\theta_{\text{E}}^{\text{WPM}}$  (WPM-ECA),  $\theta^{\text{SDM}}$  (SDM) values and equilibrium CA estimated in segmented columns in samples with homogeneous wettability. A: Silt, B: Sand, C: GB 40-70  $\mu\text{m}$ , D: GB 150-250  $\mu\text{m}$ . Note the x-axis has different scales between treatments and materials.

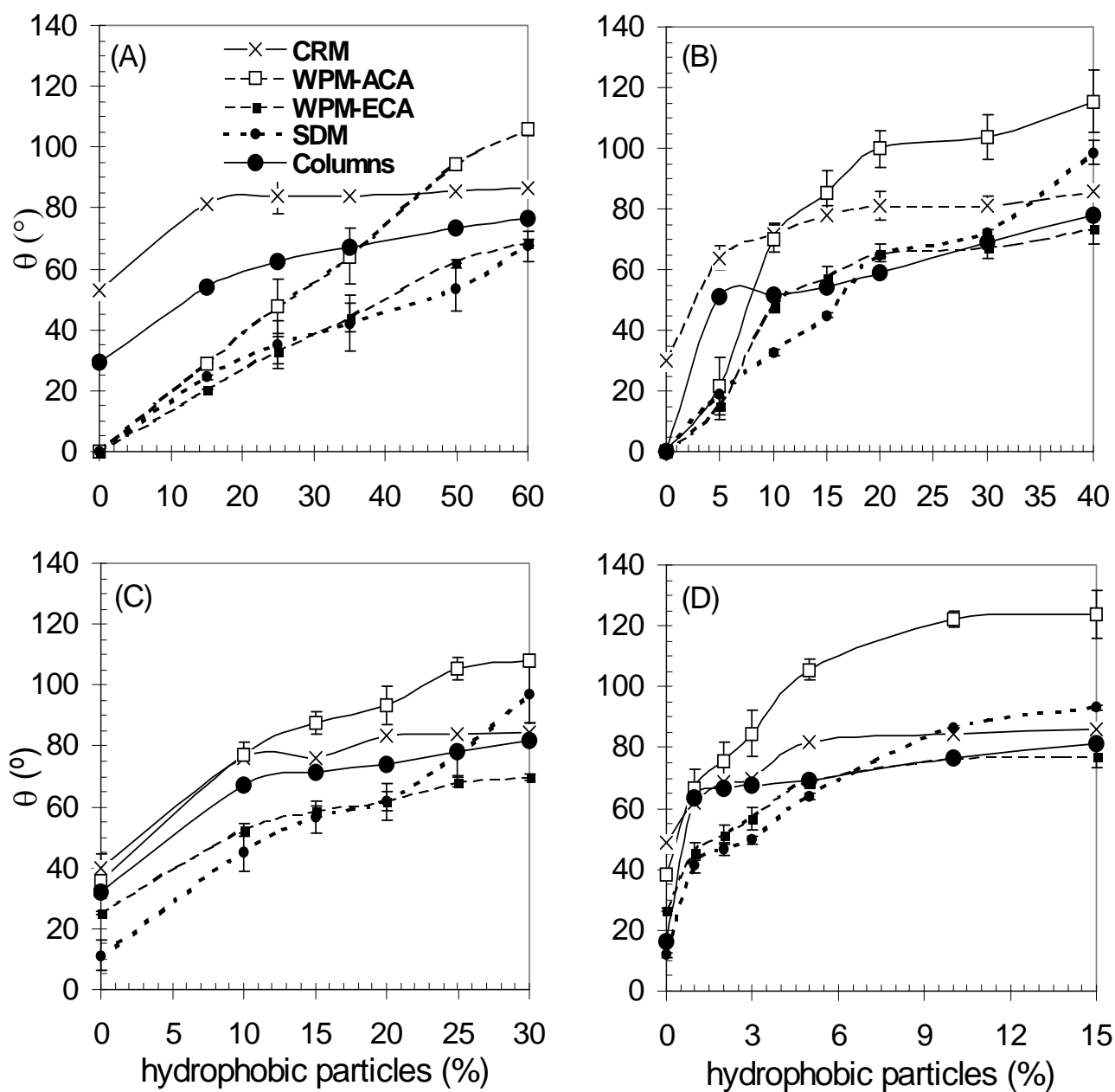


**Fig. 5** Comparison of  $\theta^{\text{CRM}}$  (CRM),  $\theta_{\text{A}}^{\text{WPM}}$  (WPM-ACA),  $\theta_{\text{E}}^{\text{WPM}}$  (WPM-ECA),  $\theta^{\text{SDM}}$  (SDM) values and equilibrium CA estimated in segmented columns in samples with mixed wettability (estimated DCDMS content in 100% hydrophobic particles =  $2.0 \cdot 10^{-3} \text{ mL g}^{-1}$  in silt and =  $5.0 \cdot 10^{-4} \text{ mL g}^{-1}$  DCDMS in sand and GB). A: Silt, B: Sand, C: GB 40-70  $\mu\text{m}$ , D: GB 150-250  $\mu\text{m}$ . Note the x-axis has different scales between treatments and materials.

maximal wettability as well as maximal water repellency of the samples. The complete range for CRM CA was only around 32° for silt, 55° for sand, 45° for GB 40-70 µm and 37° for GB 150-250 µm. It should also be kept in mind that very high values of  $\theta^{\text{CRM}}$ , i.e. CA > 85°-87°, should be merely considered as the indication for hydrophobic media with possible values between 90° to 180°, rather than exact CAs in a thermodynamical sense.

#### 2.4.2. Wilhelmy Plate Method

In agreement to the CRM ( $\theta^{\text{CRM}}$ ), the WPM angles ( $\theta^{\text{WPM}}$ ) followed for both wettability treatments (HW and MW) a monotonic trend to higher CAs with increasing hydrophobicity. The initial  $\theta_{\text{A}}^{\text{WPM}}$  for the reference materials is 0° for sand and silt, and 35°-38° for both GB fractions, which is slightly larger than the average CAs we measured on a cleaned and smooth glass slide surface ( $\theta_{\text{A}}^{\text{WPM}} = 31.3^\circ$ ). This is probably explained due to higher surface roughness of the natural materials (silt and sand) compared to the GBs, as deduced from the specific surface data (Table 1) which tends, according to the Wenzel equation, to reduce the CA when the intrinsic CA is < 90° (Adamson, 1990).

Results of  $\theta_{\text{E}}^{\text{WPM}}$  are consistent with the  $\theta_{\text{A}}^{\text{WPM}}$  characteristics, but on a considerable lower CA level. Taking the CA hysteresis as an indicator for physical and chemical surface heterogeneity (Yang, 1995; Homma et al., 2000), data show that differences between  $\theta_{\text{A}}^{\text{WPM}}$  and  $\theta_{\text{E}}^{\text{WPM}}$  are indeed increasing with increasing water repellency, while the physical surface roughness remains constant. The hysteresis is more pronounced for the MW material, e.g. mean differences between  $\theta_{\text{A}}^{\text{WPM}}$  and  $\theta_{\text{E}}^{\text{WPM}}$  were in average 22° for HW compared to 26° for MW, which confirms experimentally the higher degree of chemical heterogeneity of the surface. Roughness and chemical heterogeneity are considered as important causes for energy barriers leading to metastable conditions (Brandon and Marmur, 1986) and complicates the characterization of such natural surfaces by CA measurements. This aspect becomes possibly relevant for soils, as we assumed that MW samples should represent the nature of water repellent soils with more accuracy than HW samples. Extreme differences of  $\theta_{\text{A}}^{\text{WPM}}$  and  $\theta_{\text{E}}^{\text{WPM}}$  were found to be around 130° for silt and sand and about 100° for GBs, indicating higher energy barriers for the natural materials. While  $\theta^{\text{WPM}}$  is theoretically unrestricted between 0° and 180°, the highest  $\theta_{\text{A}}^{\text{WPM}}$  we

measured in our experiments was in the range 120-130°, which is considerably larger than the range 95-105° we measured on smooth silanized glass slides, indicating again the impact of roughness for the rough particle surfaces and probably the formation of composite surfaces with air inclusions (Bico et al., 1999).

### 2.4.3. Sessile Drop Method

The SDM contact angle ( $\theta^{\text{SDM}}$ ) might also as the WPM angle  $\theta_{\text{E}}^{\text{WPM}}$  be considered to represent better the thermodynamical equilibrium CA ( $\theta_{\text{E}}^{\text{WPM}}$ ) of a rough and heterogeneous surface as dynamic methods, i.e.  $\theta_{\text{A}}^{\text{WPM}}$  or  $\theta^{\text{CRM}}$  (Good, 1993; Meiron et al., 2004). The SDM is a fast and sensitive method in the entire CA range since we measured angles between 0°-140°. In general, a relatively good agreement between  $\theta_{\text{E}}^{\text{WPM}}$  and  $\theta^{\text{SDM}}$  was observed, especially for the MW samples. For the most hydrophilic materials, zero CAs were measured for sand and silt. The good wettability is principally confirmed with the real wetting behavior as water drops spread instantly in contact with these samples. For both GB fractions the measured  $\theta^{\text{SDM}}$  were around 11-15°. Again, these results are in line with the corresponding  $\theta_{\text{E}}^{\text{WPM}}$  measurements with slightly better agreement for the MW samples (Fig. 4). The  $\theta^{\text{SDM}} - \theta_{\text{E}}^{\text{WPM}}$  agreement for MW samples was especially good for silt, with CA differences <9° between both methods. For sand and GBs, differences were slightly higher (<13°), except the most hydrophobic samples (e.g. for sand, >40% hydrophobic particles), where the differences are around 20°, showing a very pronounced increase of  $\theta_{\text{A}}^{\text{WPM}}$  with higher content of hydrophobic particles which affects, in turn, the  $\theta_{\text{E}}^{\text{WPM}}$  angle. For HW samples,  $\theta^{\text{SDM}}$  shows a relatively good similarity with  $\theta_{\text{E}}^{\text{WPM}}$  for silt (differences <14°) and sand (differences <9°). For the GB materials, the differences between both methods tend to increase with higher hydrophobicity, although smaller than 20°.

### 2.4.4. Capillary rise in long columns

The Fig. 6A shows examples of the wetting progress for the first 30 minutes for sand (HW). As observed, there is a clear tendency of lower water uptake rates with increasing water repellency. However, a few inconsistencies are observed, e.g. a sample with a medium level of hydrophobicity (DCDMS concentration:  $5.5 \cdot 10^{-5}$  ml g<sup>-1</sup>,  $\theta^{\text{CRM}} = 67.1^\circ$ ,  $\theta_{\text{A}}^{\text{WPM}} = 70.8^\circ$ ) shows initially a higher slope than the corresponding hydrophilic material ( $\theta^{\text{CRM}} = 30.2^\circ$ ;  $\theta_{\text{A}}^{\text{WPM}} = 0^\circ$ ).



This effect might be associated with an incomplete contact between sample and soil due to initial air inclusion at the bottom of the column at the beginning of the experiment. Fig. 6B shows an example of a vertical liquid profile for water and ethanol. These data were used to calculate the value of  $\theta_E$  based on the final equilibrium height of both liquids by applying Eq. 6. The scaling of the water with respect to the ethanol curves lead finally to calculated values of  $\theta_E^{CR}$  near  $0^\circ$  for sand and to  $0-20^\circ$  for GB 150-250  $\mu\text{m}$ . For silt and GB 40-70  $\mu\text{m}$ , the differences were larger resulting in values of  $\theta_E^{CR}$  around  $30^\circ$ , whereas  $\theta^{WPM}$  and  $\theta^{SDM}$  indicated zero for these both materials.

## 2.5. General discussion

Comparing the results obtained from liquid penetration into porous media, the equilibrium approach ( $\theta_E^{CR}$ ) showed usually lower CA than the conventional two-liquid method ( $\theta^{CRM}$ ), where the instantaneous liquid penetration rate is analyzed. For all samples was  $\theta^{CRM} > 0^\circ$ , including the reference materials which were prepared to give low CAs. In the case of sand, the most hydrophilic sample (no DCDMS addition) had a  $\theta_E^{CR}$  value close to zero, while for  $\theta^{CRM}$  it was around  $30^\circ$ . For GB 150-250  $\mu\text{m}$ ,  $\theta_E^{CR}$  was  $16.3^\circ$ , compared to  $\theta^{CRM} = 48.7^\circ$ . For the finer materials, silt and GB 40-70  $\mu\text{m}$ , the determined  $\theta_E^{CR}$  has a value of around  $30^\circ$ , while  $\theta^{CRM}$  determined  $52.9^\circ$  and  $40.1^\circ$ , respectively. These deviations between  $\theta_E^{CR}$  and  $\theta^{CRM}$  are consistent with the theoretical computations of Lavi et al. (2008). They solved the extended Lucas-Washburn differential equation numerically by simulating the experimental two-liquid method in glass capillaries by including viscosity, density and surface tension of different liquids in order to determine the effect of the dynamic CA and inertia on  $\theta^{CRM}$ . It was concluded that ignoring dynamic effects while analyzing the data of the two-liquid approach with the standard procedure may lead to significant deviations between dynamic and equilibrium angles. Qualitatively, these theoretical considerations can be related to the four materials we used by estimating the average pore radius ( $r$ ) according to the approximation described by Shahidzadeh et al. (2004):  $2r = d/3$  ( $d$ : average diameter of the particles). With this information, it was possible to roughly compare the experimental error in the estimation with  $\theta^{CRM}$  by using a plot previously published by Lavi et al. (2008) (Fig. 7). This plot determines for ideal circular

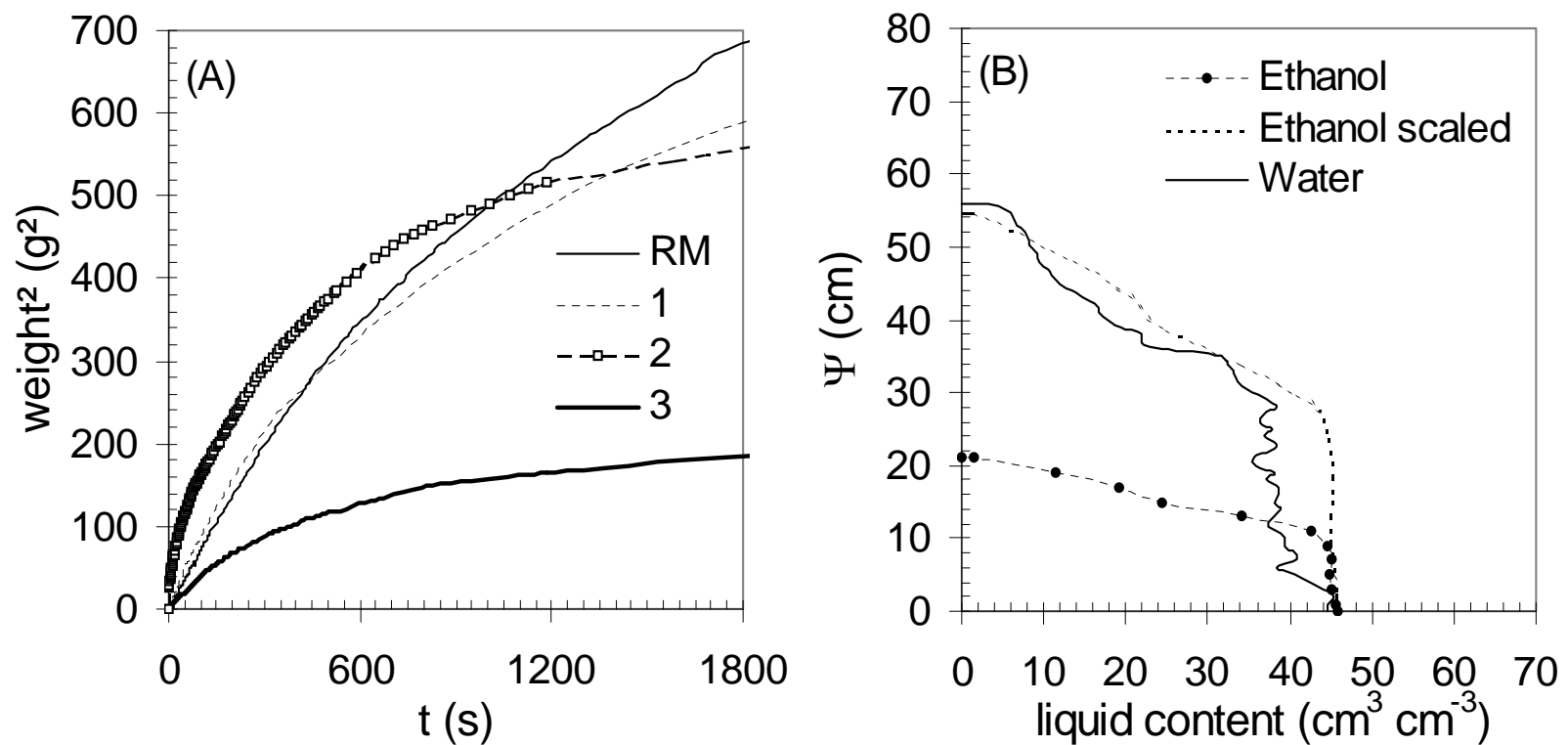


**Fig. 6** Wetting evaluation in segmented columns, examples for sand. A: Initial dynamic of wetting in homogeneous wettability samples. RM: Reference material, 1: Sample =  $2.5 \cdot 10^{-5}$  mL g<sup>-1</sup> DCDMS, 2: Sample =  $5.5 \cdot 10^{-5}$  mL g<sup>-1</sup> DCDMS, 3: Sample =  $1.0 \cdot 10^{-4}$  mL g<sup>-1</sup> DCDMS. B: Wetting retention curves of ethanol, ethanol-scaled curves and water (reference material). Note the different scales between graphics.

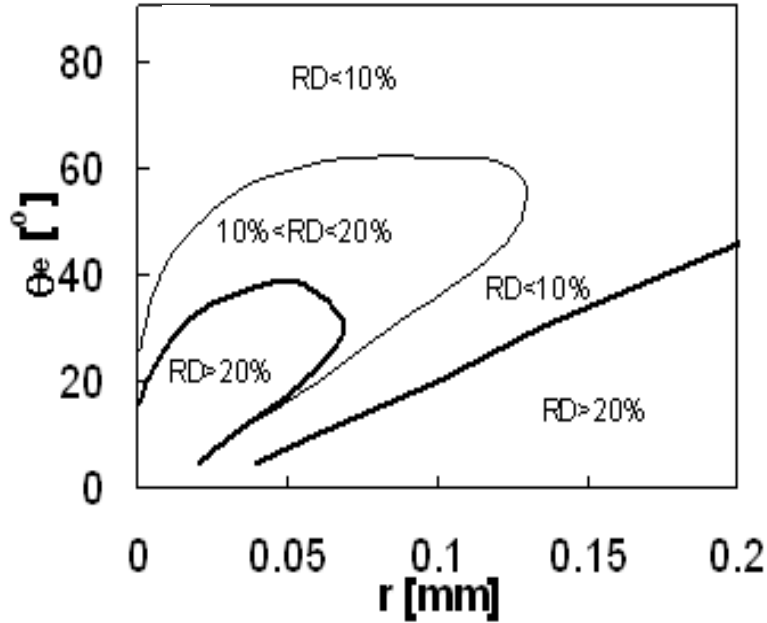


**Fig. 7** Relative deviation (RD, %) of the equilibrium contact angle ( $\theta_E$ ) and  $\theta^{\text{CRM}}$  calculated in glass capillaries. Calculations for a penetration length of 10 mm with water as test liquid ( $\sigma_L = 73 \text{ mN m}^{-1}$  and  $\rho = 1000 \text{ kg m}^{-3}$ ) (source: Lavi et al., 2008).

capillaries the theoretical relative deviation (RD) between combinations of the known  $\theta_E$  and  $r$  with respect to the RD of the observed angle determined with the standard two-liquid method CRM ( $\theta^{\text{CRM}}$ ). For silt and GB 40-70  $\mu\text{m}$ , the RD between  $\theta^{\text{CRM}}$  and  $\theta_E$  are expected to be larger in the more hydrophobic domain ( $>60^\circ$ ;  $<10\%$  of error).

The RD between dynamic and equilibrium CA is theoretically expected to increase with lower hydrophobicity. At the same time, smaller relative deviations can be expected for the coarser materials (sand and GB 150-250  $\mu\text{m}$ ) for medium CA around  $44^\circ$  ( $<10\%$  of error). This behavior is principally found for all samples (Fig.8), no matter if the source for hydrophobicity is homogenous (HW samples) or heterogeneous (MW samples). However, in comparison to Lavi et al. (2008) are the SD values for real pore systems considerable larger, i.e. up to 80%. In agreement with the theoretical prediction are the deviations significantly increasing with decreasing equilibrium CA. Linear regression analysis gave for mixed wettability a correlation of  $R^2 = 0.80$  and slightly higher ( $R^2 = 0.86$ ) for homogeneous wettability, with almost similar regression parameters. Regarding the effect of the pore geometry on the CA, Czachor (2006) showed that curved capillaries, in this case a regular axisymmetrical pore shape with a

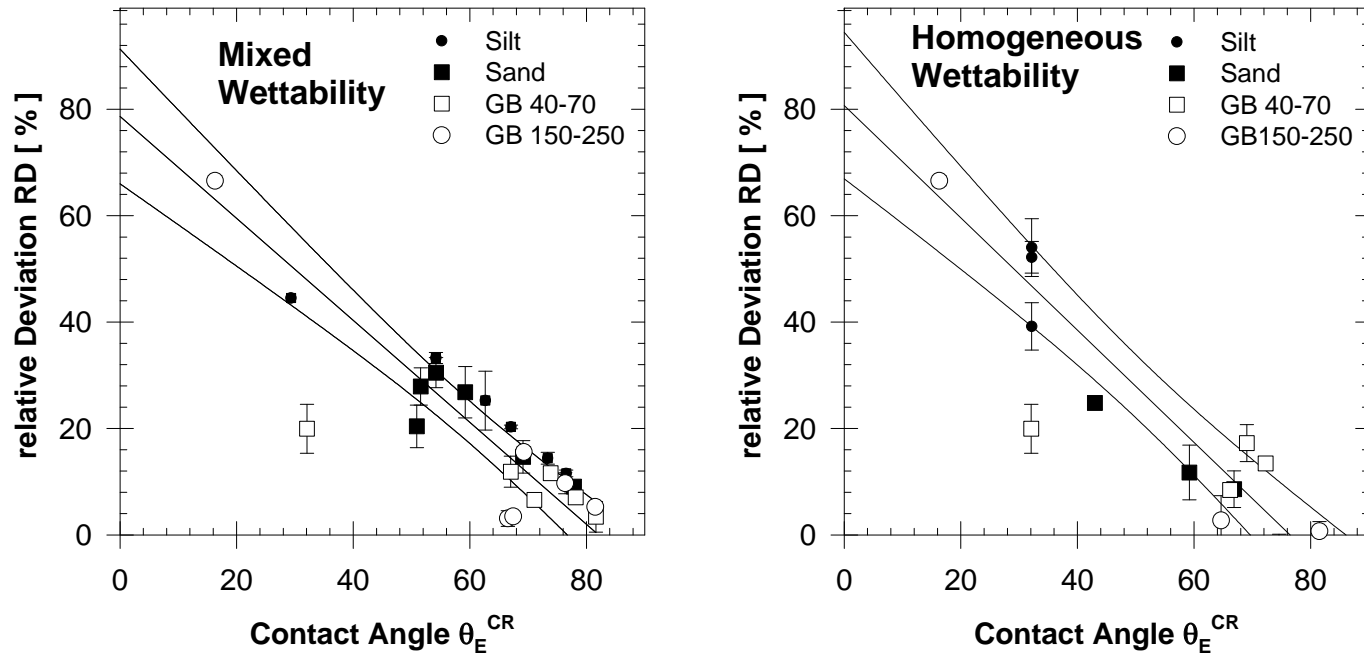


**Fig. 8** Measured relative deviation RD (%) of  $\theta^{\text{CRM}}$  with respect to  $\theta_E^{\text{CR}}$  for the material with mixed and homogeneous wettability. RD was calculated according to the expression  $100 * (\theta^{\text{CRM}} - \theta_E^{\text{CR}}) / \theta_E^{\text{CR}}$ .

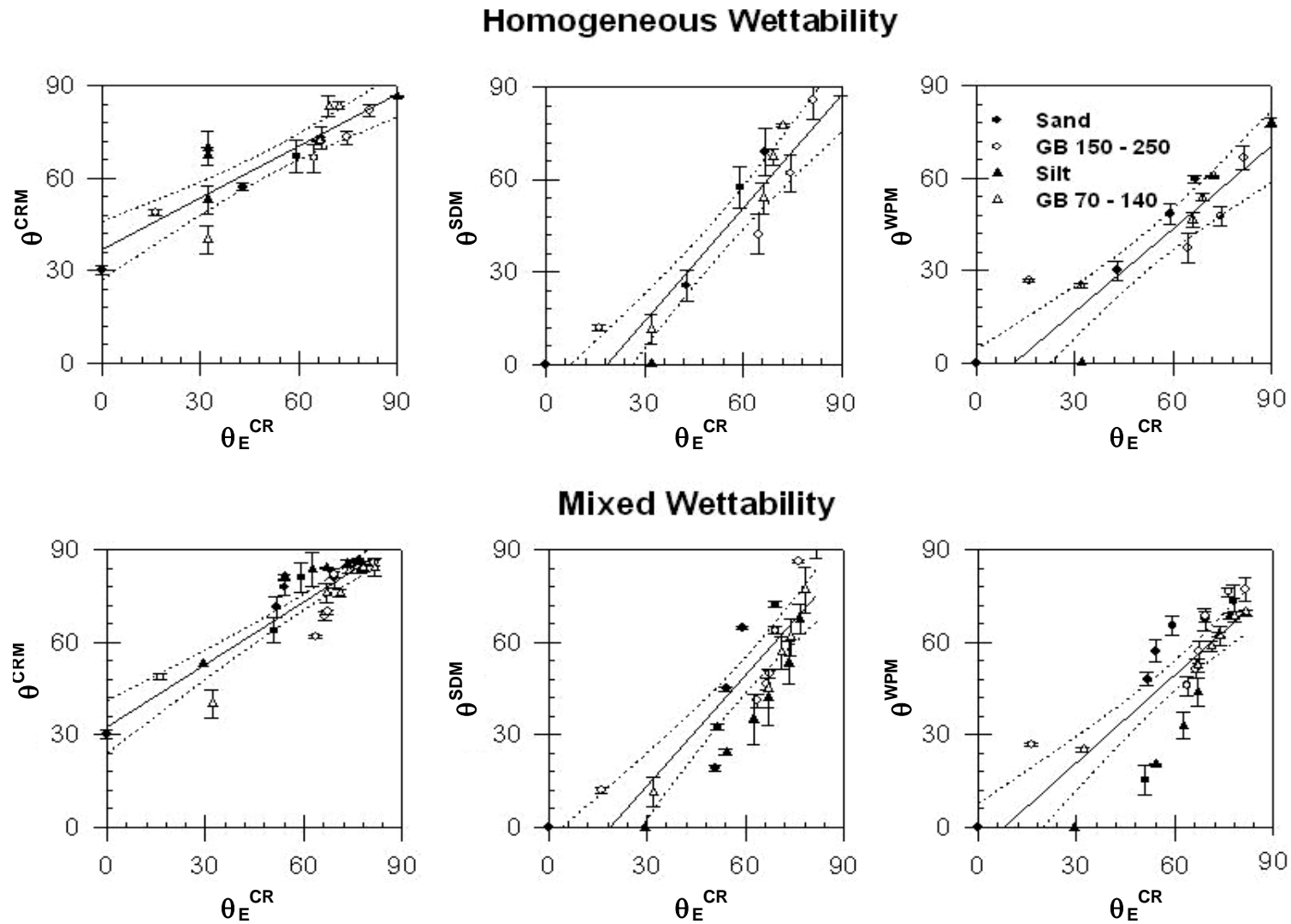
sinusoidal cross section, may increase a relatively small equilibrium CA of around 20° to apparent CAs by the factor of more than two. This effect may explain to some extent the larger  $\theta_E^{CR}$  compared with  $\theta^{SDM}$ , which were observed in particular for small CA, but does not explain the large deviation of  $\theta_E^{CR}$  with respect to  $\theta^{CRM}$ .

Fig. 9 finally summarizes the CAs of three of the experimental methods tested in this study ( $\theta^{CRM}$ ,  $\theta^{SDM}$  and  $\theta_E^{WPM}$ ) with respect to the results for the equilibrium capillary rise ( $\theta_E^{CR}$ ). This figure shows the data of all four porous materials and all wettability stages. Typically is the linear relation ( $R^2 > 0.95$ ), although the overestimation of the CA by using  $\theta^{CRM}$  is again consistent. These results suggest that it seems to be justified to predict the CA governing the equilibrium capillary rise in 3-d pore systems ( $\theta_E^{CR}$ ) with CA measurements based on quasi 2-d surfaces like the WPM and SDM technique does. It was confirmed that the CAs which are theoretically closer to the equilibrium CA ( $\theta_E^{WPM}$  and  $\theta^{SDM}$ ), were also closer to the observed  $\theta_E^{CR}$ . These diverging results are caused due to the different physical background of the methods. The SDM ( $\theta^{SDM}$ ) measures the wettability of a relatively stable small area, i.e. the liquid solid interface underneath the droplet, while  $\theta^{WPM}$  evaluates the average wettability along the perimeter of the sample of a forced moving 3-phase boundary. Summarizing,  $\theta^{SDM}$  and  $\theta^{WPM}$  estimate the CA of quasi 2-d surfaces, whereas  $\theta^{CRM}$  analyses the liquid penetration into 3-d pore systems.

## 2.6. Conclusions

We evaluated and compared different experimental methods and approaches to determine the contact angles ( $\theta^{CRM}$ ,  $\theta_A^{WPM}$ ,  $\theta_E^{WPM}$ ,  $\theta^{SDM}$ ) of porous materials (silt, sand and glass beads). We further compared these data with CAs derived from the evaluation of the capillarity ( $\theta_E^{CR}$ ) by analyzing the final height of capillary rise under gravity impact. The particles had different levels and types (homogeneous and non-homogeneous) of water repellency.

The CAs of  $\theta_A^{WPM}$  and  $\theta_E^{WPM}$  show a monotonic relation with respect to water repellency. The total range of CA is considerably larger compared with  $\theta^{CRM}$ . It was further observed that



**Fig. 9** Relation of the contact angles between the experimental methods CRM, SDM and WPM ( $\theta^{\text{CRM}}$ ,  $\theta^{\text{SDM}}$  and  $\theta^{\text{WPM}}$  respectively) and the equilibrium contact angles measured in long segmented columns ( $\theta_E^{\text{CR}}$ ) for all model materials with increasing water repellency.

$\theta_A^{\text{WPM}}$  and  $\theta_R^{\text{WPM}}$  values depend on immersion speed and depth, although the average  $\theta_E^{\text{WPM}}$  tends to remain stable for a wide range of velocities, supporting the hypothesis that the average between the advancing and receding CA may represent the apparent equilibrium contact angle  $\theta_E$ . In general,  $\theta^{\text{SDM}}$  agrees well with  $\theta_E^{\text{WPM}}$ , suggesting a Sessile Drop CA close to the equilibrium CA which also can be determined from final capillary rise heights. This has important consequences for the significance of the standard CRM. The conventional two-liquid CRM is a well established standard method for the determination of contact angles of powders in many fields of science. Our experiments show that CRM gives in particular for wettable soils considerable wrong results with respect of the equilibrium CA of the surface. This has important consequences for the determination of thermodynamic parameters derived from CA measurements, i.e. for the solid surface free energy by using the CRM technique.

The CA evaluation with long vertical columns ( $\theta_E^{\text{CR}}$ ) gives in our opinion significant information on the capillarity of a medium under the combined effect of gravity and water repellency. However, measurements are very time-consuming up to weeks.  $\theta_E^{\text{WPM}}$  and  $\theta^{\text{SDM}}$  values showed in general a better agreement with  $\theta_E^{\text{CR}}$ , making both methods suitable to predict CA-affected changes of the capillarity due to pore surface modifications. These results are valid for both HW and MW samples, indicating general results not only for model soils, as in this study, but also for natural soil systems.

Further reasons supporting differences between  $\theta^{\text{CRM}}$  and  $\theta_E^{\text{CR}}$  are probably related to the CA stability in time, especially for silt, since the time needed for the measurements is for the conventional  $\theta^{\text{CRM}}$  much shorter than for equilibrium capillary rise, but longer than for SDM and WPM. Differences in CA after different contact times are probable and caused through a time-dependency of the CA, i.e. mixing of the initial extend of hydrophobicity and its persistence. However, regarding the results of this study, time-dependency was not observed in the DCDMS treated materials, because for these materials we observed a good agreement with the liquid uptake level in the long segmented columns, as compared to  $\theta^{\text{SDM}}$  or  $\theta_E^{\text{WPM}}$ . Additional observations had shown that for DCDMS-vapor treated materials (100% hydrophobic particles) no water uptake into the columns, even after weeks, which indicates a stable persistence of the initial water repellency level. Hence, CAs obtained from SDM and WPM should also be

considered under the criterium of time-dependent wettability as very suitable for the characterization of the initial equilibrium CA of natural soils. All deviations between  $\theta^{\text{SDM}}$ ,  $\theta_{\text{E}}^{\text{WPM}}$  and  $\theta_{\text{E}}^{\text{CR}}$  observed for natural material should probably be attributed to an additional time component of soil wettability. This problem needs to be addressed in further investigations.

In general all soil materials can be investigated with the introduced methods, except very hydrophobic soils like peats or podzols with the CRM. The investigator should also be aware, that CRM gives, in particular for fine textured and well wettable materials like loess with a low carbon content, considerably larger CA due to dynamic effects, which reflects not only physical surface properties but merely a combination of pore geometry effects and wettability. On the other hand, physical interpretation of the measured angles should be related to the specific problem, i.e. the determination of apparent equilibrium contact angles. Further objectives could be the determination describing the complete wetting/dewetting behavior of water repellent porous media including desorption, i.e. by relating dynamic Wilhelmy Plate contact angles to dynamic capillary pressure – saturation relations. For natural soils, also the problem of time-dependent CA and moisture-dependent wettability is still an open question which needs to be considered in the future.



## Chapter 3

# Prediction of contact angles from solid and liquid surface free energies of model porous materials

### 3.1. Introduction

Wettability of soils affects properties like water infiltration and moisture distribution within the soil profile (Dekker et al., 2000; Doerr et al., 2000). It is known that the wettability is related to the balance of surface free energies or surface tensions ( $\sigma$ ,  $\text{mN m}^{-1}$ ) in a solid-liquid-gas system (Grundke, 2001). This balance of forces, applied to an ideal system in thermodynamic equilibrium, was firstly defined by Thomas Young (1805).

The surface free energy components of the Young equation normally are difficult to measure directly (Bachmann et al., 2006). Therefore, contact angles (CA) are used as indicators of the thermodynamic state of the system (Marmur, 2006). Different methods to assess CAs have been developed, with different levels of accuracy with respect to the intrinsic or Young angle. Empirical approaches to estimate the components of Young equation, mainly derived from the works of Zisman (1964) and Girifalco and Good (1957), are normally used in research related to wettability. The first author found a relation between the cosine of the measured CA ( $\cos\theta$ ) and the corresponding surface energies of a series of homologous test liquids. The later authors suggested an equation for the assessment of  $\sigma_{\text{SL}}$  as a function of  $\sigma_{\text{SV}}$  and  $\sigma_{\text{LV}}$ , also defining the so-called Girifalco interaction parameter ( $\Phi$ ), which describes in theory the molecular interactions of two immiscible phases in contact.

The present research compares two different experimental methods to determine the CA and the surface free energy: the Capillary Rise Method (CRM) (Washburn, 1921; Siebold et al., 2000) and the Wilhelmy Plate Method (WPM) (Wilhelmy, 1863; Bachmann et al., 2003). CAs were measured for a set of model materials (silt, sand and non-porous GB) with different levels of

water repellency. The components of the Young equation were calculated for each sample and method (CRM and WPM) by following the concept of critical surface tension ( $\sigma_C$ ) firstly described by Zisman (1964). The surface free energy components are then used to estimate the Girifalco interaction parameter  $\Phi$  (Girifalco and Good, 1957). Finally, both  $\sigma$  and  $\Phi$  data are used to re-calculate the CA by applying an equation of state (Spelt and Neumann, 1992; Bachmann et al. (2006). Therefore, the objective of the present research is to evaluate and compare the results of both experimental methods independently to proof consistency of theory (Zisman plots and equation of state approach) and the corresponding CA results. The results obtained with both methods are compared in relation to the Zisman approach (i.e.  $\sigma_C$  value versus water repellency level indicated by the mixing ratio of wettable and non-wettable grains) and secondly by comparing the relation between the measured and predicted CA by using the equation of state with its previously adjusted regression parameters  $\alpha$  and  $\beta$ . This analysis also should prove, if  $\alpha$  and  $\beta$  are soil specific or “global” variables, which might possibly reduce the number of parameters in the Young equation from four to three variables. Overall, the objective is to validate on one hand the usefulness of both measuring methods and on the other hand the usefulness of the concept of the equation of state for applications in soil science.

### 3.2. Theory

The Young equation (Young, 1805) describes the balance of forces acting at the three-phase boundary of a drop on a solid surface. This relation has the form

$$\sigma_{LV} \cos \theta_E = \sigma_{SV} - \sigma_{SL} \quad (8)$$

where ( $\theta_E$ ) is the Young or intrinsic contact angle,  $\sigma$  is the surface energy or surface tension and the indices S, V and L correspond to solid, vapor and liquid, respectively. This relation assumes ideal conditions, such as a drop of pure water placed on a smooth, chemically non-reactive, homogeneous and perfectly clean surface. However, the values of  $\sigma_{SV}$  and  $\sigma_{SL}$  are in practice almost impossible to assess, hence the experimental verification of this relation is very difficult (Bachmann et al, 2006). The linear relation found by Zisman (1964) for a series of homologous liquids normally is used to assess the value of  $\sigma_{SV}$ . This approach was proved to be also linear

for a series of aqueous ethanol solutions applied to water repellent soils (Arye et al., 2006; Bachmann et al., 2003), with the form

$$\cos \theta = b_0 + b_1 \sigma_{LV} \quad (9)$$

where  $b_0$  and  $b_1$  are fitting parameters. The graphical presentation of Eq. (9), known as Zisman plot (Zisman, 1964), allows to find the value of  $\sigma_{LV}$  where CA is zero ( $\cos\theta = 1$ ), which is assumed to correspond to  $\sigma_{SV}$ . In this way, the so-called critical surface tension ( $\sigma_C$ ) is the point where  $\sigma_{LV} = \sigma_{SV}$ , which allows to estimate  $\sigma_{SL}$  by replacing the corresponding values in Eq. (8).

An alternative approach for the assessment of  $\sigma_{SL}$  and the others Young equation components was suggested by Girifalco and Good (1957). They proposed the expression

$$\sigma_{SL} = \sigma_{SV} + \sigma_{LV} - 2\Phi \sqrt{\sigma_{SV} \sigma_{LV}} \quad (10)$$

where  $\Phi$  is a dimensionless parameter quantifying the molecular forces in the different phases of the test system (solid-liquid-gas).  $\Phi$  usually is assumed to be as near to unity, which in theory reflects that the intermolecular forces are of the same nature (Schneider et al., 1997). However, recent research carried out on soil samples with increasing water repellency, shown that  $\Phi$  significantly decreases down to a value around of 0.6 (Arye et al., 2006; Bachmann et al., 2006). The re-arrangement of Eq. (10) in order to calculate  $\Phi$  leads to

$$\Phi = \frac{\sigma_{SV} + \sigma_{LV} - \sigma_{SL}}{2\sqrt{\sigma_{SV} \sigma_{LV}}} \quad (11)$$

A research carried out by Spelt (1992) found that  $\Phi$  and  $\sigma_{SL}$  can be related with the expression

$$\Phi = \beta - \alpha \sigma_{SL} \quad (12)$$

where  $\alpha$  and  $\beta$  are fitting parameters. Eq. (12) was validated by Arye et al. (2006) in experiments carried out with hydrophobized soils. By combining Eq. (8), (9) and (12), Bachmann et al. (2006) derived an equation of state (ES), which in theory allows to predict the CA of soil with known  $\sigma_{SV}$  for any  $\sigma_{LV}$ . This equation has the form

$$\cos \theta = \frac{(2\alpha\sigma_{SV} - 2\beta) \cdot \sqrt{\sigma_{SV}\sigma_{LV}} + \sigma_{LV}}{2\sigma_{LV} \cdot \alpha \sqrt{\sigma_{SV}\sigma_{LV}} - \sigma_{LV}} \quad (13)$$

The present research focuses on comparing the measured and the corresponding predicted CAs derived with CRM and WPM by applying the Zisman's critical surface tension concept.

### 3.3. Methodology

#### 3.3.1. Materials and treatments

Four model materials were evaluated: sand, silt and solid, non-porous glass beads (GB). A description is given in Table 1. The pre-treatment of the sample as also the preparation of highly hydrophobic materials followed the guidelines given in Chapter 2 (2.3.1). A set of samples with increasing levels of water repellency were obtained by mixing hydrophilic and hydrophobic materials (0 and 100% hydrophobic particles, respectively) in different ratios. Mixtures with 10-25-50-75 and 90% of hydrophobic particles were prepared (total weight of each sample = 100 g). In this way, for each model material seven samples with increasing water repellency were prepared.

#### 3.3.2. Contact angle measurement

Contact angles (CA) were evaluated with the Capillary Rise Method (CRM) and the Wilhelmy Plate Method (WPM), by following the guidelines and set-up already mentioned in Chapter 2 (2.2, Methods). Three approaches are then compared: CRM ( $\theta^{CRM}$ ), WPM-ACA ( $\theta_A^{WPM}$ , considering the advancing CA) and WPM-ECA ( $\theta_E^{WPM}$ , considering the average between the advancing and receding CA).

### 3.3.3. Assessment of the critical surface tension

For each sample and method, the solid surface energy ( $\sigma_{SV}$ ) was estimated according to the critical surface tension concept ( $\sigma_C$ ) (Zisman, 1964; Watson and Letey, 1970) (Eq. 10). CAs were measured for deionized water and a series of aqueous-ethanol solutions (0 - 96% ethanol). For each liquid,  $\sigma_{LV}$  was measured with WPM by using a platinum-iridium rectangular plate. The data were plotted as conventional Zisman plots (i.e.  $\cos\theta$   $f(\sigma_{LV})$ ) and the corresponding  $\sigma_C$  determined. As in highly hydrophobic samples the relation  $\cos\theta$  versus  $\sigma_{LV}$  becomes curvilinear, the fit of Eq. (9) was made considering only the linear section of data.

### 3.3.4. Application of the equation of state

The prediction of CA by applying the equation of state was carried out according to the steps already described in the theory section: for each sample and method,  $\sigma_{SL}$  was estimated by replacing in Eq. (8) the values of  $\sigma_C$  previously obtained from Zisman plots, i.e. where  $\cos\theta = 1$  and  $\sigma_{LV} = \sigma_{SV}$ .

With the three components of the Young equation estimated ( $\sigma_{SV}$ ,  $\sigma_{SL}$  and  $\sigma_{LV}$ ), the value of  $\Phi$  for each sample and method was assessed by applying Eq. (11). The  $\alpha$  and  $\beta$  parameters were then determined for each sample by fitting Eq. (12) to the  $\Phi$  and  $\sigma_{SL}$  data of the seven samples (0-10-25-50-75-90 and 100% hydrophobic particles).

Finally, the different parameters ( $\sigma_{SV}$ ,  $\sigma_{SL}$ ,  $\sigma_{LV}$ ,  $\Phi$ ,  $\alpha$  and  $\beta$ ) were used to re-calculate the CA for each sample by applying Eq. (13). In order to have an independent verification of the ES, the average values of  $\alpha$  and  $\beta$  determined by Bachmann et al. (2006) were used ( $\alpha$ : 0.0126;  $\beta$ : 0.9767), which were calculated for a series of soils with different texture and level of water repellency by using  $\theta_A^{WPM}$ . The experimentally measured and predicted CAs were then compared.

### 3.4. Results and discussion

#### 3.4.1. Zisman plots and assessment of the critical surface tension

Fig. 10 shows examples of Zisman plots comparing the results of the three different experimental approaches for two samples of sand: 50% hydrophobic particles ( $\theta_A^{\text{WPM}} = 105.6^\circ$ ;  $\theta_E^{\text{WPM}} = 68.6^\circ$ ;  $\theta^{\text{CRM}} > 90^\circ$ ) and 100% hydrophobic particles ( $\theta_A^{\text{WPM}} = 129.4^\circ$ ;  $\theta_E^{\text{WPM}} = 83.6^\circ$ ;  $\theta^{\text{CRM}} > 90^\circ$ ). In general, it was observed that the standard deviation (SD) tends to decrease with increasing amount of hydrophobic particles. This better reproducibility of the CA can be explained by the sampling, as the probability in evaluating subdomains on the sample with a similar number of hydrophobic particles is significantly higher with increasing water repellency (Ustohal et al., 1998). For the same sample, both WPM approaches ( $\theta_A^{\text{WPM}}$  and  $\theta_E^{\text{WPM}}$ ) had smaller values of SD compared with CRM, showing that a better reproducibility is obtained for 2-d systems (i.e. WPM) than for 3-d (i. e. CRM).

As already mentioned, the linear relation between  $\sigma_{LV}$  and  $\cos\theta$  defined by Eq. (9) is in general observed for values of  $\sigma_{LV} < 40 \text{ mN m}^{-1}$ . For increasing hydrophobicity, the relation between both variables tends to be curvilinear when all points of the plot are considered (Fig 10, B1). These results are in good agreement with the findings of Bachmann et al. (2000), who carried out measurements with the Sessile Drop Method (SDM) and with Arye et al (2006), who applied the Zisman approach to natural water-repellent soils. A sigmoidal shape is often observed in WPM plots, especially for those materials with the lowest specific surface area (e.g. non-porous GB), as these materials reach significant hydrophobicity already with very low percentages of hydrophobic particles (e. g. up to  $\theta_A^{\text{WPM}} = 117^\circ$  for GB 150-250  $\mu\text{m}$  with 10% hydrophobic particles). It can be assumed that CRM will show a similar curvilinear tendency with increasing hydrophobicity, although it will be probably masked by its narrower range (in theory 0-90°) compared to WPM (in theory 0-180°) (Bachmann et al., 2003). It is also interesting to note that even when both WPM approaches ( $\theta_A^{\text{WPM}}$  and  $\theta_E^{\text{WPM}}$ ) measure different CAs for the same material, Zisman's surface tension concept leads to almost the same value of  $\sigma_C$  as can be seen from Fig. 10 (A1 and B1), with also similar values of  $R^2$ .

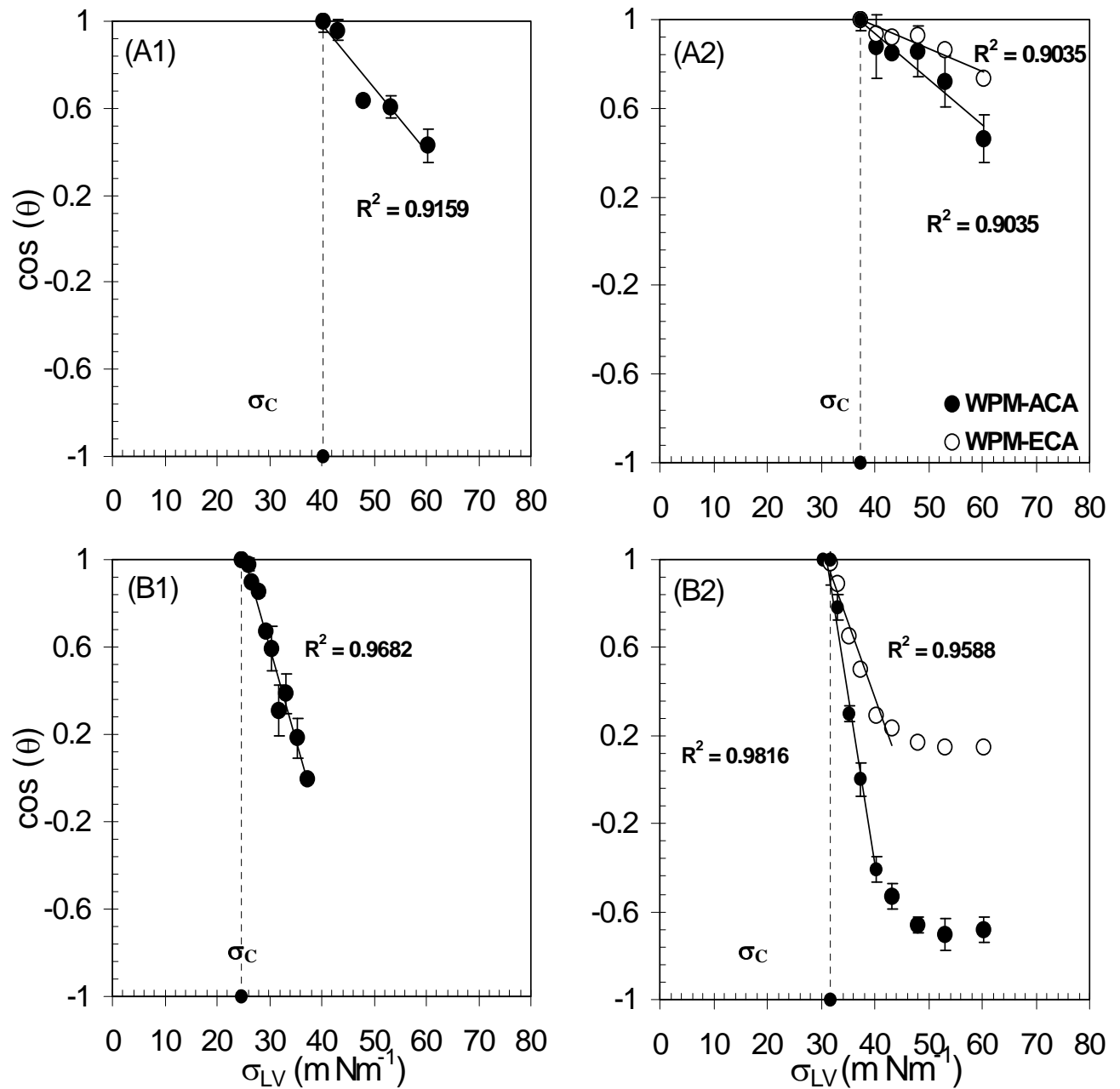


Fig. 10 Examples of Zisman plots and linear regressions to estimate  $\sigma_C$  in two samples of sand. A: 50% hydrophobic particles ( $2.5 \cdot 10^{-4} \text{ mL g}^{-1}$  DCDMS). B: 100% hydrophobic particles ( $5.0 \cdot 10^{-4} \text{ mL g}^{-1}$  DCDMS). 1: CRM data, 2: WPM data. The estimated  $\sigma_C$  for each plot is also indicated.

Fig. 11 compares  $\sigma_C$  calculated with the three experimental methods as a function of the water repellency (% of hydrophobic particles). As expected, a decrease of  $\sigma_C$  with higher amount of hydrophobic particles is observed in all cases, although with irregularities observed in CRM for some highly hydrophobic samples, e.g. sand with >75% hydrophobic particles (Fig. 11A). These results demonstrate the suitability of both experimental methods (CRM and WPM) when the critical surface tension approach is applied, although differences in the calculated  $\sigma_C$  for the same sample can be expected depending on the experimental approach. In this line,  $\sigma_C$  is usually lower in CRM than in WPM. Arye et al. (2006) explained the differences between both methods as in WPM some liquid uptake due to the rugosity of the particles can happen, which will reduce the estimated CA of the corresponding sample. In the present research, the most significant  $\sigma_C$  decrease was observed in the transition from reference (0% hydrophobic particles) to 20% hydrophobic particles in silt and sand (e.g. a decrease from 64.6 to 36.9 mN m<sup>-1</sup> for sand in WPM measurements), and from 0% to 10% hydrophobic particles for GB (e.g. a decrease from 44.9 to 28.6 mN m<sup>-1</sup> for GB 150-250  $\mu$ m with WPM). This kind of two-slopes behavior can be explained with the results observed by Steenhuis et al. (2005), who assessed water repellency in terms of the percolation theory. They concluded that even very small percentages of hydrophobic particles can induce significant water repellency in soils otherwise hydrophilic, by blocking the paths where water drains. This explanation can directly be applied to CRM experiments, due to the importance of the geometrical arrangement of particles in the estimation of CA (as already discussed in Chapter 2). This is especially relevant for those materials with greater pore radius and lower specific surface area (e.g. GB), where one single water-repellent particle can have a bigger relative effect than in a more complex pore-system constituted by small-radius particles (e.g. silt) (Goebel, 2007). At the same time, as WPM is not based on the pore-system configuration and apparently has a wider range and better resolution compared to CRM, it is possible to expect a more gradual decrease of  $\sigma_C$  with increasing water repellency (i.e. Fig. 11C). Finally, with WPM, with higher amounts of hydrophobic particles (10-80%)  $\sigma_C$  decreases to 31-38 mN m<sup>-1</sup> for silt and sand, and 25-28 mN m<sup>-1</sup> for both GB. Significantly lower values are observed with CRM, in general from 20 to 30 mN m<sup>-1</sup> for silt and sand, and around 20 mN m<sup>-1</sup> for both GB materials.



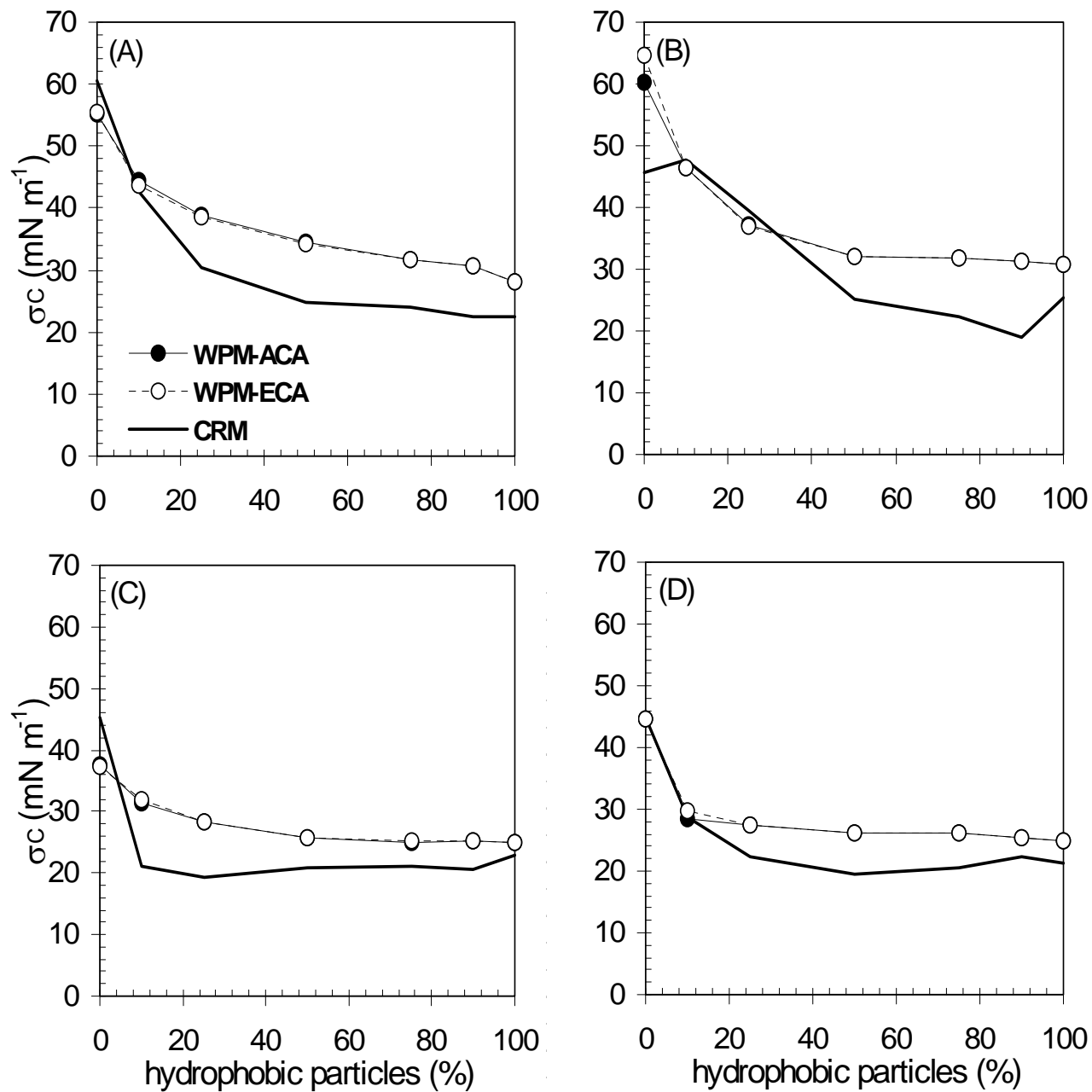


Fig. 11 Critical surface tension ( $\sigma_C$ ) as a function of the water repellency (% hydrophobic particles). A: Silt. B: Sand. C: GB 40-70  $\mu\text{m}$ . D: GB 150-250  $\mu\text{m}$  (100% hydrophobic particles are equivalent to  $5.0 \cdot 10^{-4} \text{ mL g}^{-1}$  DCDMS in sand and GB, and to  $2.0 \cdot 10^{-3} \text{ mL g}^{-1}$  DCDMS in silt).

### 3.4.2. Equation of state approach

Spelt et al. (1992) defines the ES as a relation with the form  $\sigma_{SL} = f(\sigma_{SV}, \sigma_{LV})$ . In theory, the ES allows to estimate  $\sigma_{SV}$  and  $\sigma_{SL}$  by using a liquid of known  $\sigma_{LV}$  and measuring the corresponding CA on the solid. According to Bachmann et al. (2006), the ES approach, despite positive findings, has normally been criticized regarding its suitability to estimate the surface free energy components of the Young equation, given its weak theoretical background. In this line, the results of the ES derived by Bachmann et al. (2006) (Eq. 13) should be considered as approximations in testing the experimental approaches.

#### 3.4.2.1. Estimation of the parameters $\Phi$ , $\alpha$ and $\beta$

Fig. 12 shows the  $\Phi$  parameter (calculated by fitting Eq. (12) to the Young surface free energy components) for sand, as a function of the water repellency (% hydrophobic particles). Table 2 shows the values of the regression parameters  $\alpha$  and  $\beta$ , determined from the relation  $\Phi = f \sigma_{SL}$  (Eq. 12), for the different model materials and methods. Fig. 13 shows an example for sand of the relation between  $\alpha$  and  $\beta$  as a function of  $\sigma_{SV}$  for the three experimental methods.

It was observed that  $\Phi$  decreases directly with higher water repellency (Fig. 12), although for CRM the decrease showed some irregularities in the more hydrophobic samples (i.e. >80% hydrophobic particles). This is possibly related, as previously observed e.g. for sand (Fig. 11A), to a not completely accurate estimation of  $\sigma_C$  in Zisman plots, given the relatively low resolution capability and range of CA estimation of CRM compared to WPM. Considering all the materials and samples,  $\Phi$  was located around the unity (range 1.0-1.2) mainly in the more wettable domain (i.e. <20% hydrophobic particles), decreasing to 0.8-0.6 for CRM and WPM-ECA, and to 0.3-0.2 for WPM-ACA. These results are in good agreement with Arye et al. (2006), who observed that in natural soils the assumption  $\Phi = 1$  is not correct for significant water repellency, where  $\Phi$  decreases to 0.5-0.6. As observed in Fig. 12, the estimation of  $\Phi$  based in WPM-ACA data usually leads to lower values (range 0.2-0.3) in comparison to CRM and WPM-ECA (range 0.6 - 0.8), especially in the most hydrophobic samples (>50% hydrophobic particles).

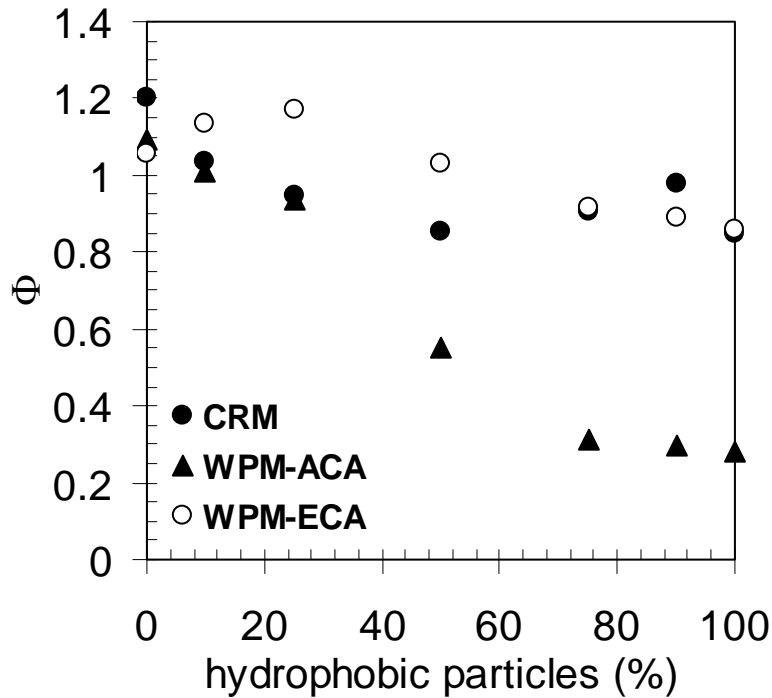


**Fig. 12** Girifalco's interaction parameter ( $\Phi$ ) as a function of the water repellency (% of hydrophobic particles) for sand.

As previously described by Spelt et al. (1992), a direct relation between  $\Phi$  and  $\sigma_{SL}$  (Eq. 12) was calculated in all cases ( $R^2 > 0.80$  for CRM,  $> 0.98$  for WPM-ACA and  $> 0.94$  for WPM-ECA) (Table 2). In general, when all data are considered,  $\alpha$  (the slope of Eq. 12) shows a bigger scattering than  $\beta$  (the intercept of Eq. 12) (Fig. 13).

Regarding the samples with  $< 25\%$  hydrophobic particles (silt and sand), the calculated  $\alpha$  and  $\beta$  are in agreement with the findings of Spelt et al. (1992). These authors concluded that for different ideal polymeric surfaces (e.g. MMM methacrylic polymer S with fluorinated side chain), the best fit of Eq. (12) occurs when  $\alpha = 0.0075$  and  $\beta = 1.000$ . Regarding both GBs, although  $\beta$  tends to remain near the unity,  $\alpha$  shows relatively higher values compared to the soil materials (silt and sand). These results can indicate a certain level of dependence on texture-related properties, although the relatively low number of samples ( $n = 28$ ) here evaluated does not allow to establish definitive conclusions.

**Table 2:** Regression parameters  $\alpha$  and  $\beta$  for each sample and experimental method, calculated by fitting the data of the Girifalco's interaction parameter ( $\Phi$ ) and solid-liquid surface free energy ( $\sigma_{SL}$ ) to the equation  $\Phi = \beta - \alpha\sigma_{SL}$ .

Material	Hydrophobic particles (%)	CRM		WPM-ACA		WPM-ECA	
		$\alpha$	$\beta$	$\alpha$	$\beta$	$\alpha$	$\beta$
Silt	0	0.0082	1.0032	0.0082	1.0030	0.0071	0.9999
	10	0.0108	0.9988	0.0105	1.0001	0.0101	1.0099
	25	0.0064	1.0118	0.0131	0.9991	0.0220	1.0207
	50	0.0092	0.9647	0.0060	0.9868	0.0146	0.9968
	75	0.0104	0.9522	0.0094	0.9870	0.0179	0.9974
	90	0.0106	0.9303	0.0096	0.9709	0.0175	0.9899
	100	0.0109	0.9280	0.0093	0.9696	0.0187	0.9875
	Average	0.0095	0.9699	0.0094	0.9881	0.0154	1.0030
	SD	0.0017	0.0350	0.0022	0.0137	0.0052	0.0116
Sand	0	0.0079	1.0001	0.0076	0.9991	0.0099	1.0039
	10	0.0082	1.0085	0.0106	1.0008	0.0102	1.0057
	25	0.0071	1.0099	0.0142	0.9983	0.0084	1.0032
	50	0.0092	0.9718	0.0045	1.0064	0.0089	1.0002
	75	0.0101	0.9440	0.0095	0.9883	0.0141	0.9934
	90	0.0101	0.9262	0.0094	0.9785	0.0161	0.9973
	100	0.0108	0.9454	0.0101	0.9843	0.0158	0.9934
	Average	0.0091	0.9723	0.0094	0.9937	0.0119	0.9996
	SD	0.0014	0.0345	0.0030	0.0101	0.0033	0.0050
GB 40-70 $\mu\text{m}$	0	0.0088	0.0998	0.0123	1.0027	0.0115	1.0048
	10	0.0086	0.9671	0.0201	1.0228	0.0078	0.9893
	25	0.0102	0.9443	0.0087	0.9953	0.0105	0.9703
	50	0.0155	0.9284	0.0110	0.9908	0.0163	0.9868
	75	0.0117	0.9123	0.0108	0.9755	0.0183	0.9860
	90	0.0116	0.8954	0.0107	0.9686	0.0183	0.9860
	100	0.0116	0.8937	0.0113	0.9756	0.0185	0.9907
	Average	0.0111	0.8059	0.0121	0.9902	0.0145	0.9877
	SD	0.0023	0.3124	0.0037	0.0189	0.0044	0.0101
GB 150-250 $\mu\text{m}$	0	0.0108	1.0003	0.0102	1.0018	0.0098	1.0030
	10	0.0099	0.9494	0.0098	1.0046	0.0070	0.9744
	25	0.0107	0.9444	0.0094	0.9940	0.0172	0.9991
	50	0.0105	0.8860	0.0089	0.9617	0.0182	0.9896
	75	0.0111	0.9080	0.0088	0.9459	0.0188	0.9898
	90	0.0111	0.9072	0.0090	0.9459	0.0188	0.9896
	100	0.0114	0.9155	0.0093	0.9518	0.0193	0.9830
	Average	0.0108	0.9301	0.0093	0.9722	0.0156	0.9898
	SD	0.0005	0.0380	0.0005	0.0268	0.0050	0.0095

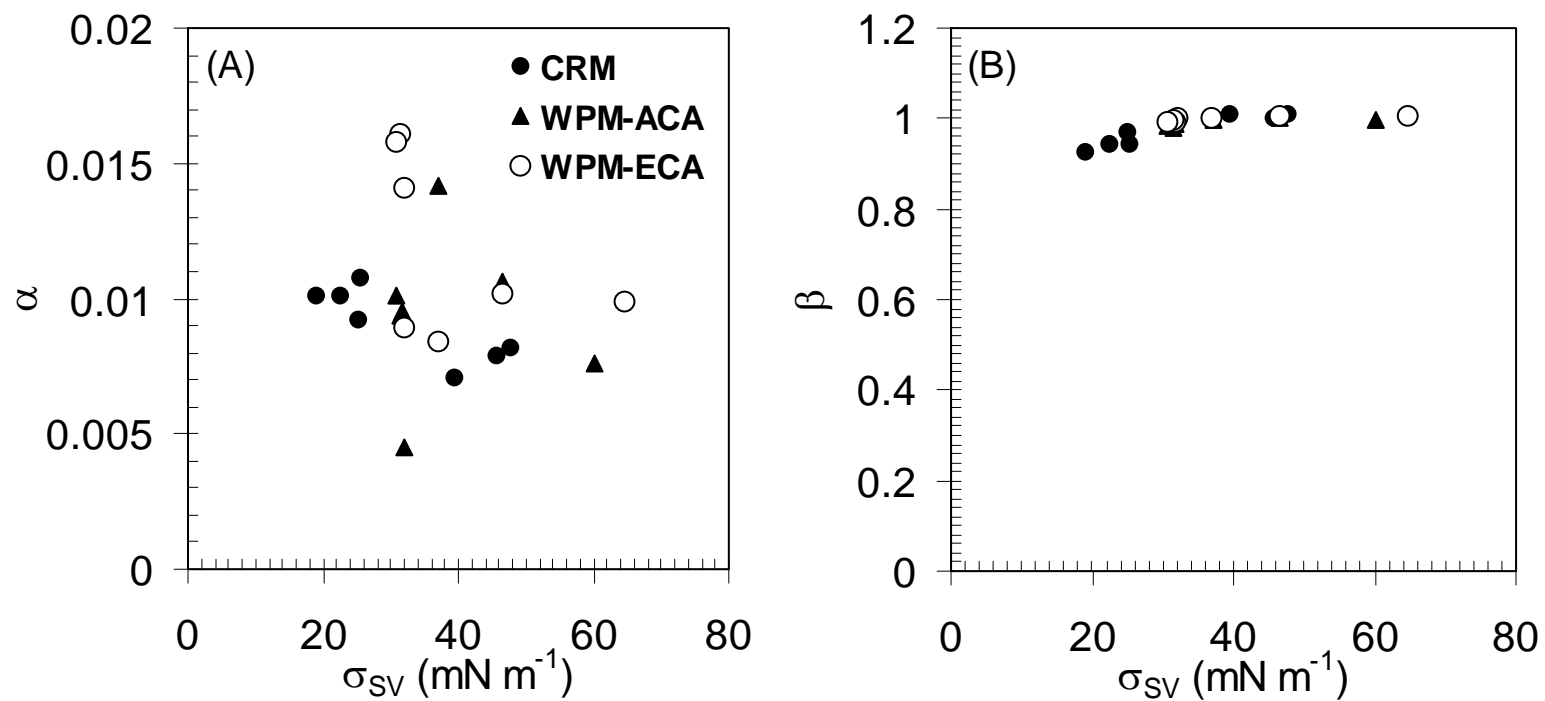


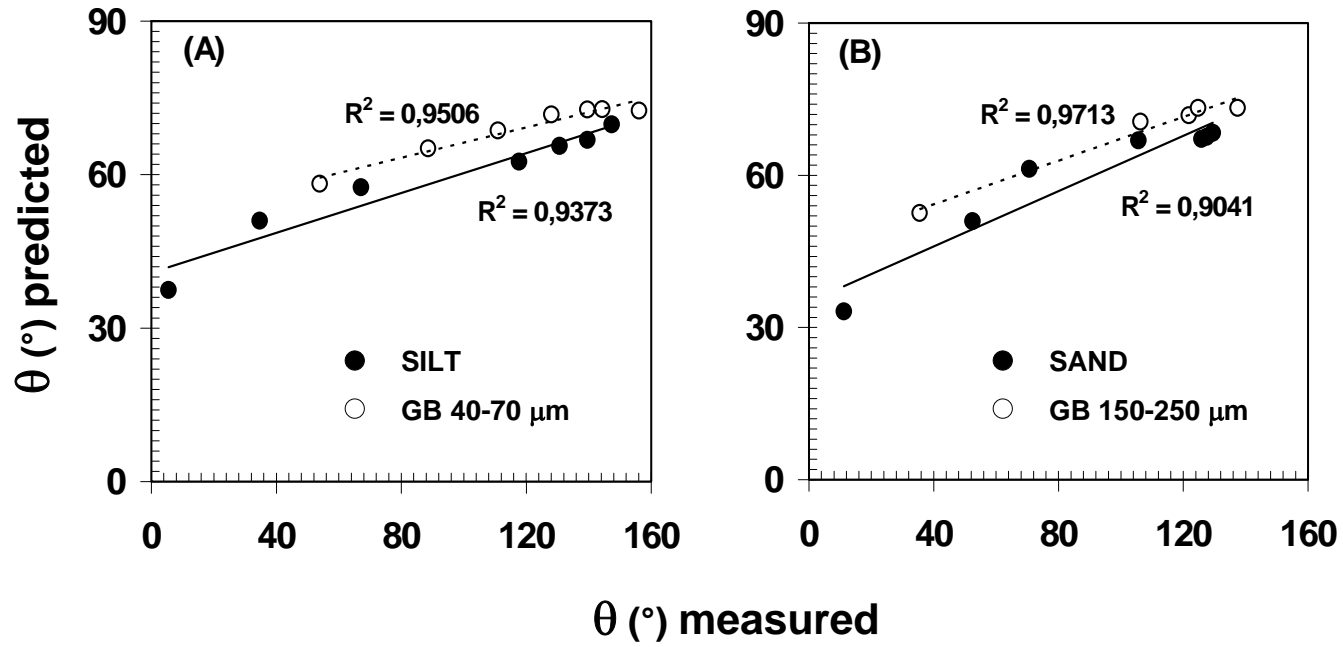
**Fig. 13** Regression parameters  $\alpha$  and  $\beta$  as a function of the solid-vapor surface free energy ( $\sigma_{SV}$ ) for the three different experimental methods. Examples for sand.

As seen in Table 2 and Fig. 13, while  $\alpha$  does not present a clear tendency with increasing water repellency (e.g. lower  $\sigma_{SV}$ ),  $\beta$  decreases slightly. Considering the average of the complete set of materials and samples, no significant differences between the different experimental methods were observed:  $\alpha$  results  $\sim 0.0101$  in CRM and WPM-ACA, and  $\sim 0.0143$  in WPM-ECA.  $\beta$  results = 0.9200, 0.9860 and 0.9943 in CRM, WPM-ACA and WPM-ECA respectively. These values are in line with the results of Bachmann et al. (2006) (i.e.  $\alpha = 0.126$  and  $\beta = 0.9767$ ), who applied WPM-ACA. These results show that  $\alpha$  and especially  $\beta$  can be considered as constants, as previously suggested by Spelt et al. (1992) for solid systems, independent of the experimental method used to calculate the  $\sigma$  components of the Young equation.

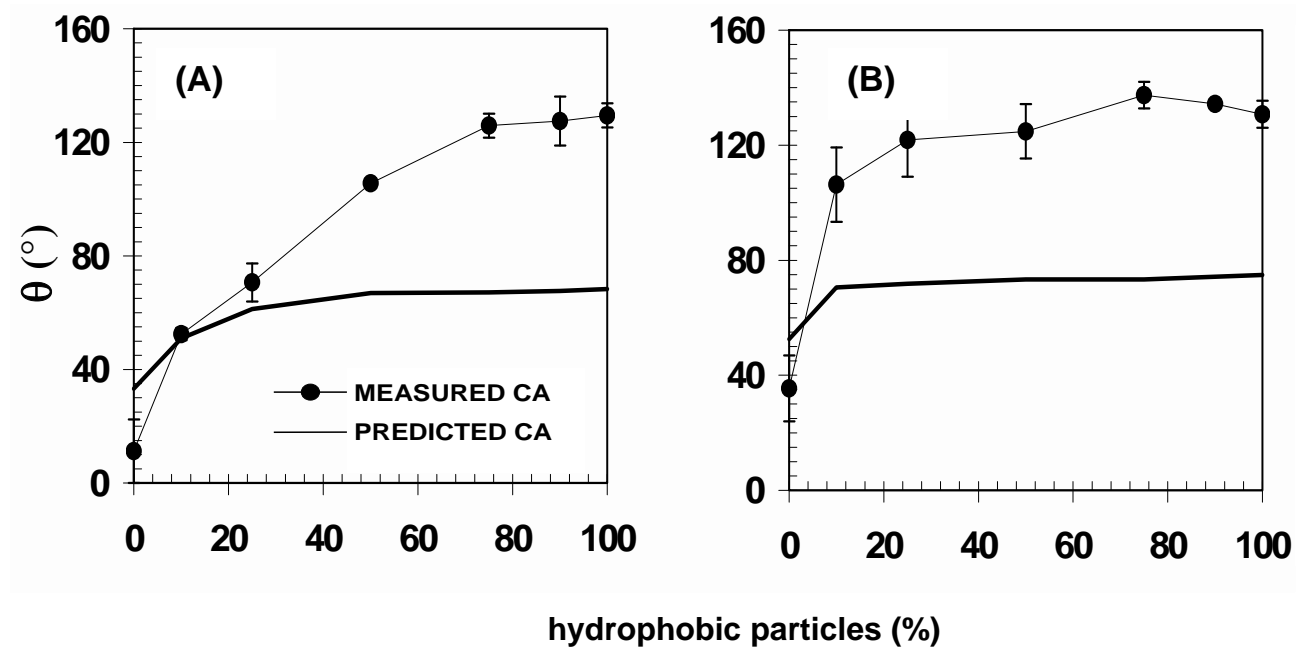
#### 3.4.2.2. Prediction of contact angles and comparison of methods

Fig. 14 shows the results of linear regression analysis between the directly measured CA (WPM-ACA) and predicted CA (ES approach) for the different model materials. As observed, in all cases  $R^2$  showed values  $>0.9$ , which is assumed as an indicator of a good agreement between measured and predicted CAs.

Fig. 15 compares the experimentally measured and the predicted CAs (ES) as a function of the water repellency (% of hydrophobic particles) for sand and GB 150-250  $\mu\text{m}$ . As observed, the predicted CAs (ES approach) showed a significant narrower range compared to the directly measured CAs. As example, the predicted CAs ranged between  $30^\circ$  and  $70^\circ$  for sand and  $44^\circ$  and  $72^\circ$  for GB 150-250  $\mu\text{m}$ . In general, it was observed that the maximum predicted CA was reached with a relatively low amount of hydrophobic particles (e.g.  $\sim 40\%$  hydrophobic particles for sand and  $\sim 15\%$  for GB 150-250  $\mu\text{m}$ ). Similar values were observed for silt and GB 40-70  $\mu\text{m}$  compared to sand and GB 150-250  $\mu\text{m}$ , respectively. At the same time, even when Fig. 13 shows a good agreement between the directly measured and predicted CAs, the deviation between both was significant, and higher with increasing water repellency (e.g. difference up to  $\sim 70^\circ$  in sand with 100% hydrophobic particles). In terms of standard error (SE), determined from the seven pairs of measured and predicted CAs (0-10-25-50-75-90 and 100% hydrophobic particles), it showed values of 58.7 in silt, 48.0 in sand, 62.1 in GB 40-70  $\mu\text{m}$  and 57.4 in GB 150-250  $\mu\text{m}$ . Given that the Young equation is based on the estimation of an ECA (Morra and Della Volpe, 1998; Chibowski et al., 2002), it can be expected the agreement directly measured CA / predicted



**Fig. 14** Linear regressions between the directly measured CA versus the predicted CAs (ES approach).  
 A: Silt and GB 40-70  $\mu\text{m}$ . B: Sand and GB 150-250  $\mu\text{m}$ .



**Fig. 15** Comparison of measured and predicted contact angles (WPM-ACA) as a function of the water repellency (% hydrophobic particles). A: Sand. B: GB 150-250  $\mu\text{m}$ .



CA to be better for WPM-ECA approach, although this remark cannot be directly proved in the present research, due to the absence of independent values for  $\alpha$  and  $\beta$  with this experimental approach (WPM-ECA). Further research in this topic is needed in order to validate the present results, especially regarding the values of  $\alpha$  and  $\beta$  calculated with CRM and WPM-ECA. This aspect becomes very important due to the test materials consisted of mixtures between hydrophilic and hydrophobic particles, where effects like metastability can be present, affecting the estimation of CAs and surface free energies (Marmur, 1993; Karbowiak et al., 2006) through the application of the ES approach.

### 3.5. Conclusions

Three experimental approaches (CRM, WPM-ACA and WPM-ECA) assessing CAs and surface free energies were compared. By applying the critical surface tension concept to Zisman plots, the components of the Young equation ( $\sigma_{SV}$ ,  $\sigma_{SL}$  and  $\sigma_{LV}$ ) and the Girifalco interaction parameter ( $\Phi$ ) were calculated for a set of model materials with increasing amounts of hydrophobic particles. Both  $\sigma$  and  $\Phi$  data were used to calculate the regression parameters  $\alpha$  and  $\beta$  between  $\sigma_{SL}$  and  $\Phi$ . Finally, this information (plus independent values of  $\alpha$  and  $\beta$ ) was used to re-calculate the CAs for each sample with the WPM-ACA method, by applying a previously proposed SE (Bachmann et al., 2006). In this way, the present research focused in evaluating and comparing the calculated values of  $\Phi$ ,  $\alpha$  and  $\beta$  parameters of the different experimental methods, to proof the consistency of the theory related to surface free energies and the corresponding comparison between directly measured and predicted CAs for WPM-ACA, for future applications of the methods in soil research.

For all methods,  $\sigma_C$  decreased directly with higher water repellency. It was observed that although both WPM approaches (WPM-ACA and WPM-ECA) measure different CAs, they tend to estimate similar values of  $\sigma_C$  for all samples in Zisman plots. In agreement with recent works it was observed that the Girifalco interaction parameter ( $\Phi$ ), usually considered as = 1, consistently decreases with higher water repellency, which potentially can affect the application of the ES approach to predict CAs of solid surfaces. The regression parameters of the relation

$\Phi = \beta - \alpha\sigma_{SL}$  showed values consistent with previous researches, although the effect of texture-related properties (e.g. specific surface) in the final estimation of  $\alpha$  and  $\beta$  is not completely clear.

CAs predicted by the equation of state (ES) showed a very restricted range compared to the direct assessment of CA. In general, the CAs predicted by the ES reached a maximum value (around 75° - 80°) at low amounts of hydrophobic particles (around 40% for silt and sand and 15% for GB), which confirms some possible limitations of the empirical ES approach mentioned in previous works. The agreement between the directly measured CAs and the predicted CAs was low for all materials, especially those with a high level of water repellency. Comparison of these results with CRM and WPM-ECA methods was not possible, due to absence of independent values of  $\alpha$  and  $\beta$  parameters in the literature for similar materials. Further research is needed considering e.g. the possible effects of the metastable condition on the estimation of CAs. Additionally, given the already mentioned limitations of the ES approach, the validity of the experimental methods in function of other ES approaches should also be considered.

## Chapter 4

# Assessing contact angles in porous media by evaluating the kinetics of capillary rise and hydraulic properties

### 4.1. Introduction

The evaluation of the wettability and its relation to hydraulic properties is a relevant topic of research in soil science, as it affects directly processes like erosion and infiltration (DiCarlo et al., 1999; Regalado et al., 1993). Authors like Ishakoglu and Filiz (2005) and Naasz et al. (2008) analyzed the consequences of water repellency on hydraulic properties, especially the hysteretic phenomena associated with drying-wetting cycles. They found a significant impact on water distribution and the air regime around the root system.

Marmur and Cohen (1997) introduced a model for the characterization of the wettability of porous media by the kinetics of capillary rise. This model assumes an ideal system consisting of an assembly of parallel capillaries, whose wetting properties can be averaged and described in terms of one single-equivalent capillary. In a more recent article, Marmur (2003) derived a set of equations to describe the kinetics of capillary rise using the Darcy equation instead of the Hagen-Poiseuille law, thus re-defining and generalizing the original model by relating the wetting kinetics and the corresponding hydraulic properties of the pore system under test. Compared to the standard two-liquid Capillary Rise Method (CRM) (Siebold, 2000), where the first stage of the liquid penetration rate is analyzed in order to estimate the CA, the generalized model has the advantage to avoid the use of a reference liquid to estimate the geometry factor, although much longer samples than with the standard CRM are needed (Siebold, 2000; Dang-Vu and Hupka, 2005; Lavi et al, 2008). Although Marmur and Cohen (1997) carried out some initial evaluations in sand and Whatman filter paper, the experimental evaluation of the generalized model for real porous media is still missing. In the present research, a set of model materials with different levels of water repellency were packed in long segmented columns fixed vertically to consider beside capillarity also gravity. In these samples, the kinetics of capillary rise, the hydraulic and

the geometric properties (i.e. permeability and shape of the particles, respectively) were assessed. The validity of the model was then experimentally tested, following the theoretical guidelines given by Marmur and Cohen (1997) and Marmur (2003): for each sample, the dynamic CA ( $\theta_D$ ) and the so-called intrinsic or true one ( $\theta_I$ ), as defined by the Young equation (Young, 1805), were calculated.  $\theta_D$  (or equivalent CA, as originally defined by Marmur and Cohen, 1997) corresponds to the CA estimated by the model during the capillary rise, while  $\theta_I$  is the CA of the same medium estimated under assumed equilibrium conditions. These results were then compared with the equilibrium CA ( $\theta_E$ , which under ideal conditions is in theory equal to  $\theta_I$ ) estimated by fitting and scaling the data of height-dependent saturation degree ( $\text{cm}^3 \text{ cm}^{-3}$ ) of the same long segmented columns to the van Genuchten function for capillary pressure - saturation curves (van Genuchten, 1980). Therefore, the main objective is to test the validity of the generalized model (Marmur and Cohen, 1997 and Marmur, 2003) for describing the dynamics of capillary rise under the impact of gravity and for estimating  $\theta_I$ . These results should improve the understanding of the impact of water repellency on hydraulic properties in porous media. A next step should be the application of the same procedure on natural soils.

## 4.2. Theory

### 4.2.1. Equivalent Capillary model

The Lucas-Washburn (LW) equation (Lucas, 1918; Washburn, 1921), which is based on the application of the Hagen-Poiseuille law, describes the advancing movement of a water meniscus due to capillary forces into a cylindrical tube. This equation has been often applied to describe the wettability of porous media by assessing the dynamic CA (e. g. Siebold et al., 1997). It has the form

$$x^2 = \frac{r \sigma \cos \theta}{2\eta} t \quad (14)$$

where  $x$  is the height the wetting front (m),  $t$  is the time (s),  $r$  the capillary radius (m),  $\sigma$  and  $\eta$  are the surface free energy or surface tension ( $\text{mN m}^{-1}$ ) and viscosity ( $\text{kg m}^{-1} \text{ s}^{-1}$ ) of the test liquid, respectively, and  $\theta$  is the contact angle (CA). The LW equation, which predicts a linear

relation between  $x^2$  and  $t$ , is suitable for the evaluation of liquid penetration in horizontal capillaries, where the effect of gravity is neglected (Zhong et al., 2001). Marmur and Cohen (1997) proposed a model based on the LW equation, where the effect of gravity is included, that is suitable for the evaluation of much longer sized columns. These authors suggested that the best way to describe wetting kinetics in such complex systems as porous media is i) to analyze the case of a single vertical capillary, and ii) to extend this evaluation to an assembly of vertical parallel capillaries, where an equivalent capillary, which averages the behavior of the complete system, can be assumed. This model has the form

$$At = -Bx - \ln(1 - Bx) \quad (15)$$

$A$  and  $B$  correspond to fitting parameters defined by

$$A \equiv \frac{\rho^2 g^2 r^3}{16\sigma\eta\cos\theta} \quad (16)$$

$$B \equiv \frac{\rho g r}{2\sigma\cos\theta} \quad (17)$$

where  $\rho$  is the density of the liquid ( $\text{kg m}^{-3}$ ),  $g$  is the acceleration due to gravity ( $9.81 \text{ m s}^{-2}$ ). This model, due to  $r$  and  $\theta$  contribute independently to the capillary rise, avoids one of the main problems of the standard CRM to estimate the dynamic CA, that is the use of a reference liquid (in addition to the test liquid) to calculate the apparent pore radius. In order to fit the experimental data to the model (i.e. to find the exact value of  $A$  and  $B$ ), Marmur and Cohen (1997) suggested to make a plot between the expression  $-Bx - \ln(1 - Bx)$  versus  $t$ , which in theory is always linear. In such a plot, by varying the value of  $B$ , the linear regression with the highest  $R^2$  is searched. The slope of this regression will then give the best possible estimation of  $A$ . Marmur and Cohen (1997) determined that the dimensionless coefficient  $(Bx)^3/At$  (for a detailed description of the model refer to the original paper) has a maximum value = 0.68692, reached at a time  $(At) = 0.39066$ . Both values are in theory universal for both a single capillary as also for an assembly of capillaries with homogeneous properties, since  $(Bx)^3/At$  is independent of  $r$ , although

not the time ( $At$ ). For an assembly of capillaries with heterogeneous distribution, experiments carried out by Marmur and Cohen (1997) showed that the model has some limitations, as it assumes the same CA and geometric properties for all capillaries, which increases the difficulty in defining a unique equivalent capillary. Marmur (2003) re-defined the wetting model (Eq. 15) by using the Darcy equation (Darcy, 1856; Kissa, 1996) instead of the Hagen-Poiseuille law. This approach includes the permeability ( $\kappa$ ,  $m^2$ ), specific surface area ( $S$ ,  $m^{-1}$ ) and porosity ( $\varepsilon$ ) of the test medium. To relate these variables, Marmur (2003) proposed the following form of the Kozeny-Carman equation (Kozeny, 1927; Carman, 1937 and 1938):

$$\kappa = C \frac{\varepsilon^3}{S^2(1-\varepsilon)^2} \quad (18)$$

where  $C$  is a dimensionless geometrical constant related to pores geometry (Salem, 2001). Marmur (2003) found that, theoretically,  $C = 0.5$  for a system consisting of completely cylindrical capillaries. However, for real porous media, a value of  $C < 0.5$  should be expected. Considering this new approach, the fitting parameters of the model (Eq. 15) are then defined as

$$A^* \equiv \frac{C\varepsilon^3\rho^2g^2}{S^3(1-\varepsilon)^3\sigma\eta\cos\theta} \quad (19)$$

$$B^* \equiv \frac{\varepsilon\rho g}{S(1-\varepsilon)\sigma\cos\theta} \quad (20)$$

and

$$\frac{(B^*)^3}{A^*} = \frac{\rho g \eta}{C\sigma^2 \cos^2 \theta_D} \quad (21)$$

where  $\theta_D$  is the predicted dynamic CA, that means, the one estimated in relation to the radius of the equivalent capillary. A theoretical analysis of the equations carried out by Marmur (2003), shows that more than one unique expression to define the equivalent pore radius ( $r_{EQV}$ ) of

the porous-system is possible. So,  $r_{EQV}$  derived from  $A$  and  $A^*$  has the form

$$r_{EQV}^A = 2(2C)^{1/3} E^* \quad (22)$$

with

$$E^* \equiv \frac{\varepsilon}{S(1-\varepsilon)} \quad (23)$$

and  $r_{EQV}$  derived from  $B$  has the form

$$r_{EQV}^B = 2E^* \quad (24)$$

According to the model, Eq. (22) and (24) will coincide when  $C$  is theoretically = 0 or = 0.5. It is theoretically possible to equate the rate of penetration into a uniform porous medium with that of a cylindrical capillary, so  $A = A^*$  and  $B = B^*$  and  $r_{EQV}$  can be calculated from  $A/B = A^*/B^*$  as

$$r_{EQV} = (8C)^{1/2} E^* \quad (25)$$

The predicted dynamic CA ( $\theta_D$ ) is then calculated from the expression  $A/B^3 = A^*/(B^*)^3$ , which leads to

$$\cos\theta_D = (2C)^{1/2} \cos\theta_I \quad (26)$$

and  $\theta_I$ , corresponding to the intrinsic CA of the medium. Theoretically, when  $C$  decreases (increasing tortuosity of pores), the calculated  $\theta_D$  will be systematically higher than  $\theta_I$  when the capillary penetration is evaluated.

#### 4.2.2. Capillary pressure-saturation curves

Water retention or capillary pressure-saturation curves (WRC), are normally used in soil science for the modelling and description of hydraulic properties (Prunty and Casey, 2002). A standard model used to fit the experimental data to mathematical closed-form WRC, is the sigmoidal function proposed by van Genuchten (1980). This model has the form

$$V = (1 + (\omega \cdot \Psi)^n)^{-m} \quad (27)$$

where  $V$  represents the normalized degree of saturation ( $\text{m}^3 \text{m}^{-3}$ ),  $\omega$  is a scale-factor ( $\text{m}^{-1}$ ) and  $\Psi$  ( $\text{m}$ ) is the capillary pressure or matric suction. Both  $n$  and  $m$  are dimensionless parameters,  $n$  corresponds to the pore-size distribution index, and  $m$  corresponds in many investigations to the expression  $(1-1/n)$ . The expression  $1/\omega$  is known as the air entry value, corresponding to the matric suction at which the drainage of a saturated material starts (Spohrer et al., 2006). When a capillary system has reached an equilibrium state, i.e. the water uptake ceases, the final height of the wetting front can be used to estimate the corresponding equilibrium CA ( $\theta_E$ ) when in a second measurement a reference liquid is used (Letey et al., 1962; Arye et al., 2007). The reference liquid is assumed to have a CA =  $0^\circ$ . In such evaluations, the information from WRC fitted to the van Genuchten function (Eq. 27) can be used to assess the corresponding  $\theta_E$  by scaling the  $\omega$  parameter, obtained from the reference liquid to the corresponding sample evaluated in water (Arye et al., 2007), according to the expression

$$\theta_E = \arccos \left( \frac{\omega_0}{\omega_1} \right) \quad (28)$$

where  $\omega_0$  and  $\omega_1$  correspond to the scale-factors of the capillary pressure-saturation curves fitted to Eq. (27), and the numbers 0 and 1 correspond to the reference liquid (ethanol) and water, respectively.



### **4.3. Methodology**

#### **4.3.1. Materials and treatments**

Four materials were evaluated: two natural materials (silt and sand) and glass beads (GB) of two grain sizes, comparable to silt and sand (see Table 1). All materials were pre-treated in order to get highly hydrophilic samples. A set with increasing water repellency was prepared, following the guidelines of the Chapter 2 (2.3.1). For each model material, three samples with homogeneous wettability (HW, with all particles have near same level of water repellency) and six samples with mixed wettability (MW, mix of hydrophilic and hydrophobic particles) were used beside the reference material (with no addition of DCDMS). For HW samples, the DCDMS amount ranged from  $5.5 \cdot 10^{-6}$  to  $1.0 \cdot 10^{-2}$  mL g<sup>-1</sup>. For MW, the amount of hydrophobic particles ranged between 1.5 and 60% by weight.

#### **4.3.2. Evaluation of kinetics of capillary rise and fit to the Van Genuchten model**

All samples (reference, HW and MW materials) were packed into long segmented columns, the kinetics of capillary rise measured, and the gravimetric liquid content as a function of height determined, by following the procedure already described in Chapter 2 (2.3.2.4, Capillary rise under gravity impact). The samples were evaluated in duplicate. All samples were evaluated with water, while the reference materials were also evaluated with ethanol. The gravimetric liquid content (water and ethanol) per segment was plotted for all samples as capillary pressure-saturation curves (cm and cm<sup>3</sup>cm<sup>-3</sup>, respectively). The curves were fitted to the Van Genuchten model (Eq. 27) with the RETC-1D software (van Genuchten et al., 1991).  $\theta_{EQ}$  of each sample was estimated by using the information of the fitted curves (parameter  $\omega$ ), according to Eq. (28).

#### **4.3.3. Evaluation of the C geometry factor and shape of the particles**

The C geometry factor of Kozeny-Carman equation (Eq. 18) was estimated for reference materials (no addition of DCDMS), by using the information of S and  $\varepsilon$  (Table 1). For each reference material, the saturated hydraulic conductivity ( $K_C$ , m s<sup>-1</sup>) was measured in columns (column height = 50 cm, filling height = 30 cm, inner diameter = 2.08 cm) closed at the bottom with a silk sheet and a plastic ring. The material was filled into the columns and gently compacted with a plastic stick each 5 cm, in order to reproduce the same bulk density obtained in the previous experiments with long segmented columns. The columns were submerged (about 4

cm) into a bottle with a defined water table (7 cm) and the velocity of the drainage of a water column (length = 20 cm) measured. Ten replications were made. For the reference materials,  $\kappa$  ( $\text{m}^2$ ) was estimated from the expression (Hillel, 1998) (for water,  $\rho = 998.29 \text{ kg m}^{-3}$  and  $\eta = 0.001 \text{ kg m}^{-1} \text{ s}^{-1}$  at 20 °C):

$$K_c = \kappa \frac{\rho g}{\eta} \quad (29)$$

C was then estimated by solving Eq. (18) with the corresponding values of  $\kappa$ , S and  $\varepsilon$  of each reference material. As in Eq. (18) S ( $\text{m}^2 \text{ g}^{-1}$ ) must be expressed in  $\text{m}^{-1}$ , S was previously converted to  $\text{m}^2 \text{ kg}^{-1}$  and multiplied by the bulk density of the material (expressed as  $\text{kg m}^{-3}$ ) determined in the long segmented columns (see original data in Table 1).

In order to infer the general geometry of the pore system, pictures of the materials were taken with an optical microscope, randomly sampling 50 individual particles. The average deviation of the particles from a circular shape was estimated by applying the following definition of circularity (Ci) (Hawkins, 1993; Narsilio and Santamarina, 2008):

$$Ci = \frac{Ar_1}{Ar_2} \quad (30)$$

where  $Ar_1$  is the area of the particle ( $\text{m}^2$ ) and  $Ar_2$  the area of the smallest circle circumscribing it ( $\text{m}^2$ ). A perfect circular shape is defined by  $Ci = 1$ .

## 4.4. Results and discussion

### 4.4.1. Equivalent Capillary model

#### 4.4.1.1. Kinetics of capillary rise

Fig. 16 shows examples of the wetting kinetics observed in reference materials for sand and GB 150-250  $\mu\text{m}$ . Shown are a complete measurement of the capillary rise process (about one week for all samples) (Fig. 16A) and the corresponding rate of liquid uptake (g) per second (s) (i.e.  $\Delta W/\Delta t$ ) of the first three hours (Fig. 16B). As observed, when the complete measurement of

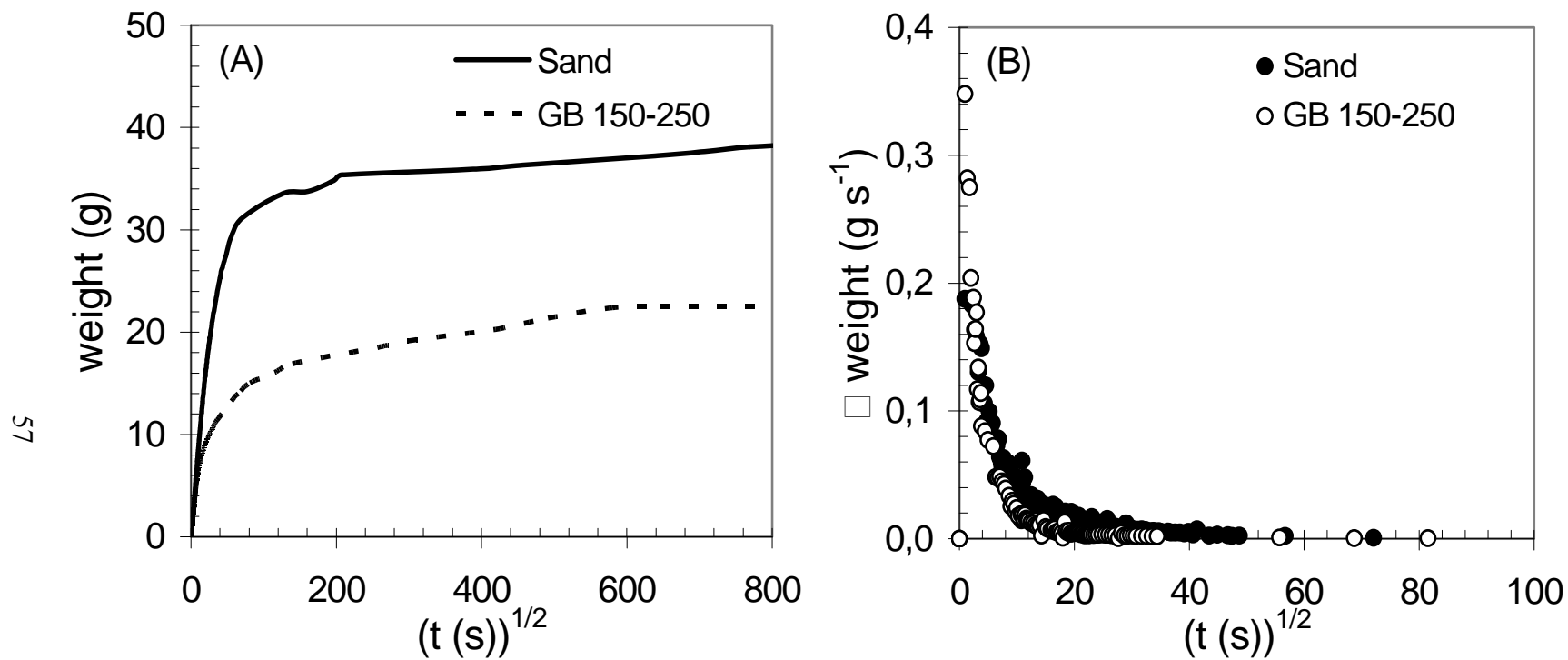
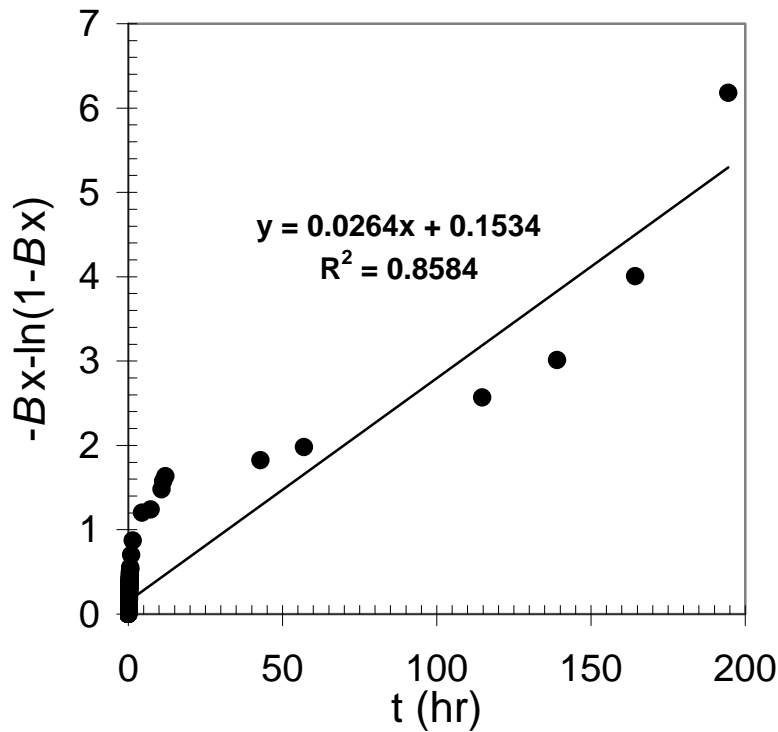


**Fig. 16** Wetting kinetics in segmented columns for sand and GB 150-250  $\mu\text{m}$  (reference materials, no addition of DCDMS). A: Complete measurement determined after one week. B: Rate of liquid uptake ( $\text{g s}^{-1}$ ) (first three hours of the measurement).

capillary rise is considered (Fig. 16A), the capillary process usually shows a two-slope behavior, where the linearity assumed by the LW equation is observed only in the first stages of the measurement (in general, <180 min for silt and GB 40-70  $\mu\text{m}$ , and <80 min for sand and GB 150-250  $\mu\text{m}$ ). When the initial rate of the liquid uptake is considered (Fig. 16B), it is observed that the maximum level of liquid uptake normally is reached within the first minutes of the measurement (<5 min). After this time, a constant decrease of the rate is observed, showing a very low and stable value (although positive in relation to the evaporation rate) until the equilibrium height is reached. These results confirm the observation of authors like Stange et al. (2003), who concluded from tests in glass capillaries, that the LW equation is not able to describe the entire capillary infiltration process, especially under the effect of gravity. Regarding the Equivalent Capillary model (Eq. 15), Fig. 17 shows an example of the relation between the expression  $-Bx - \ln(1 - Bx)$  versus time (t) for sand (wetable reference material), considering a complete measurement (about one week). As observed, the theoretical linearity of this plot (correlation coefficient  $R^2 = 1$ ) (Marmur and Cohen, 1997) is generally not observed when the complete capillary process is considered. In the present research,  $R^2$  was in the range 0.81 - 0.91 for samples with  $\theta_E^{\text{WPM}} < 90^\circ$ , being even lower for hydrophobic materials ( $\theta_E^{\text{WPM}} > 90^\circ$ ) ( $R^2 < 0.7$ , e.g. GB 150-250  $\mu\text{m}$  with >40% hydrophobic particles), for both types of wettability, HW and MW samples, respectively. Similar results were found by Marmur and Cohen (1997) by using data of paraffin oil in sand collected by Hackett (1921). These data correspond to a measurement running for about 3000 hours. The authors concluded that the theoretical linearity of the plot  $-Bx - \ln(1 - Bx)$  versus t is observed only in the first stages of the entire capillary process. From these results, it becomes clear that the Equivalent Capillary model has limitations, especially in those time domains where the rate of liquid uptake is low (<0.01  $\text{g s}^{-1}$ ), but still positive in relation to the evaporation level, which must be considered during the long-term experiment.

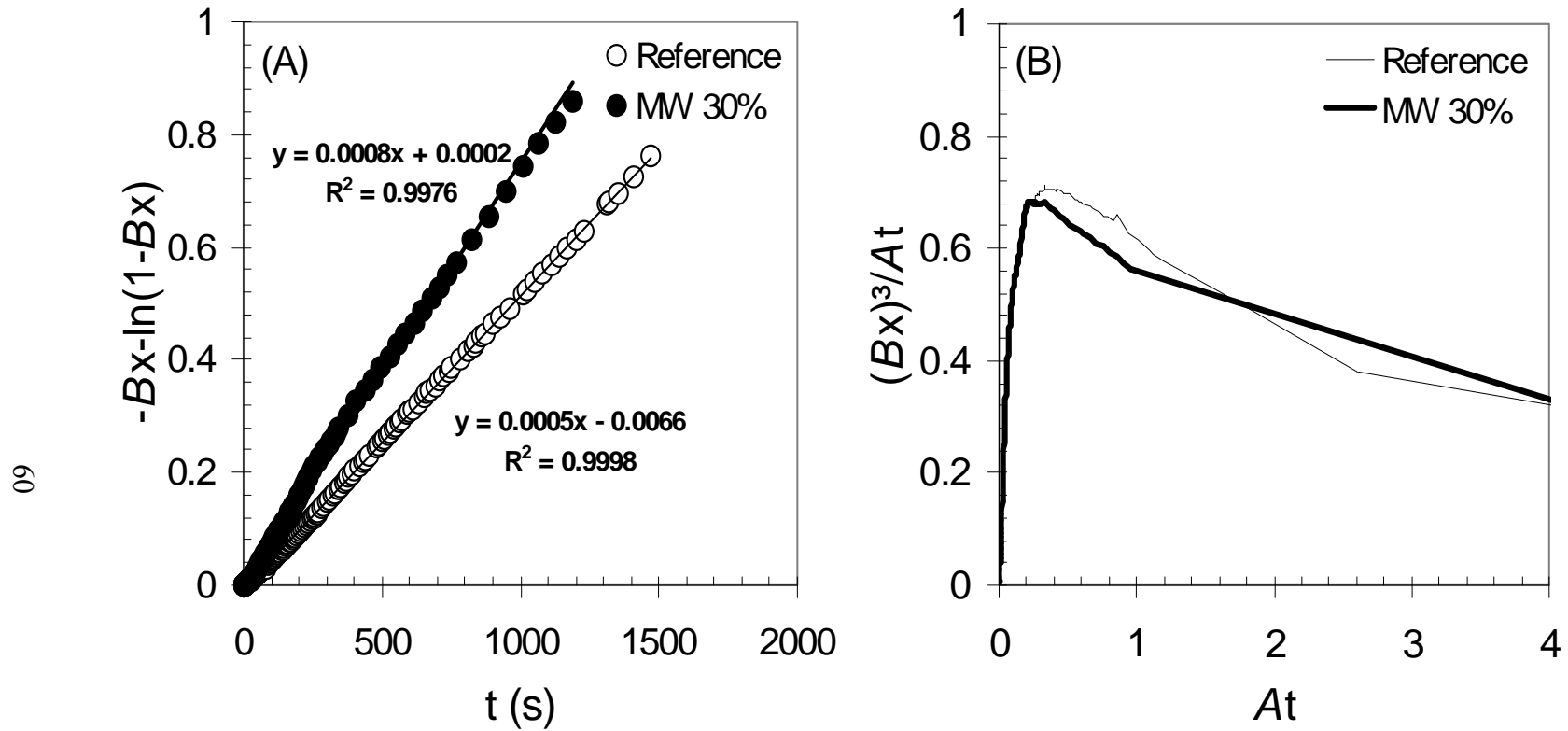
#### 4.4.1.2. Fit of the wetting model

Fig. 18 shows an example of the application of the Equivalent Capillary Model for sand (reference and MW samples) considering only the first stages of the capillary process (<2000 s). It is observed how the linearity of the plot  $-Bx - \ln(1 - Bx)$  versus time (t) is significantly better than considering the entire process (Fig. 18A). In general,  $R^2$  was in the range 0.97-0.99 for all samples, with a slight decrease with increasing water repellency (no significant differences between HW and MW samples were observed). For the same samples, Fig. 18B shows the



**Fig. 17** Relation between the expression  $- Bx - \ln(1 - Bx)$  versus time ( $t$ ) for a complete measurement of the capillary process (about one week). Example for sand (wetttable reference material).

relation  $(Bx)^3/At$  versus  $t$ , based on the previous estimation of the parameters  $A$  and  $B$ , by considering only the section of the curves where the linearity of  $- Bx - \ln(1 - Bx)$  versus  $t$  is observed. In near all cases the curves were in good agreement with the expected behavior described by the model of Equivalent Capillary developed by Marmur and Cohen (1997) and Marmur (2003). As previously mentioned, an ideal porous medium (i.e. cylindrical straight pores of the same radius) has a theoretical maximum of  $(Bx)^3/At = 0.68692$  at  $At = 0.39066$ . Gradually, with increasing repellency, the first value (corresponding to the liquid uptake due to capillary rise) will decrease, while the second value (the moment where the maximum liquid uptake occurs) will increase. In the present research,  $(Bx)^3/At$  showed in general higher values than for the ideal expected case, especially for silt. The ranges observed were 0.9-1.6 for silt and 0.7-0.9 for the other materials. These differences can be explained qualitatively when the complexity of the pore system is considered, especially in materials like silt, material with higher specific surface and tortuosity due to particles shape in relation to sand (Mauran et al, 2000; Manthey, 2006). At the same time,  $At$  showed increasing values with higher water repellency



**Fig. 18** Application of the Equivalent Capillary model on sand (reference material) and one MW sample (30% hydrophobic particles particles =  $1.5 \cdot 10^{-4}$  mL  $g^{-1}$  DCDMS) considering the first stages of capillary rise. A: Plots between the expression  $-Bx - \ln(1 - Bx)$  versus time ( $t$ ) and the corresponding linear regressions, used to estimate the fitting parameters  $A$  and  $B$ . B: Relation between the dimensionless expressions  $(Bx)^3/At$  and  $(At)$ .

for both HW and MW samples. This behavior is in good agreement with the theory of the Equivalent Capillary model, as the time  $t$  of liquid penetration is expected to increase with higher water repellency. The ranges observed for  $At$  were 1.1-1.5 for silt and 0.2-0.7 for the rest of materials (sand and GB).

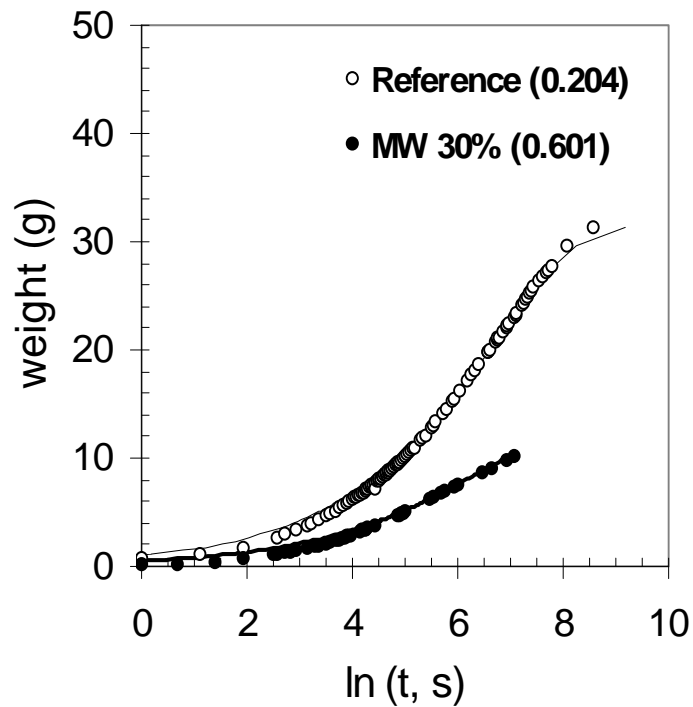
Table 3 summarizes the fitting parameters ( $A$  and  $B$ ) and the expressions ( $(Bx)^3/At$  and  $At$ ) for the four model materials tested. Shown are the values corresponding to the most hydrophilic (reference) and the most hydrophobic samples (both HW and MW). In general, the fitting parameters had similar range and tendencies in relation to the experimental results presented by Marmur and Cohen (1997). However, it must be noted that these authors presented only a restricted set of data (two kinds of filter paper and sand), which does not allow a good comparison with the results of the present research. It must be noted that for the most hydrophobic sample of silt ( $1 \cdot 10^{-1}$  mL  $g^{-1}$  DCDMS, HW),  $A$  and  $B$  are equal zero due to no water uptake by capillary rise was observed into the corresponding columns.

Fig. 19 shows an example of the fit of the Equivalent Capillary model to the experimental data of the sand samples (reference material and MW 30% hydrophobic particles). The plot shows the weight of the liquid uptake ( $g$ ) versus the time ( $t$ ) ( $t$  is expressed as  $\ln$  in order to reduce the scale of the x-axis). A good agreement between the experimental and fitted values was observed in almost all cases, except for samples with high hydrophobicity (e.g.  $>50\%$  hydrophobic particles in sand and  $>10\%$  in GB 150-250  $\mu m$ , with  $\theta_A^{WPM} > 110^\circ$ ). The standard error (SE) between the measured and predicted data was significantly better (i.e. smaller) for the wettable materials (e.g.  $<10\%$  hydrophobic particles for sand, MW samples, with  $\theta_A^{WPM} < 60^\circ$ ). SE had a range of 0.1 - 0.7, reaching 3.2 for GB 150-250  $\mu m$  with 15% hydrophobic particles, which was the highest SE observed in this study. The lower quality of the fit of the wetting model in hydrophobic samples is possibly related to a not completely accurate estimation of the parameters  $A$  and  $B$ , due to the smaller number of points where the linearity assumed by the plot  $- Bx - \ln(1 - Bx)$  versus  $t$  is observed, compared to the hydrophilic samples. It can then be concluded that the Equivalent Capillary Theory shows limitations to model the complete measured capillary rise process in large columns under the effect of gravity. However, reasonable approximations are obtained (especially in materials located in the sub-critical range of hydrophobicity) when the fit of the parameters  $A$  and  $B$  is based on the first stages of the process ( $<2000$  s).

**Table 3:** Values of the fitting parameters  $A$  and  $B$  and the dimensionless expressions  $(Bx)^3/At$  and  $At$  for the reference (no addition of DCDMS) and the most hydrophobic materials (HW and MW samples).

Material	Reference				HW					MW				
	$A$	$B$	$(Bx)^3/At$	$At$	DCDMS (mL g <sup>-1</sup> )	$A$	$B$	$(Bx)^3/At$	$At$	DCDMS (%)	$A$	$B$	$(Bx)^3/At$	$At$
Silt	$1.0 \cdot 10^{-5}$	$9.0 \cdot 10^{-3}$	1.585	1.094	$1 \cdot 10^{-1}$	0	0	0	0	60	$6.0 \cdot 10^{-4}$	$4.5 \cdot 10^{-2}$	0.944	1.451
Sand	$2.0 \cdot 10^{-4}$	$2.7 \cdot 10^{-4}$	0.705	0.378	$1 \cdot 10^{-4}$	$1.7 \cdot 10^{-3}$	$7.0 \cdot 10^{-2}$	0.694	0.285	40	$1.3 \cdot 10^{-3}$	$1.5 \cdot 10^{-1}$	0.696	0.332
GB 40-70 μm	$1.0 \cdot 10^{-4}$	$2.1 \cdot 10^{-2}$	0.887	0.286	$4 \cdot 10^{-5}$	$1.6 \cdot 10^{-3}$	$5.0 \cdot 10^{-2}$	0.636	0.427	30	$6.0 \cdot 10^{-4}$	$1.2 \cdot 10^{-1}$	0.879	0.244
GB 150-250 μm	$1.9 \cdot 10^{-3}$	$8.8 \cdot 10^{-2}$	0.982	0.200	$3 \cdot 10^{-5}$	$5.7 \cdot 10^{-3}$	$2.6 \cdot 10^{-1}$	0.725	0.651	15	$1.7 \cdot 10^{-3}$	$8.0 \cdot 10^{-1}$	0.920	0.033





**Fig. 19** Fit of the Equivalent Capillary model on sand (reference and MW 30 % hydrophobic particles =  $1.5 \cdot 10^{-4}$  mL g<sup>-1</sup> DCDMS). The standard error (SE) is indicated in brackets.

#### 4.4.1.3. Hydraulic properties, shape of the particles and C geometry factor

Fig. 20 shows pictures of the particles of the different model materials. As observed, both GB fractions are characterized by an almost perfect spherical shape (>90% of the particles), while the particles of sand and especially silt, exhibit mainly irregular shape.

Table 4 shows the average values of hydraulic conductivity ( $K_C$ ), permeability ( $\kappa$ ), circularity of the particles ( $C_i$ ) and the C geometry factor from the Kozeny-Carman equation, estimated for the reference materials. Considering  $K_C$  and  $\kappa$ , the estimated values are consistent with those commonly expected for silty and sandy textures in soils (Donoso, 1981; Hillel, 1998). According to the scale defined by Bear (1972) based on  $K_C$ , all materials can be classified as semi-pervious, with silt limiting with the impervious range, GB 40-70  $\mu\text{m}$  and sand located in the middle of the range, and GB 150-250  $\mu\text{m}$  limiting with the pervious materials. These results ( $C_i$ ,  $K_C$  and  $\kappa$ ) lead to conclude that the pore system should be closer to the ideal case defined by Marmur (2003) (i.e. cylindrical pores) especially in GB 150-250  $\mu\text{m}$  in relation to GB 40-70  $\mu\text{m}$ , as also

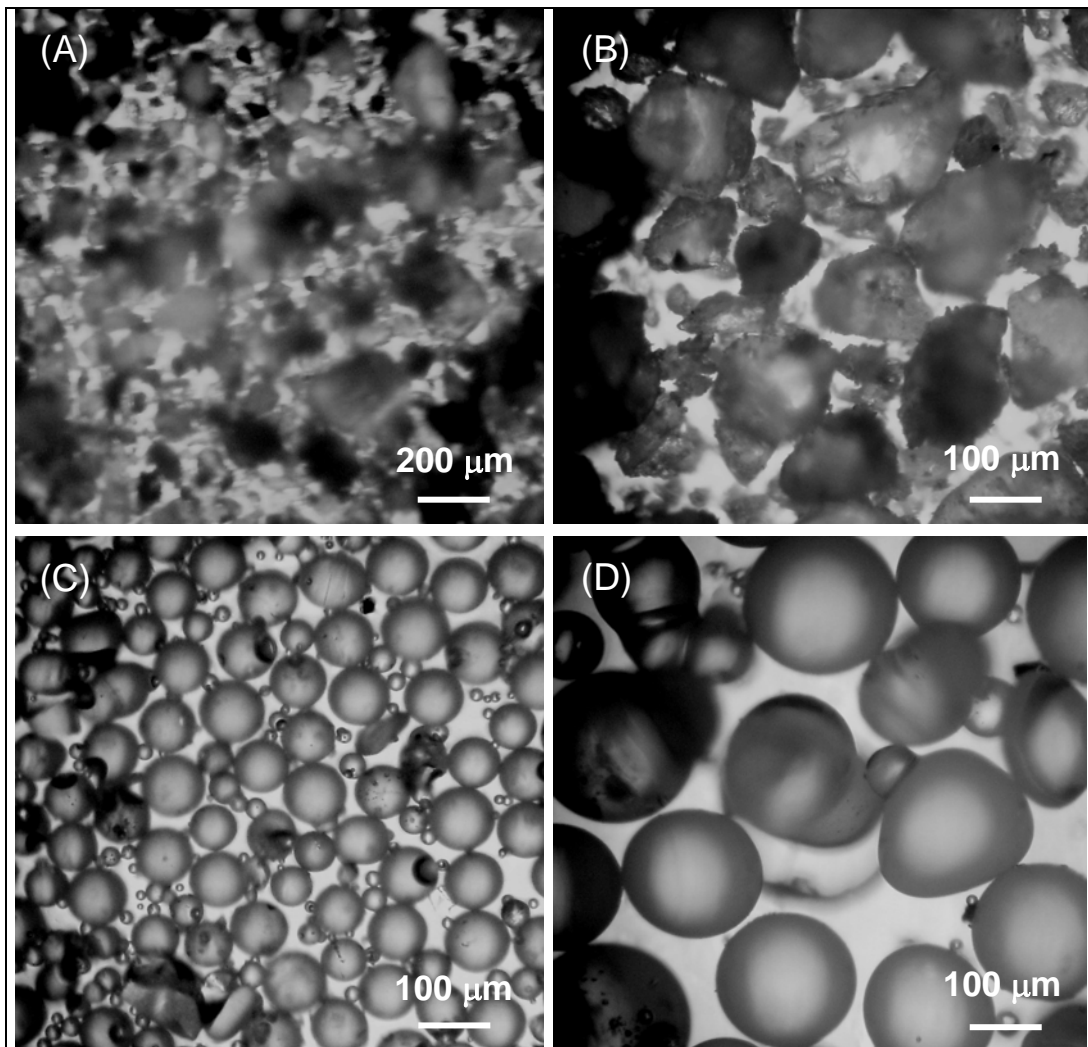


**Fig. 20** Photographs of the particles of the model materials. A: Silt, B: Sand, C: GB 40-70  $\mu\text{m}$ , D: GB 150-250  $\mu\text{m}$ . Note the different scale of silt.

**Table 4:** Values of hydraulic conductivity ( $K_C$ ), permeability ( $\kappa$ ), Circularity ( $C_i$ ) and C geometry factor estimated for reference materials.

Material	$K_C$ ( $\text{m s}^{-1}$ )	$\kappa$ ( $\text{m}^2$ )	$C_i$		C	
			average	SD	range	average
Silt	$1.81 \cdot 10^{-7}$	$1.85 \cdot 10^{-14}$	0.52	0.06	0.050 - 0.130	0.090
Sand	$9.57 \cdot 10^{-6}$	$9.82 \cdot 10^{-13}$	0.64	0.05	0.006 - 0.526	0.266
GB 40-70 $\mu\text{m}$	$4.32 \cdot 10^{-6}$	$4.42 \cdot 10^{-13}$	0.92	0.03	0.001 - 0.040	0.021
GB 150-250 $\mu\text{m}$	$5.59 \cdot 10^{-5}$	$5.73 \cdot 10^{-12}$	0.94	0.05	0.117 - 0.205	0.161

$K_C$  /  $\kappa$ : Average of 10 measurements.

$C_i$ : Average of 50 particles.

sand with respect to silt. As observed in Table 4, the calculated average values of  $C$  are in line with this assumption. The lower  $C$  for silt and GB 40-70  $\mu\text{m}$  in relation to sand and GB 150-250  $\mu\text{m}$  can be expected, as this empirical parameter is defined as the product between a factor of tortuosity ( $l$ , deviation of the pore from a straight line) and one of shape of particles and pore channels ( $k_0$ ) (Carman, 1937 and 1938, Salem, 2001; Rodriguez et al., 2004). According to the results of Czachor (2006), the tortuosity is assumed to be higher for silt and GB 40-70  $\mu\text{m}$ , increasing their theoretical deviation from an ideal pore system, reducing the estimated  $C$  (i.e. cylindrical capillaries of similar size) (Marmur, 2003). Contrary as expected, both soil materials (silt and sand, particles with irregular shape) have higher  $C$  in comparison with the GB (40-70  $\mu\text{m}$  and 150-250  $\mu\text{m}$ , particles with almost perfect spherical shape). From this, it becomes evident that the use of the particle shape as the only indicator of the pore system configuration can eventually lead to erroneous conclusions. At the same time, the results demonstrate that the accurate assessment of  $C$  can be a critical factor affecting the correct estimation of  $\theta_l$  through the Equivalent Capillary Model. In this line, the high sensitivity on  $C$  of parameters like  $S$  and  $K_C$  leads to values of  $C$  higher than the theoretical range (0-0.5) (Marmur, 2003), as experimentally observed for sand (see Table 4, highest value of  $C$ ).

#### 4.4.2. Capillary pressure-saturation curves

Fig. 21 shows examples of capillary pressure-saturation curves and the corresponding fit of the van Genuchten model. For all the samples in the subcritical range of hydrophobicity ( $\theta_E^{\text{WPM}} < 90^\circ$ ), the correlation between the experimental data and the model is high ( $R^2 > 0.98$ ), while for hydrophobic samples  $R^2$  decreases to values around 0.8 (HW and MW samples).

The curves in general do not show the regular sigmoidal form proposed by the van Genuchten model, especially not for GB and for the samples with increasing water repellency. In these cases, there is normally a sharp transition of the liquid content, from wet to dry at the wetting front (e.g. MW samples with more than 15% hydrophobic particles in GB 40-70  $\mu\text{m}$  and more than 5% in GB 150-250  $\mu\text{m}$ ). Slightly more sigmoidal character of the moisture versus height curves were usually observed for sand. This behavior is possibly related to wetting resistance during the capillary rise supporting sharp contrast between wetted and non-wetted grain surfaces (Dekker and Ritsema, 2000; Ellies et al., 2002; Pagliai and Vignozzi, 2002). Comparing the air entry

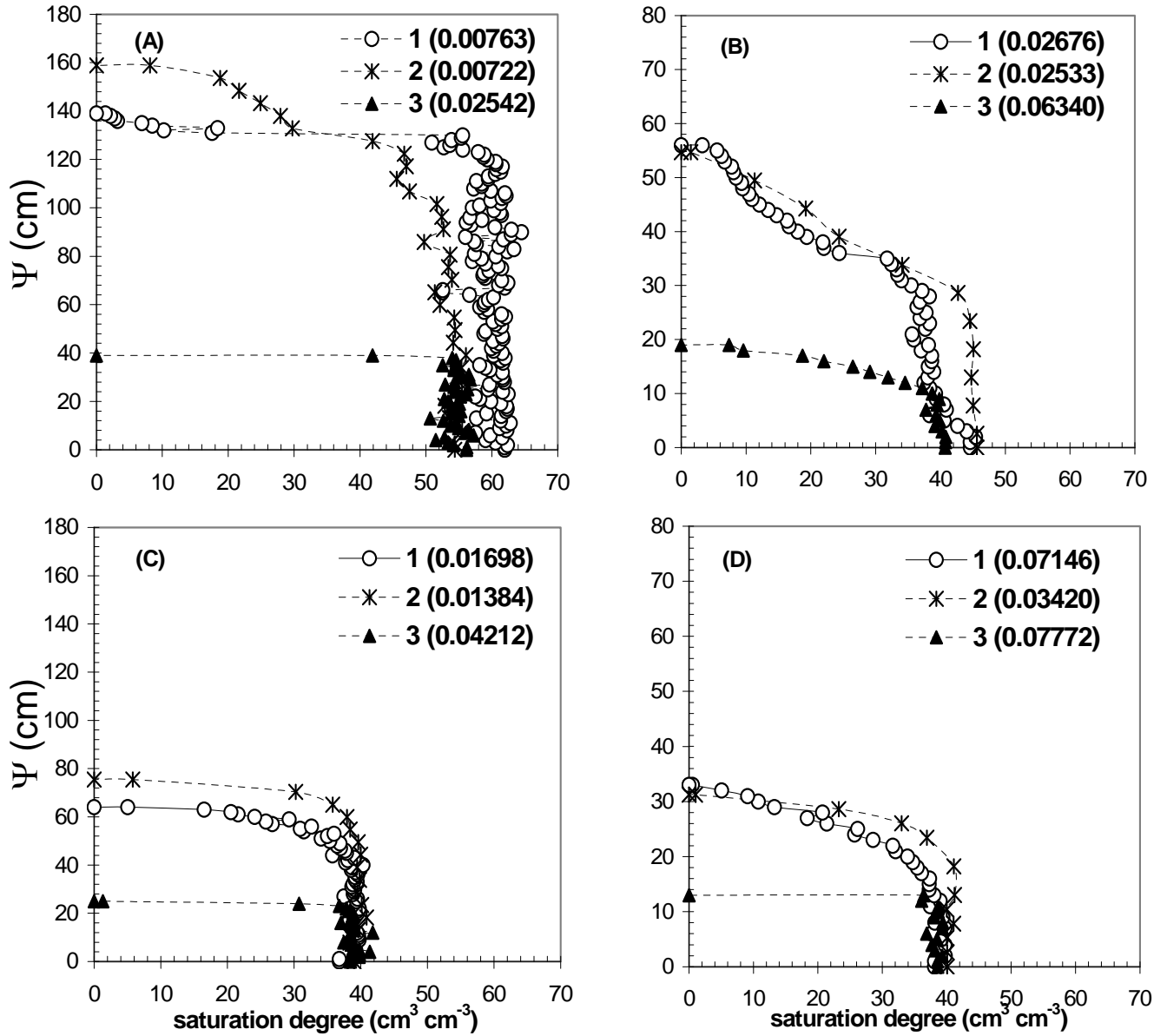


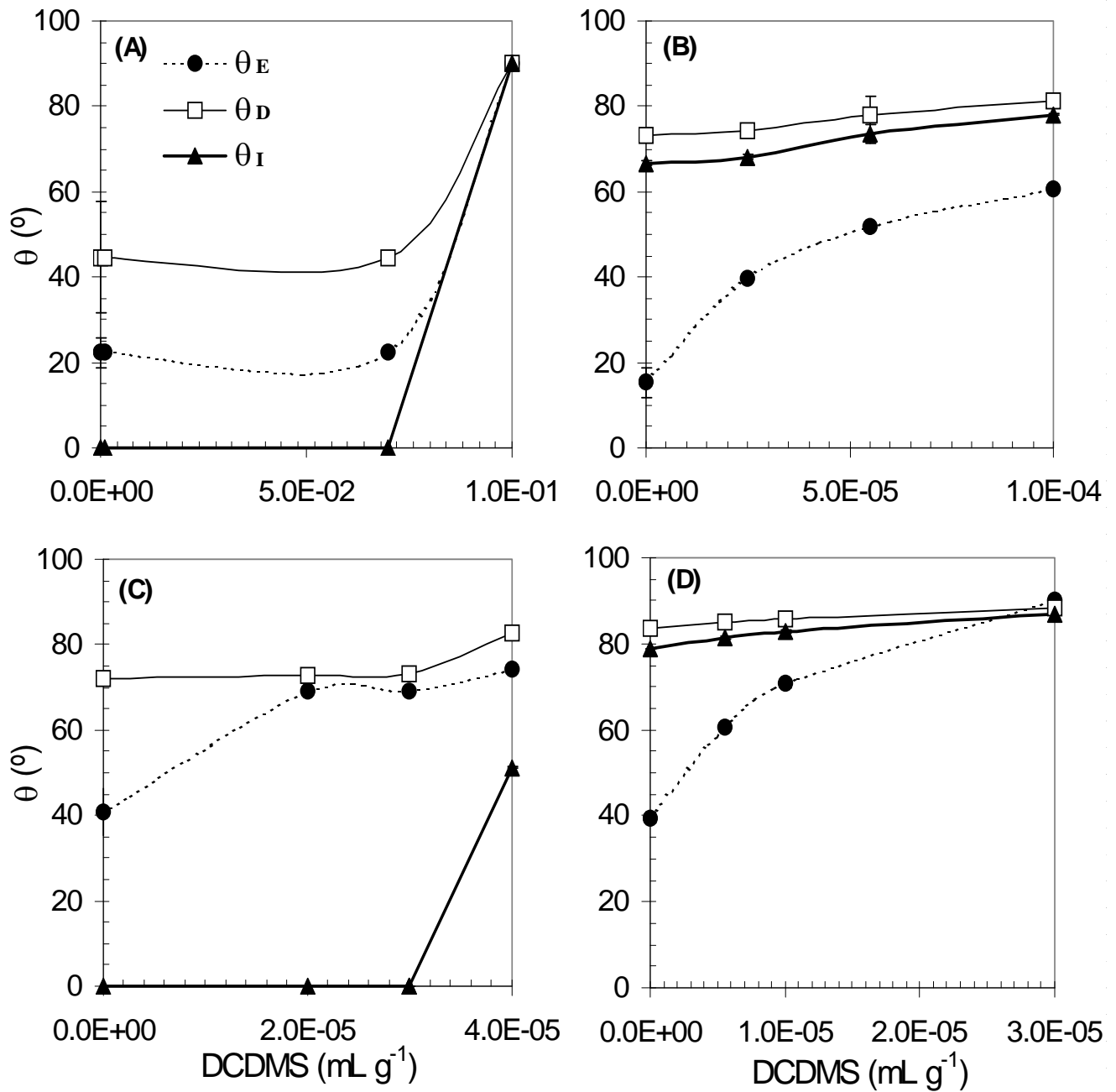
**Fig. 21** Capillary pressure-saturation curves fitted to the van Genuchten model. A: Silt, B: Sand, C: GB 40-70  $\mu\text{m}$ , D: GB 150-250  $\mu\text{m}$ . 1: Water uptake in reference material. 2: Ethanol scaled curve. 3: Water uptake in a MW sample (Silt = 60% hydrophobic particles, sand = 30%, GB 40-70  $\mu\text{m}$  = 15%, GB 150-250  $\mu\text{m}$  = 5%). The van Genuchten  $\omega$ -parameter is indicated in brackets. Note the different scales of the y-axis.

value ( $=1/\omega$ ) of the reference materials (Fig. 21), higher values for silt ( $= 131.1$ ) were observed in relation to sand ( $= 37.4$ ). A similar tendency was observed for GB 40-70  $\mu\text{m}$  in relation to GB 150-250  $\mu\text{m}$ . These differences are expected and confirm that silt and GB 40-70  $\mu\text{m}$  have pores with a lower equivalent radius, where water will be retained with higher capillary forces than for sand and GB 150-250  $\mu\text{m}$  at the same degree of saturation (Täumer, 2007). The air entry value showed further in general an inverse relation with increasing water repellency (HW and MW samples). The relation between the air entry value and CA was already observed in experiments carried out by Shahidzadeh et al. (2003 and 2004). These authors used columns filled with hydrophilic and hydrophobic GB. They demonstrated that in hydrophilic samples a higher amount of residual water left after drainage under the influence of gravity as compared with samples with higher water repellency. Residual water is then constituted of capillary bound water located between particles (water bridges) and water films covering particle surfaces. In hydrophobic samples, the water bridges are smaller and the water films are not retained by capillary forces.

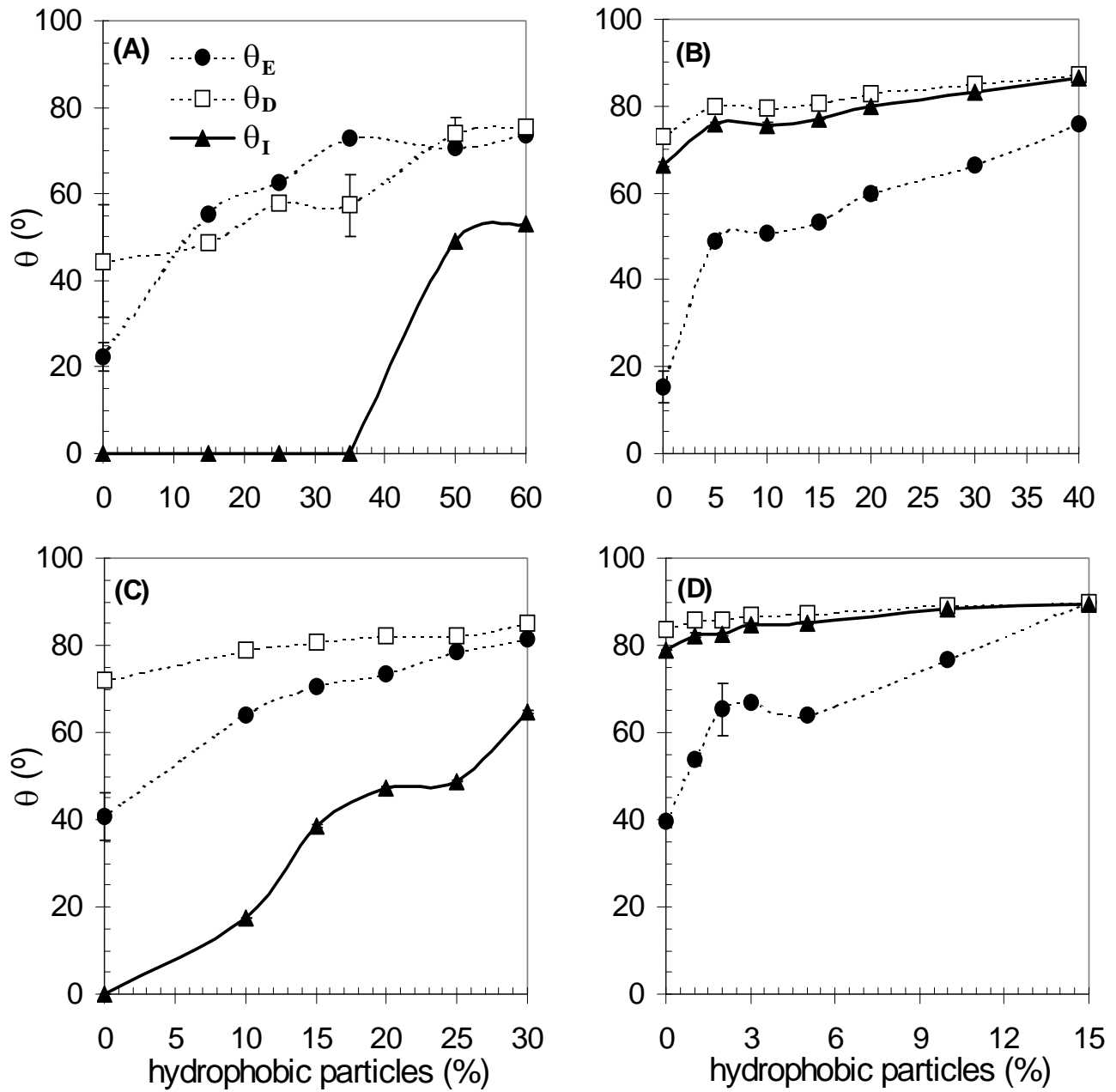
#### 4.4.3. Comparison of contact angles

Fig. 22 and 23 summarize for the HW and MW samples the corresponding CAs evaluated in this chapter:  $\theta_D$  (Eq. 21, dynamic CA estimated by applying the Equivalent Capillary Model),  $\theta_I$  (Eq. 26, intrinsic or true CA, estimated by applying the C factor) and  $\theta_E$  (Eq. 28, equilibrium CA, calculated from scaling the  $\omega$ -parameter of the van Genuchten function). It must be noted that the standard deviation (SD) is also indicated, but for almost all samples its value is  $<1$

Largest differences between the three CAs ( $\theta_E$ ,  $\theta_D$  and  $\theta_I$ ) were observed for silt and for the smaller glass beads fraction (GB 40-70  $\mu\text{m}$ ) compared with sand and GB 150-250  $\mu\text{m}$ , especially in the more wettable domain, no matter if HW or MW samples were compared. In almost all cases (excepting three samples of silt MW),  $\theta_D$  seems to be overestimated in relation to  $\theta_E$  (near  $30^\circ$  for silt and GB 40-70  $\mu\text{m}$  and near  $50^\circ$  for sand and GB 150-250  $\mu\text{m}$ ). These results are in agreement with the findings of Chapter 2, by comparing the CA between the standard two-liquid CRM with equilibrium approaches (e.g. SDM). At the same time, for reference materials, values of  $\theta_D$  around  $44^\circ$  are estimated for silt,  $73^\circ$  for sand,  $72^\circ$  for GB 40-70  $\mu\text{m}$  and  $83^\circ$  for GB 150-250  $\mu\text{m}$ . These values are also in agreement with the results of Marmur and Cohen (1997), who



**Fig. 22** Contact angles (CA) calculated for samples with homogeneous wettability ( $\theta_E$ : Equilibrium CA calculated from water retention curves;  $\theta_D$ : Dynamic CA from Equivalent Capillary Model;  $\theta_I$ : Intrinsic CA) A: Silt, B: Sand, C: GB 40-70  $\mu\text{m}$ , D: GB 150-250  $\mu\text{m}$ .



**Fig. 23** Contact angles (CA) calculated for samples with mixed wettability ( $\theta_E$ : Equilibrium CA calculated from water retention curves;  $\theta_D$ : Dynamic CA from Equivalent Capillary Model;  $\theta_I$ : Intrinsic CA) A: Silt, B: Sand, C: GB 40-70  $\mu\text{m}$ , D: GB 150-250  $\mu\text{m}$ .

measured values of about  $71^\circ$  and  $77^\circ$  even for hydrophilic materials (filter paper and sand, respectively). Taking into account that the model is able to describe the wetting process with satisfactory accuracy, the overestimation of  $\theta_D$  can be related to the nature of the dynamic CA itself, and its relation to the equilibrium CA. So, Marmur and Cohen (1997) explained the high CA with the fact that  $\theta_D$  is different to  $\theta_I$ , corresponding to an apparent CA during the process of wetting. According to Marmur (2003), the difference between both angles, as can be seen from Eq. (26), will be greater when the geometry of the pore system (described by the C factor) deviates from the ideal one (i.e. an assembly of straight-cylindrical capillaries of the same diameter). In agreement with these results, different authors have concluded that the dynamic CA normally will be greater than the equilibrium or intrinsic one, resulting from kinetic effects (Lavi et al., 2008) as well as from geometry-related aspects (Siebold et al., 1997 and 2000; Czachor, 2006).

As previously mentioned, it is assumed that  $\theta_D$  and  $\theta_I$  have a better agreement in ideal porous media like circular capillaries and getting systematically more different when the pore system becomes more complex (Marmur and Cohen, 1997; Lavi et al., 2008). The results show that  $\theta_I$  is significantly lower compared to  $\theta_D$  for silt and GB 40-70  $\mu\text{m}$  (e.g.  $\theta_I = 0^\circ$  in almost all samples of silt and GB 40-70  $\mu\text{m}$  for HW samples), while both CA show similar values for sand and GB 150-250  $\mu\text{m}$  ( $\theta_I$  between  $69^\circ$  and  $83^\circ$  in all cases). As previously observed by authors like Czachor et al. (2006) and Goebel (2007), the present results suggest a significant dependence of the CA on the geometry of the system. The lack of sensitivity of the Equivalent Capillary Model is then confirmed when the different CAs ( $\theta_D$ ,  $\theta_I$  and  $\theta_E$ ) are compared, which is also in line with the results already introduced in Chapter 2. Given the dependency on geometry to estimate the CA, it can be concluded that the correct assessment of C is essential in order to apply the model for the estimation of  $\theta_I$ . In this line, different authors have mentioned that the Kozeny-Carman equation is suitable for evaluation of sand, but it shows limitations to predict hydraulic properties when powdered materials with particles of very small diameter are tested (Singh and Wallender, 2006). Dmitriev (1996) concluded that the equation is valid only for completely anisotropic media. It must be also noted that according to authors like Sciffer (2000) and Marmur (2003), the very complex nature of heterogeneous porous media complicates significantly the development of models describing wettability, which can be rated as still insufficient. The



necessity for further research on the topic becomes clear considering that the description of the wetting process and especially the dynamic CA gives information about the test medium (e.g. the pore system configuration) not possible to infer directly with the only value of the equilibrium CA (Grader, 1986; Siebold et al., 2000; Stange et al., 2003). According to the results, the present form of the Equivalent Capillary Model can be considered as suitable to define degrees of water repellency and to describe the general geometry characteristics of the medium, but not to estimate  $\theta_I$  with accuracy. At the same time, even when the measurements needed are time consuming, it was observed that the modelling based on the evaluation of the first stages of capillary rise can render reasonable estimation of the entire process. Finally, authors like Shirtcliffe et al. (2006) state that the test of natural porous media (i.e. soils) seen as a bundle of capillary tubes is a very simplified approximation of the capillary process. However, in the specific case of the Equivalent Capillary model, even when its accuracy to determine  $\theta_I$  is still possible to improve, its relative simplicity of application should be considered as a major advantage.

#### **4.5. Conclusions**

The easy-to-apply Equivalent Capillary Model (Marmur and Cohen, 1997; Marmur, 2003) was experimentally tested using model materials with different particle diameter, particle shape and level of water repellency. Following the method proposed by the authors to evaluate the kinetics of the capillary rise, the wettability was described in terms of the dynamic CA ( $\theta_D$ ) and the intrinsic CA ( $\theta_I$ ). Both CAs were compared to the equilibrium CA obtained for the same materials, by fitting and scaling the van Genuchten model to capillary pressure-saturation data, using ethanol as reference liquid. It was observed that, in agreement with the findings of Marmur and Cohen (1997), the evaluation of the fitting parameters is restricted when the entire capillary process is considered, as the linearity of the relation  $W = f(t)^{1/2}$  predicted by the Lucas-Washburn equation is observed only in the first stages of the complete measurement (about one week). However, the fit of the linear section of the capillary rise (always observed within the first 24 hours of the complete measurement) gives reasonable results, especially for the most hydrophilic samples ( $\theta_E^{WPM} < 60^\circ$ ). The dynamic CA ( $\theta_D$ ) predicted by the model seems to be overestimated in relation to the equilibrium one ( $\theta_E$ ) for almost all samples. These results were in agreement with previous researches, like Lavi et al. (2008), who compared the dynamic CA versus the equilibrium CA in glass capillaries with the standard two-liquid CRM (Bachmann et

al., 2003). The significant difference between  $\theta_D$  and  $\theta_E$  supports the suitability of the application of the van Genuchten model in order to calculate  $\theta_E$  when a reference liquid is used. It was observed that the estimated intrinsic CA ( $\theta_I$ ) decreases significantly in almost all samples compared to  $\theta_D$  for the materials with the smallest particle diameter (silt and GB 40-70  $\mu\text{m}$ ), but not for those with larger diameter (sand and GB 150-250  $\mu\text{m}$ ). These results show a restriction of the model in estimating  $\theta_I$ , possibly related to the accurate assessment of the  $C$  factor from the Kozeny-Carman equation (MacMullin and Muccini, 1956). In this sense, further research is needed in order to determine the value of  $C$  more accurately, considering especially that the experiments of the present research were carried out in model materials (i.e. defined particle size), as the final target shall be the application on natural soils. It is concluded that the Equivalent Capillary Model is suitable to define degrees of water repellency and to describe the general behavior of wetting kinetics of porous media. However, it still lacks of resolution in modelling the entire process, as also in estimating  $\theta_I$ , especially in porous media with significant particle diameter and with increasing water repellency. However, its reasonable accuracy and simplicity should be considered as significant advantages.

## Chapter 5

# Comparing capillary rise contact angles of soil aggregates and homogenized soil

### 5.1. Introduction

Wettability of soil affects physical properties at the soil surface such as aggregate stability, surface runoff and erosion, as well as processes in the unsaturated zone, like preferential flow and solute transfer. All these factors may have important implications on chemical and biological processes or, more general, on soil-water-plant interaction (Ellies et al., 2002a). To describe the wetting properties of soil, the soil-air-water contact angle (CA) is often used. The CA, in general, is a fundamental variable to describe interfacial properties (Zisman, 1964; Adamson, 1990) and in the past has also been used to describe the wetting behavior of porous media (Dullien, 1992; Marmur, 1992 and 2003), whereby an increasing CA indicates increasing water repellency. Quantitative wettability measurements of soil particles that eliminate factors modifying the wettability of real grain surfaces, like roughness and chemical heterogeneity, are almost impossible. Therefore, semi-quantitative methods like the Capillary Rise Method (CRM), the Sessile Drop Method (SDM) and the Wilhelmy Plate Method (WPM) are often applied to describe the soil wetting behavior with sufficient reproducibility (Bachmann et al., 2003).

Land use, especially in humus topsoil, often influences the wetting behavior of soil because of site-specific modifications of the quantity and quality of soil organic matter (SOM). Greater organic matter content tends to increase water repellency, which, in turn, increases the stability of soil aggregates against dispersion or slaking (Ellies et al., 2003). The effects of SOM on the wettability of particle surfaces can be very significant; even the presence of only a single molecular film of organic components can alter the wetting properties (Chenu et al., 2000; Ellerbrock et al., 2005). Different species of plants, kinds of manures or the soil tillage system can produce organic matter very different in quantity and quality (Woche et al., 2005). Pine forest

soils where organic matter has accumulated tend to be more water repellent ( $CA = 90^\circ$  or  $>90^\circ$ ) than agricultural soils, which often exhibit slightly reduced wettability (subcritical water repellency,  $CA < 90^\circ$  and  $> 0^\circ$ ) (Woche et al., 2005).

Under any land use or vegetation, the spatial distribution of organic matter in soils is influenced considerably by aggregation (Hassink and Whitmore, 1997). Different studies show that the distribution of soil organic matter differs with aggregate size (Balesdent et al., 2000; Ellies et al., 2002b). Further, Ellies et al. (1995) found that the organic matter content also depends on the location in the soil matrix, e.g. the skins of aggregates had different carbon content than the interior.

Aggregation also influences the development of flow paths in soils, so water transport is usually much different in intact vs. homogenized bulk soil. To date, however, bulk homogenized soil has been used for almost all CA measurements. As aggregation is an important physical process affecting parameters like aeration, water conductivity and protection of soil organic matter against degradation (e.g. Oades, 1993; Hassink and Whitmore, 1997; Huygens et al., 2005), it seems to be important to determine soil wettability not only for homogenized bulk soil but also for intact aggregates. The wettability of soil aggregates has been explicitly determined in only a few studies. For example, Hallett et al. (2001) assessed a water repellency index R for individual soil aggregates, from a range of cultivation practices with different fertilizer inputs. They found that a change from ploughing to zero-tillage could increase R by a factor of two in some cases. Further, soil aggregates from zero-tillage than from ploughed treatments were more repellent and that higher levels of N added to field soil did not affect R. Ellies et al. (2005) reported for peeled aggregates, sieved from volcanic ash soils, that the wetting resistance, determined with SDM on homogenized aggregate layers, increased from the exterior to the center of the aggregates. However, a direct comparison between the wettability of intact aggregates compared with corresponding homogenized aggregates is missing, mainly because standard methods have not been established to measure the wettability of soil aggregates. Hence, the objectives of the present study are to analyze the wetting behavior in terms of CAs of intact soil aggregates and to compare the results with those obtained by using the corresponding crushed aggregates. The latter preparation technique is the standard application of the CRM where, in practice, homogeneous powder generally should be used. The wettability of single aggregates is also determined in this study and compared with the CAs of packed intact aggregates or homogeneous

beds of soil. So three cases will be investigated: A system with inter- and intra- aggregate pore space (aggregate packings), a system with only intra-aggregate pore space (single aggregates), and a system with only inter-particle pore space (homogenized aggregates). To compare all soils the present research was focused on the 1-2 mm aggregate fraction which abundantly was found at all sites. Further, it was assumed that using this fraction allows also the determination of the CA with packings of aggregates due to sufficiently small inter-aggregate pores.

## **5.2. Methodology**

### **5.2.1. Materials**

The selection of the samples, aside from abundance of 1-2 mm aggregates, considered aspects like land use (forest, grassland, agricultural), type of manuring, texture, and total soil organic carbon content (SOC). Twelve samples from five sites, all located in Germany, were investigated. All samples were from humus horizons, which includes nine topsoils (B, H<sub>NPK</sub> 1, H<sub>FYM</sub> 1, RTM, SK, WS<sub>AEH</sub>) and three humus subsoils (H<sub>NPK</sub> 2, H<sub>FYM</sub> 2, WS<sub>BH</sub>). The textures varied between sandy loam and silt loam. Steinkreuz (SK) and Waldstein (WS) have 11 and 30% gravel contents, respectively. The air-dried samples were prepared according to the procedure established by Goebel et al. (2004). The dry material was gently sieved to the fraction 1-2 mm by preserving the small aggregates. A part of the 1-2 mm fraction was homogenized by gentle crushing to give visually a single-grain structure.

The total organic carbon content was bigger for the two forest soil (SK and WS), smaller for the agricultural soils (B and H) and intermediate for the grassland soils (RTM). While the forest soils are acidic (around pH 3), the agricultural soils showed pH values between 6 and 7. The pH of the grassland soils ranges from 3.1 to 4.5, depending on the kind of manure. The forest soil horizons generally had higher organic carbon contents of 4.6 to 6.1%, whereas all other samples had a range from 0.3 to 1.4%. Locations and basic soils data are given in Tables 5 and 6. More details of the soils can be found in Woche et al. (2005).

### **5.2.2. Contact angle measurements**

Fig. 24 shows the experimental set-ups for the three different methods of wettability measurements in natural soil samples.

**Table 5:** Location and land-use data of the samples.

Site, horizon, manure variant, depth	Designation	Coordinates	Soil type (parent material)	Land use
Banteln Ap 0-30 cm	B <sub>Ap</sub>	52° 05'N, 9° 45'E	Luvisol (loess)	Agricultural (wheat)
Halle Ap NPK 0-30 cm Ah NPK 30-60 cm AP FYM 0-30 cm Ah FYM 30-60 cm	H <sub>NPK</sub> 1 H <sub>NPK</sub> 2 H <sub>FYM</sub> 1 H <sub>FYM</sub> 2	51° 30'N, 11° 57'E	Chernozem (loess)	Agricultural (maize)
Rotthalmuenster Ah 0-6 cm N control NPK, acid NK, alkaline NK, acid	RTM 1 RTM 2 RTM 3 RTM 4	48° 22'N, 12° 13'E	Gleyic Luvisol (loess)	Grassland
Steinkreuz Ah 0-5 cm	SK <sub>Ah</sub>	49° 54'N, 10° 22'E	Dystric Cambisol (sandstone with clayey and silty intersections)	Forest ( <i>Fagus sylvatica</i> )
Waldstein Aeh 0-10 cm Bh 10-12 cm	WS <sub>Aeh</sub> WS <sub>Bh</sub>	50° 06'N, 12° 06'E	Haplic Podzol (granitic solifluction layer)	Forest ( <i>Picea</i> sp.)

NPK: Nitrogen phosphorus potassium manure.

FYM: Farmyard manure.

**Table 6:** Data of particle-size distribution, total organic carbon content (SOC), and pH (all determined on bulk soil < 2 mm diameter).

Soil	Particle-size distribution (%)				Texture class	SOC (%)	pH <sub>CaCl2</sub>
	Gravel	Sand	Silt	Clay			
Ap	0	5.7	81.9	12.4	Silt loam	1.33	7.2
Ap	0	69.0	23.0	8.0	Sandy loam	0.90	5.8
Ah	0	69.0	23.0	8.0		0.30	6.5
AP	0	69.0	23.0	8.0		1.56	5.8
Ah	0	69.0	23.0	8.0		0.81	7.3
N	0	8.3	72.2	19.5	Silt loam	2.38	4.5
NPK	0	8.3	72.2	19.5		2.28	3.4
NK	0	8.3	72.2	19.5		2.81	4.3
NK	0	8.3	72.2	19.5		2.76	3.1
Ah	2	54.9	35.1	10.0	Sandy loam	7.00	3.2
Aeh	30	47.4	37.9	14.7	Loam	3.80	2.8
Bh	30	43.2	41.6	14.7		9.30	3.2

The Capillary Rise Method (CRM) is commonly performed with homogenized material (Fig. 24A) which is filled into a glass tube with a sintered bottom. A weight of approximately 50 g was placed on top of the sample, compacting it slightly, in order to improve the replication of bulk density between measurements. To avoid heaving of the sample surface during liquid penetration, the empty portion of the sample glass was filled with a sand layer. Before the measurement, the resulting filling height of the sample was recorded to calculate the bulk density. The glass was then lowered to the liquid surface of the reservoir, until the sintered glass bottom touched the liquid surface. The change in mass of the sample was recorded until the final height of the capillary uptake was reached. In extension to the regular CRM technique, aggregates were also investigated, either by using packings of aggregates or single aggregates according to Goebel et al. (2004, 2007). For the measurements of aggregate packings, the samples were prepared using a similar approach, apart from the additional pressing and with no sand coverage (Fig. 24B). The CA was determined according to Bachmann et al. (2003) and Goebel et al. (2004) with a dynamic contact angle tensiometer (DCAT 11, DATA PHYSICS; Filderstadt, Germany; resolution  $10^{-5}$  g,

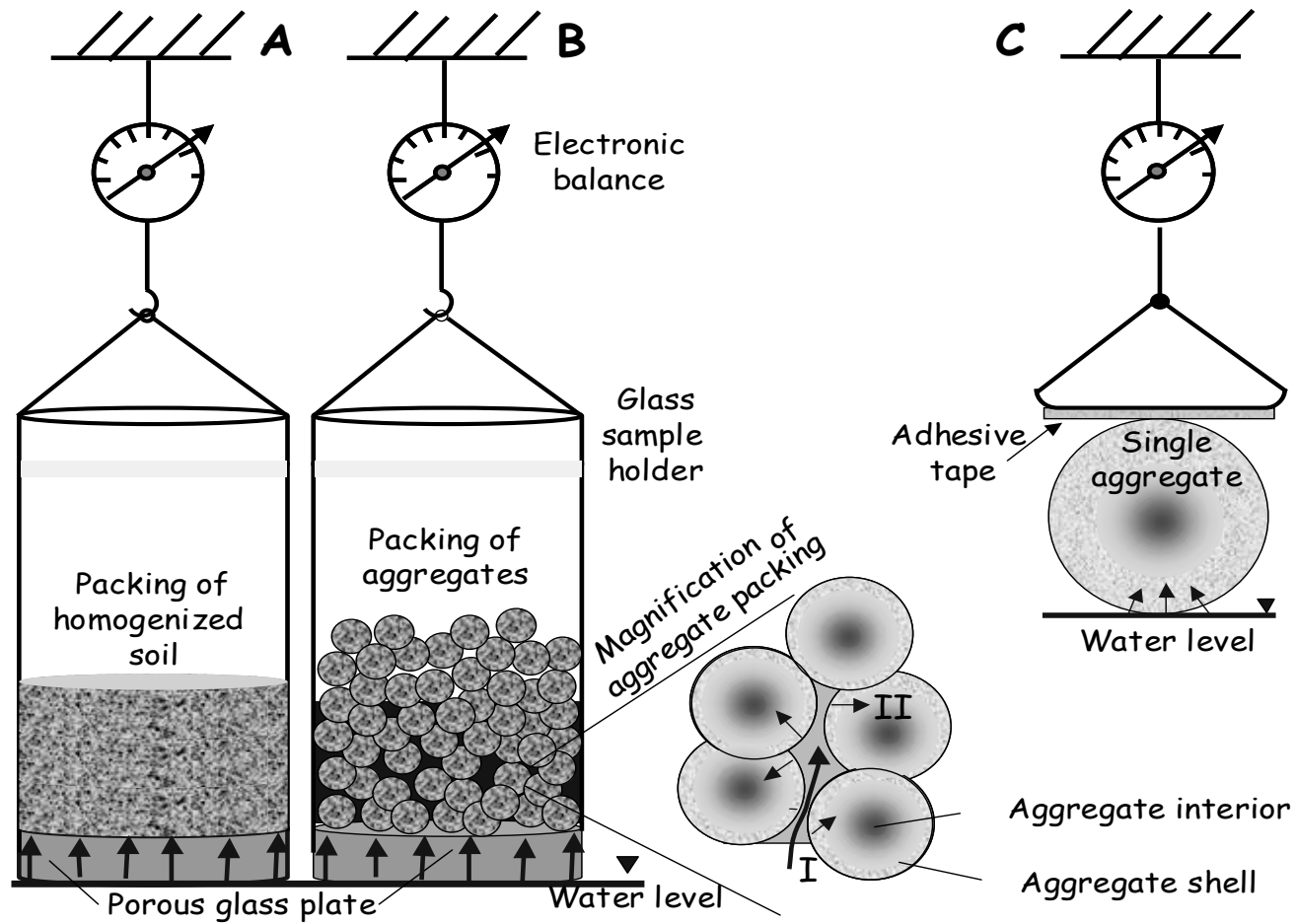


**Fig. 24** Scheme of Capillary Rise Method (CRM) sample arrangement for homogenized aggregates (A), aggregate packings (B) and single aggregates (C). The testing fluid is on a lifting stage to establish contact with the sample.



frequency of data sampling 20-30 s<sup>-1</sup>). The mass increase of the sample during the capillary rise is recorded as a function of time  $W = f(t)$  by the high precision balance. At the start of the test the balance is tared, so the mass increase corresponds to the mass of fluid sorbed by the sample. At least two independent measurements have to be made with a similar pore structure, e.g. indicated by the bulk density of the sample (Siebold et al., 1997). The contact angle  $\theta^{\text{CRM}}$  is calculated with the Washburn equation, which is derived from Poiseuille's law of liquid flow through a capillary tube (Washburn, 1921):

$$x^2 = \frac{r\sigma\cos\theta}{2\eta}t \quad (31)$$

where  $x$  is the height of the rising liquid front in the column (m),  $r$  is the effective radius of the uniform pores (m), that represents the idealized pore system of the granular material,  $\sigma$  is the surface free energy or surface tension of the liquid (mN m<sup>-1</sup>),  $\eta$  is the viscosity of the liquid (kg m<sup>-1</sup> s<sup>-1</sup>) and  $t$  is the time (s). From Eq. (31) an expression for the mass increase of the soil during the capillary rise process can be derived (Siebold et al., 1997). This expression can be written as:

$$W^2 = K \frac{\rho^2\sigma\cos\theta}{2\eta}t \quad (32)$$

where  $W$  is the weight increase of the sample (kg),  $\rho$  is the liquid density (kg m<sup>-3</sup>), and  $K$  is a geometry factor (m<sup>5</sup>) that reflects the porosity and tortuosity of the capillaries, and depends on particle-size and bulk density. If a liquid with a non-zero contact angle is used, two unknown variables have to be determined in Eq. (32). For this, the factor  $K$  has to be evaluated independently in a second run using the same soil with identical bulk density and by using a reference liquid, generally n-hexane, that wets the soil particles completely ( $\theta = 0^\circ$ ). The accurate determination of  $K$  is essential for a correct application of the modified Washburn equation. It is noted that the Washburn equation only accounts for the capillary pressure and not for the hydrostatic pressure. However, considering only the early stages of capillary rise, the hydrostatic pressure can be approximately neglected, because its contribution is very small in comparison to

capillary pressure (Washburn, 1921). For a more detailed description of the methods see Bachmann et al. (2003) and Goebel et al. (2004).

The difficulty in achieving a constant bulk density to insure that  $K$  is similar between water and n-hexane measurements is one important source of error of CRM. Bulk densities were controlled by using the information of sample weight (g), filling height (cm) and internal diameter of the glass tubes (0.9 cm) of each sample preparation. On average, the differences in bulk density for measurements with water and n-hexane, respectively, were smaller than  $0.02 \text{ g cm}^{-3}$  for aggregate packings and smaller than  $0.03 \text{ g cm}^{-3}$  for homogenized aggregates. Table 7 shows the bulk densities. Aggregate packings were  $0.25 \text{ g cm}^{-3}$  less dense than homogenized samples.

The CA for the homogenized and aggregated material of the 12 samples was determined by averaging four replicates. The fitting ranges usually were 1-3 s for n-hexane and 2-5 s for water. In general, the relation  $W^2 = f(t)$  can be expected to be linear for homogeneous packings of non-swelling particles when gravity has minor impact. This standard experimental set-up (method A, Fig. 24) is described in detail by Siebold et al. (1997). To test further the liquid penetration characteristic of coarse material comparable with the aggregate size, homogeneous packing of a coarse sand fraction 1-2 mm were also investigated (Fig. 25).

After 5 s, the filling of the pore space is completed for water and further reduced mass increase is probably caused by the vertical migration of water across the inner glass walls above the sample. From these results it is concluded that the liquid uptake with a clear linear characteristics of  $W^2 = f(t)$  takes approximately 5 s for water in the sand. The corresponding time for n-hexane was about 3 s resulting in a mean CA of about  $61^\circ$ . For the packings of aggregates, the inter-aggregate pore space was estimated as the mean of the possible packing of spheres (cubic, tetragonal, pyramidal, tetrahedral) resulting in an inter-aggregate macropore volume of about 34%. For water a quite good agreement between calculated and measured values have been found for the B, H and  $WS_{Bh}$ , while for RTM, SK and  $WS_{Aeh}$  with higher CA, the amount of water recorded did not fill the entire inter-aggregate pore space before the transition from the first linear slope to the curvilinear part of the infiltration curve was observed. An increasing CA leads to a lower final capillary rise height in the macropore system according to the general capillary rise equation, including in the inverse relation between capillary height and equivalent pore size radius

**Table 7:** Bulk density  $\rho_B$  ( $\text{g cm}^{-3}$ ) and standard deviation (SD) of sample tubes filled with aggregates packings and with homogenized aggregates.

Soil	Water				n-Hexane			
	Aggregates		Homogenized A		Aggregates		Homogenized A	
	$\rho_B$	$\pm\text{SD}$	$\rho_B$	$\pm\text{SD}$	$\rho_B$	$\pm\text{SD}$	$\rho_B$	$\pm\text{SD}$
B <sub>Ap</sub>	0.91	0.02	1.23	0.03	0.91	0.03	1.21	0.06
H <sub>NPK</sub> 1	0.91	0.01	1.32	0.06	0.96	0.04	1.32	0.09
H <sub>NPK</sub> 2	0.95	0.04	1.38	0.07	0.90	0.02	1.31	0.05
H <sub>FYM</sub> 1	0.97	0.01	1.40	0.04	0.95	0.02	1.40	0.05
H <sub>FYM</sub> 2	0.93	0.02	1.38	0.00	0.94	0.05	1.37	0.03
RTM 1	0.65	0.02	0.89	0.03	0.58	0.01	0.85	0.00
RTM 2	0.67	0.02	0.91	0.03	0.66	0.01	0.91	0.08
RTM 3	0.72	0.02	0.90	0.02	0.67	0.03	0.87	0.03
RTM 4	0.66	0.03	0.90	0.02	0.61	0.02	0.88	0.03
SK <sub>Ah</sub>	0.56	0.02	0.94	0.03	0.56	0.02	0.93	0.02
WS <sub>Aeh</sub>	0.74	0.02	1.11	0.03	0.77	0.04	1.08	0.06
WS <sub>Bh</sub>	0.79	0.04	1.09	0.06	0.80	0.06	1.10	0.04

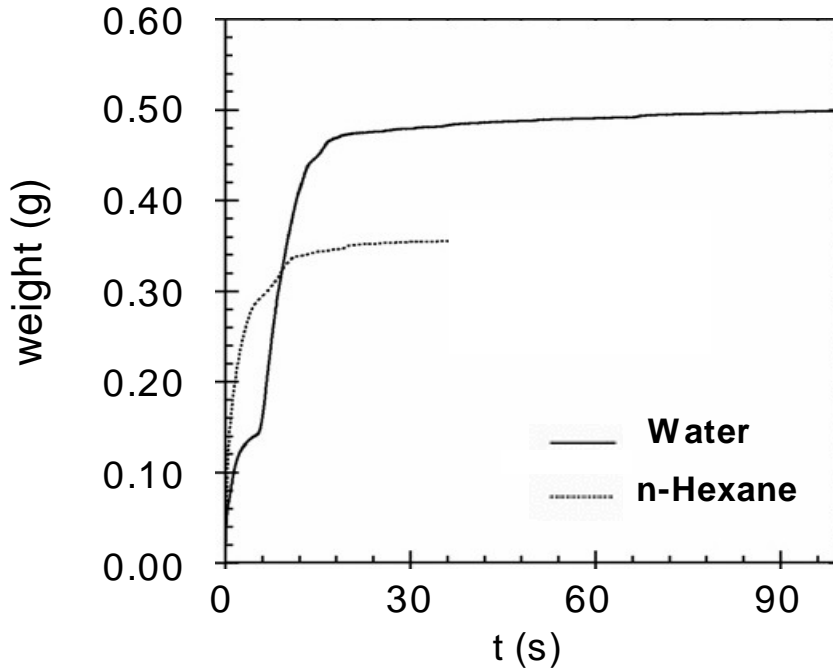


**Fig. 25** Weight increase as a function of time for sand fraction 1-2 mm,  $\theta^{\text{CRM}} = 61^\circ$ .

(Marmur, 1992). Fitting ranges for aggregate packings for Slope I were 1-3 s for n-hexane and 2-5 s for water. Within this interval, at least 30% of the entire liquid uptake was reached. Regarding Slope II, fitting ranges varied for individual soils, but mostly were within the range of 8-60 s for n-hexane and water. The Slope II time interval was considered as not so well defined as Slope I, but approximately started at filling heights around 55 to 60% of the total pore volume. However, due to the relatively poor definition of this interval, one of the objectives was therefore to test the agreement of this approach with independent measurements as described below.

Wetting properties inside the aggregates were measured using single aggregates (method C, Fig. 24). Aggregates were selected for similar shape and weight to make them comparable as much as possible. Single aggregates (1-2 mm) of each soil sample were selected randomly for the CA determination and combined to give two subgroups with the same number of aggregates and similar total aggregate mass. They were fixed using adhesive tape to the DCAT (Goebel 2007; Fig. 24C). The fitting range here considers the whole infiltration process from the first contact with the fluid until saturation. For each soil, 6 to 10 replications were made with n-hexane and with water, respectively. The fitting range for single aggregates was soil-dependent but generally in the range 0.05 - 0.4 s for both liquids.

Some aggregates dispersed after full saturation with water (Fig. 26, left). However, in all cases the destruction of aggregates always occurred after saturation and could be distinguished very clearly from the weight changes caused by infiltration. The average slopes for each liquid were calculated after elimination of the extreme curves (curves outside the confidence interval of the remaining curves), always keeping a minimum of at least 6 individual measurements.

### **5.3. Results and discussion**

First is presented the general shape of the infiltration curves for water and n-hexane, for the methods A to C. Fig. 27 shows typical results for an almost water-repellent soil ( $WS_{Bh}$ , forest) and for a wettable soil ( $H_{NPK}$  1, arable land). In Fig. 27 are displayed the curves as  $W = f(t^{1/2})$  to allow a comparison of the absolute mass changes, according to the different methods rather than linear time behavior. Generally, the n-hexane curves of the two soils were quite similar, whereas the water curves show distinctly different slopes, particularly for the measurement of aggregate packings. Results for the homogenized samples as the standard preparation technique for CRM

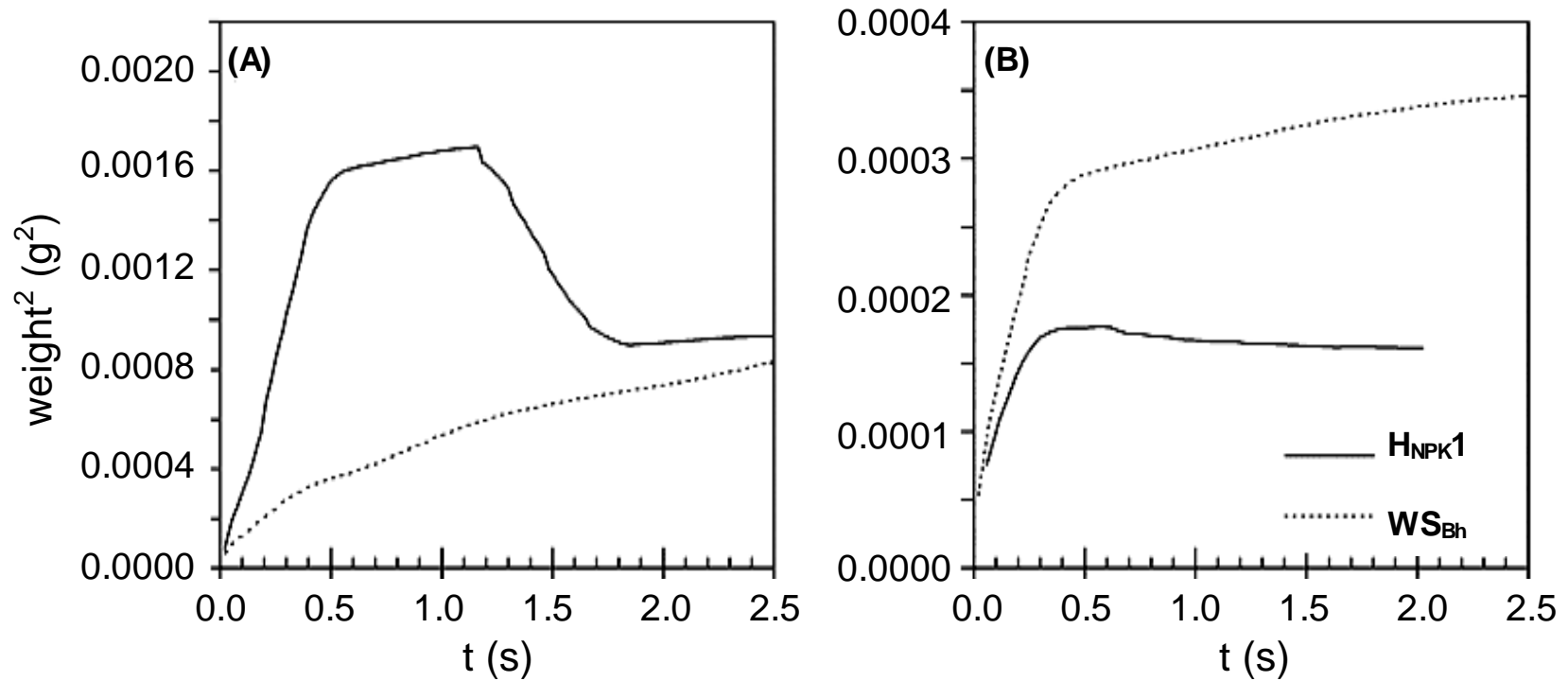


**Fig. 26** Weight increase (squared,  $W^2 = f(t)$ ) as a function of time in single aggregates, for the sites Halle and Waldstein. The decrease in weight for Halle after 1.3 s (water) corresponds to the dispersion of the aggregate.

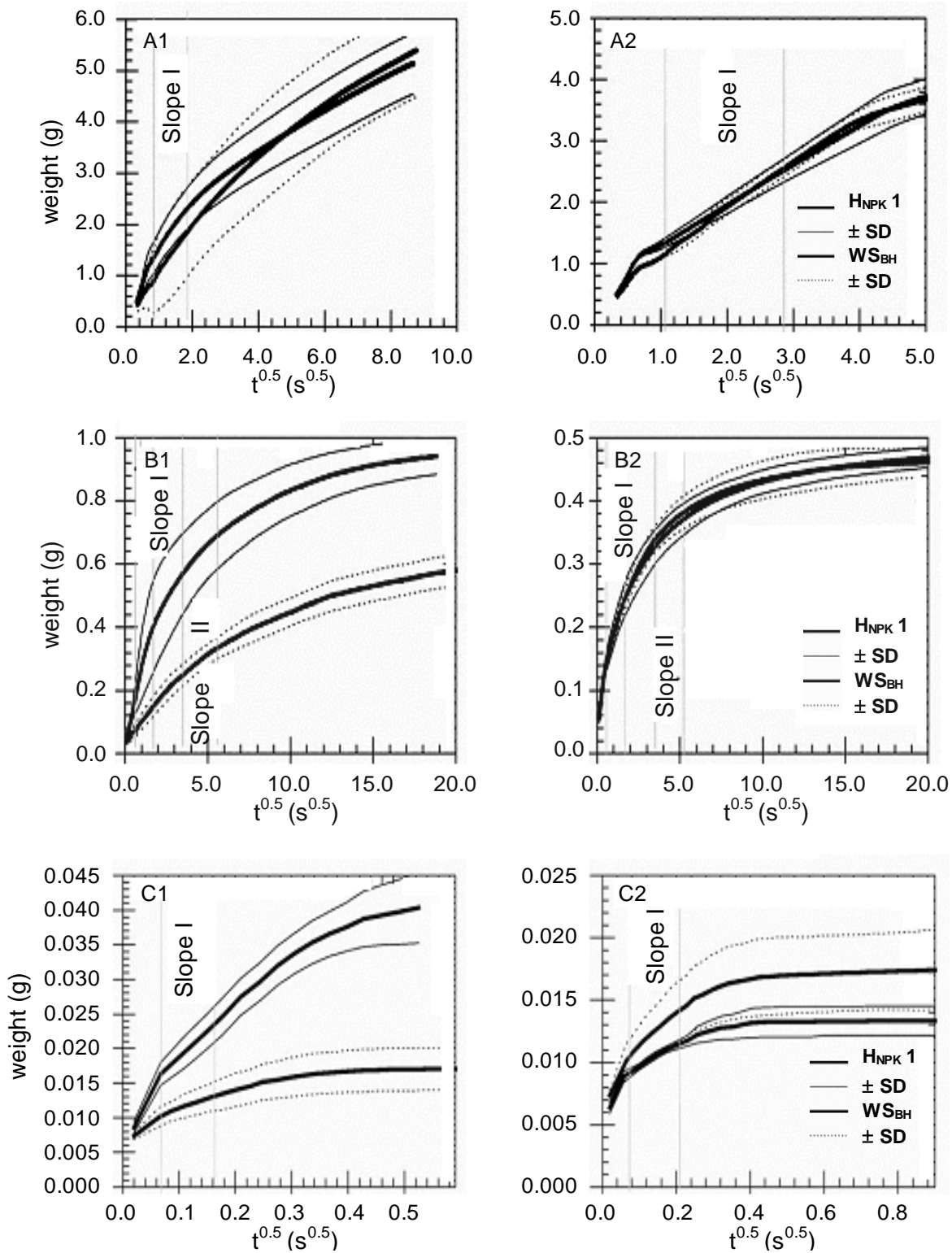


**Fig. 27** Water (1) and n-hexane (2) uptake curves  $W = f(t^{1/2})$  for the wettable soil Halle H<sub>NPK</sub> 1 and the almost non-wettable forest soil Waldstein WS<sub>BH</sub>. A: Homogenized aggregates, B: Aggregate packings, C: Single aggregates. Also indicated are the domains for analyzing Slope I (homogenized aggregates, single aggregates) and Slope I/II (aggregate packings) by grey vertical lines. Note the different scales between the graphics.

(Fig. 27A), show the linear slope of the water uptake curve, which can be observed after 2 to 10 s. For n-hexane and water the slopes here were quite similar, resulting in CAs of  $62 \pm 11^\circ$  for  $H_{NPK} 1$  and  $77 \pm 6^\circ$  for  $WS_{BH}$  (Table 8). Here a rapid linear increase for water within an interval of 1-5 s was observed. For single aggregates (Fig. 27C), the results were different: for the Waldstein forest soil, the infiltration rates into the aggregates are generally low during the entire infiltration process, whereas the Halle soil aggregates adsorbed water much faster. Greater slopes for water of the  $H_{NPK} 1$  curves (Fig. 27B, C) resulted in a distinctly smaller CA as compared to  $WS_{BH}$  (Table 8). In contrast, the graphs obtained for aggregate packings (Fig. 27B) seemed to indicate two linear domains (two-slope behavior; Goebel et al., 2004; Goebel et al., 2007) before the curve turns into the non-linear stage, which ends up with the zero slope after saturation or after reaching the final capillary rise height. The first slope was apparently associated with the rapid infiltration into the inter-aggregate (macropore) system (process I, Fig. 24B). The second slope seemed to be more attributed to the infiltration into the intra-aggregate pore space (process II, Fig. 24B) from the already filled inter-aggregate pore space. These processes were probably not exactly defined on the time scale, since both infiltration processes may have overlapped to a certain extent. However, such a two-slope infiltration behavior was not observed for capillary rise experiments done with samples without inter-aggregate porosity by Goebel et al. (2004), who used solid GB packings of 1-2 mm diameter, or for the coarse sand measurement shown in Fig. 25. The corresponding curves for the CA determined for aggregate packings and single aggregates and organic carbon content. According to Ellies et al. (2003) and Woche et al. (2005), pH may be considered as a suitable qualitative indicator for organic matter composition to predict the general wetting behavior of terrestrial soils. A linear regression analysis for the relation  $CA = f(\text{pH})$  for the CA determined from Slope I gave  $R^2 = 0.56$  and for Slope II  $R^2 = 0.57$ . For the single aggregates a higher coefficient of determination of about  $R^2 = 0.76$  was obtained, whereas for the homogenized material  $R^2$  was  $<0.1$ . In line with the pH variations, differences between arable land and other land-use systems were clearly detectable for the CA measurements by using intact aggregates, no matter if packings of aggregates or single aggregates were analyzed. Physical abrasion, reduced fungal populations and organic matter mineralization could all potentially diminish CA in arable soils (Hallett et al., 2001). Differences in wetting behavior between different land uses were not found by the conventional homogenized sample, already indicated by the low correlation of CA with pH. For minor pH variations (Rotthalmuenster, profiles 2 to 4), a similar correlation of CA and pH was not observed.

**Table 8:** Results of CRM measurements: contact angle ( $\theta^{\text{CRM}}$ ) and wetting coefficient (k).

Soil	Aggregate packing				Single aggregates		Homogenized aggregates	
	Slope I		Slope II		k = cos $\theta$	$\theta^{\text{CRM}}$	k = cos $\theta$	$\theta^{\text{CRM}}$
	k = cos $\theta$	$\theta^{\text{CRM}}$	k = cos $\theta$	$\theta^{\text{CRM}}$				
B <sub>Ap</sub>	1.645±0.965	0	2.599±1.369	0	2.798±0.686	0	0.325±0.117	71±7
H <sub>NPK 1</sub>	0.955±0.126	19±15	0.961±0.323	23±26	2.877±0.969	0	0.460±0.171	62±11
H <sub>NPK 2</sub>	1.264±0.280	0	1.736±0.133	0	0.999±0.208	17±20	0.430±0.109	64±7
H <sub>FYM 1</sub>	0.916±0.124	20±18	1.203±0.185	0	1.971±0.357	0	0.393±0.100	67±6
H <sub>FYM 2</sub>	0.667±0.068	48±5	1.470±0.194	0	2.500±0.433	0	0.443±0.100	64±6
RTM 1	0.100±0.023	84±2	0.248±0.017	76±1	0.217±0.033	77±2	0.266±0.091	75±5
RTM 2	0.806±0.316	29±33	2.338±0.779	0	0.323±0.185	71±11	0.594±0.008	54±1
RTM 3	0.074±0.023	86±1	0.120±0.042	83±2	0.048±0.010	87±1	0.462±0.127	62±8
RTM 4	0.040±0.010	88±1	0.127±0.030	83±2	0.083±0.020	85±1	0.367±0.184	68±11
SK <sub>Ah</sub>	0.014±0.001	89±0	0.023±0.006	89±0	0.033±0.036	88±2	0.220±0.107	77±6
WS <sub>Aeh</sub>	0.083±0.015	85±1	0.129±0.038	83±2	0.479±0.287	59±21	0.277±0.122	74±7
WS <sub>Bh</sub>	0.252±0.033	75±2	0.481±0.134	61±9	0.230±0.132	77±8	0.432±0.253	63±18



However, due to the relatively small number of samples we only can draw some preliminary conclusions about the wetting behavior of aggregates in relation to land-use systems. It was found for some completely wettable soils that the cosine of the CA was  $>1$  (Table 8). In this case, CAs were defined as zero. Due to the non-linearity of the  $\cos\theta$  to  $\theta$  relation and the restricted values between -1 and 1, some differences observed become much more pronounced when considering  $\cos\theta$  instead of the CA itself. The wetting coefficients ( $k$ ) were significantly greater than unity for  $B_{Ap}$  (single aggregates),  $H_{NPK}$  2 (aggregate packing, single aggregates),  $H_{FYM}$  1 (S2 and single aggregates),  $H_{FYM}$  2 (S1 and single aggregates) and RTM 2 (S2). They indicate extremely good wettability, enhancing the absolute differences observed between aggregates and homogenized material in terms of  $k$  (see Table 8).

Table 9 shows the P-values obtained by a t-test (two-tailed) for differences in mean wetting coefficient  $\cos\theta$  measured on homogenized aggregates, single aggregates and aggregate packings. The statistical analysis of the data indicated for most soils that there were no significant differences between mean  $\cos\theta$  measured on single aggregates and those obtained from aggregate packings (Slope II). This supports the assumption that the information gained from Slope II in measurements of aggregate packings can be attributed to the wetting properties of the aggregate interior. On the other hand, for the arable soils there were significant differences between mean  $\cos\theta$  measured on homogenized aggregates and those calculated from Slope II (aggregate packings). The fact that CAs measured on homogenized aggregates were significantly ( $P < 0.001$ ) larger than those determined on single aggregates and on aggregate packings (Slope II) supports this assumption statistically. Results show further that the standard deviation (SD) of the determination of  $\cos\theta$  and CA, given in Table 8, seems not to be related specifically to the type of sample preparation (aggregate packing, single aggregate and homogenized aggregates). The tendency of increasing SD with decreasing CA was observed, as evident from linear regression. This probably indicates greater spatial and quality heterogeneity of the matrix for small CA.

#### **5.4. Conclusions**

According to Siebold et al. (1997), the packing procedure is one of the most sensible factors to ensure reproducible results with the Capillary Rise Method (CRM). It was found that for

**Table 9:** P-values for differences in mean wetting coefficient  $k=\cos\theta$  obtained for homogenized aggregates, single aggregates and aggregate packings of the soils investigated.

Soil	HOM <sup>A</sup> vs. AGG <sup>B</sup>	S1 <sup>C</sup> vs. AGG	S2 <sup>D</sup> vs. AGG	S1 vs. HOM	S2 vs. HOM
B <sub>Ap</sub>	0.005 <sup>**E</sup>	n.s.	n.s.	n.s.	0.044*
H <sub>NPK 1</sub>	0.014*	0.027*	n.s.	0.003**	0.045*
H <sub>NPK 2</sub>	0.006**	n.s.	n.s.	0.001**	0.000***
H <sub>FYM 1</sub>	0.000***	0.001**	n.s.	0.001**	0.000***
H <sub>FYM 2</sub>	0.002**	0.003**	n.s.	0.004**	0.000***
RTM 1	n.s. <sup>F</sup>	0.001**	n.s.	0.013*	n.s.
RTM 2	n.s.	n.s.	0.008**	n.s.	0.041*
RTM 3	n.s.	0.016*	0.001**	n.s.	n.s.
RTM 4	n.s.	0.007**	n.s.	n.s.	n.s.
SK <sub>Ah</sub>	0.016*	n.s.	n.s.	0.031*	0.034*
WS <sub>Aeh</sub>	n.s.	n.s.	n.s.	0.049*	n.s.
WS <sub>Bh</sub>	n.s.	n.s.	0.036*	n.s.	n.s.

<sup>A</sup>: HOM =  $\cos\theta$  obtained for homogenized aggregates.

<sup>B</sup>: AGG =  $\cos\theta$  obtained for single aggregates.

<sup>C</sup>: S1 =  $\cos\theta$  obtained for aggregate packings (Slope I).

<sup>D</sup>: S2 =  $\cos\theta$  obtained for aggregate packings (Slope II).

<sup>E</sup>: \*\*\* =  $P < 0.001$ ; \*\* =  $0.001 < P < 0.01$ ; \* =  $0.01 < P < 0.05$ .

<sup>F</sup>: n.s. = Not significant value ( $P > 0.05$ ).

conventional (homogenized) samples as well as for aggregate packings, good reproducibility of sample bulk density density was achieved, as indicated by the variance of the bulk densities. In line with the findings of Goebel et al. (2004), the experiments have shown that CRM can be applied not only on homogenized soil (the standard sample preparation technique), but also by using single aggregates or aggregate packings. Liquid uptake curves for aggregate packings shown a two-slope behavior, which was interpreted as the transition process of rapid inter-aggregate liquid uptake (Slope I) and subsequent infiltration into aggregates (Slope II). Data derived from Slope II agreed surprisingly well with the CA approximately from individual aggregates, except for one sample (RTM 2). This result was not obvious, because the dynamics of liquid uptake was different between single aggregates and aggregate packings. Additionally, it

could also be demonstrated that the CRM technique could be applied to individual small aggregates of 1 to 2 mm in diameter. Single liquid uptake curves for individual aggregates also shown in some cases a great deal of variability compared to the mean of all replicates for a particular soil. This was probably caused by the small-scale pore and aggregate surface structure. However, the standard deviation of the CA obtained on single aggregates was comparable with the other modes.

Contact angles (i.e.  $k = \cos\theta$ ) determined for aggregate packings and single aggregates were similar to homogenized aggregates only for the grassland and forest soils (RTM, SK and WS) but not for the agricultural soils (B and H). A comparison of the texture of the B and RTM samples (both silt loam) exclude a systematic impact of soil texture on this effect. The soils with low pH (RTM, SK and WS) show relatively high CAs at the aggregate surface (Slope I) and also high CAs inside the aggregate (Slope II). Homogenized aggregates had only slightly smaller CA which indicates a homogeneous distribution of hydrophobic organic components within the entire aggregate. The soils with generally lower carbon content and higher pH (B and H) were characterized by small CAs of the aggregates (surface and inside the aggregate), but rather uniform CAs for homogenized material. In this case it was assumed that for the undisturbed aggregates potentially hydrophobic organic matter was not exposed on pore surfaces and had low impact on the water infiltration rate. The example using 1-2 mm aggregates suggests that the wetting behavior, particularly of arable soils, is a complex property that cannot be easily assessed by standard CRM measurements using homogenized soil samples. Whenever possible, CRM measurements should include investigations of intact aggregates and the wetting coefficient  $k = \cos\theta$  should also be considered to distinguish clearly between completely wettable soils and soils with very small levels of repellency. Finally it should be noted that the methods proposed are only applicable to soil with CA  $>0^\circ$  to CA  $<90^\circ$ . The measured CA with the CRM should also only be considered as a relative value in order to distinguish the wetting behavior of soil. It is finally concluded, that this study may have direct implications on the investigation of a wide range of physical processes in soil. These include overland and preferential flow, wetting properties following organic amendments and soil stability to slaking stresses.

## Chapter 6

# Final discussion and conclusions

The present thesis was focused on testing different experimental approaches to assess the wettability in porous media, regarding especially a future application to natural soils. It is organized in a series of individual chapters, covering in detail the different objectives of the entire research. Chapter 1 introduced the general problem and the objectives of the entire research. Chapter 2 evaluated different experimental methods assessing CA (CRM, WPM and SDM) and compared the results with the capillarity of the same porous media including the impact of gravity. These evaluations were applied to a set of model materials with different degrees of water repellency. Chapter 3 compared two of the methods under test (CRM and WPM) in assessing the CA and surface free energies. Chapter 4 focused on the experimental validation of a new generalized Lucas-Washburn model for characterization of capillary rise and estimation of CA in porous media. The model is based on the assumption that an equivalent capillary, representing the average properties of the porous system, can be defined. This evaluation was applied, as in the previous experiments, to a set of model materials with different degrees of water repellency. In Chapter 5, the suitability of the standard CRM in describing the wetting behavior of real soil samples is tested. This evaluation was focused on comparing the CAs of intact aggregates versus the corresponding homogenized material.

In this context, two main hypotheses were established:

- I. CRM usually overestimates CAs in comparison with other experimental approaches due to different factors (i.e. porous-system geometry), resulting in verifiable deviations from the equilibrium or intrinsic CA.
- II. WPM can be used as a reliable and accurate method for the estimation of the CA of soil material.

## 6.1. Experimental and theoretical assessment of wettability in model porous media

The main conclusions regarding the comparison of the different experimental approaches assessing CA and surface free energy can be summarized as follows:

### assessing contact angles

- *CRM showed a more restricted range in relation to the others approaches, with a significant overestimation of the CA, especially in the small diameter range (silt and GB 40-70  $\mu\text{m}$ ) and in the wettable domain ( $\text{CA} < 60^\circ$ ). However, as CRM never estimates a  $\text{CA} = 0^\circ$ , it is difficult to completely elucidate if this overestimation is due to the effect of dynamic and/or geometric factors.*
- *WPM shows a monotonic relation between CA and water repellency, with a significantly better resolution than CRM. Both advancing and receding CA showed a strong dependency on the set-up parameters as immersion speed and depth, although their mean CA (equilibrium CA) tends to remain stable in almost all cases.*
- *WPM (equilibrium approach) and SDM showed a better agreement with the equilibrium CA measured in segmented columns with increasing water repellency (both in homogeneous and mixed wettability), than CRM and WPM (dynamic approach).*

### assessing surface free energies and predicting contact angles

- *The critical surface tension ( $\sigma_C$ ) estimated according to the method proposed by Zisman (1964) showed a decrease with higher water repellency, with some irregularities observed for CRM. Both WPM approaches (dynamic and equilibrium) estimated very similar values of  $\sigma_C$  for all samples.*
- *The equation of state applied, based on the assessment of the components of the Young equation and the Girifalco's interaction parameter, showed a low resolution capacity in predicting CAs for all materials with WPM-ACA.*

### testing the Equivalent Capillary model for capillary rise

- *The model is based on a generalization of the Lucas-Washburn equation, however, the linearity predicted by this relation between the liquid uptake versus time was not observed when the entire capillary process (near one week) is considered. A reasonable fit between experimental data and the model is observed when only the initial section of the wetting process is considered (within the first 24 hours of the process).*

- *The C factor of the Kozeny-Carman equation, a well-known expression relating permeability to texture properties, showed values of 0.27 and 0.16 for sand and GB 150-250  $\mu\text{m}$ , and  $<0.1$  for silt and GB 40-70  $\mu\text{m}$ . As GB have a near-perfect sphere shape and C is also defined as the product between tortuosity and shape, the low value of C in silt and GB 40-70  $\mu\text{m}$ ) can be explained by the high tortuosity of the pore system.*
- *The estimated dynamic CA is overestimated in almost all samples compared to the equilibrium CA, estimated from capillary pressure-saturation curves. The intrinsic CA shows a significant decrease in relation to the dynamic CA for silt and GB 40-70  $\mu\text{m}$  (up to  $70^\circ$ ), but is small for sand and GB 150-250  $\mu\text{m}$  ( $<15^\circ$ ). These results suggest a lack of resolution of the wetting model related to the geometry of the test medium, although aspects like simplicity of application and reasonable fit should be considered as advantages for future research.*

Considering that different CAs can be estimated for the same porous system, a logical discussion is related to the question which CA represents in a better way the wetting behavior of the sample, as also which method has to be used. Firstly, as already mentioned, it should be considered that all methods are approximations to the intrinsic or true CA of the Young equation, which at the same time requires a number of assumptions normally not observed in heterogeneous porous media (Sedev et al., 2004). In fact, the validity of the Young equation itself and its application are still a matter of discussion (Marmur, 1986 and 2003). For instance, as already mentioned in Chapter 2, multiple thermodynamic equilibrium states (metastability) are possible to observe on non-ideal surfaces, determining that a wide range of apparent CAs can be measured<sup>3</sup>. This is also valid when the difference between the dynamic and equilibrium CA is considered. Authors like Hoffman (1975), Grader (1986) and Siebold et al. (2000) correlated the difference dynamic-equilibrium CAs in terms of wetting kinetics. Such differences were experimentally demonstrated in this research, as the estimated CAs can be very different according to the method used. In the case of CRM (dynamic-advancing CA), Goebel (2007) observed that this approach apparently is biased according to texture-related characteristics (e.g. diameter of the particles). In the present research, differences were observed by comparing the dynamic versus equilibrium CA in near ideal systems (GB) and natural materials (silt and sand). The findings are in good agreement with authors like Ericksson et al. (2002) and more recently Czachor (2006). These authors found a

---

<sup>3</sup> Marmur, A. 2008. Personal communication. Department of Chemical Engineering, Technion-Institute of Technology. Haifa, Israel.

significant dependency between water repellency and the configuration of the pore-system in assessing higher dynamic CA with increasing tortuosity in porous media like soils and GB systems, validating affirmations of authors like Philips (1971) regarding the LW equation. The last author concluded that in some cases, the geometry of the pore system can be even more important than the true CA regarding the wetting behavior. It is then clear that the basic question which CA estimates the intrinsic or true CA of Young (1805) more accurately is still opened. An example for the extreme difficulty to characterize a sample in terms of CA is shown in Fig. 28. As observed, WDPT confirms the high hydrophobicity of the DCDMS-treated silt sample (CA >115°), although with CRM and even with WPM, some liquid uptake is observed. Different reasons can explain these discrepancies, such those related to the initial treatment (heat and/or DCDMS application), CA as a function of time, as also those related to the experimental methods themselves, reinforcing the observation that more than one unique apparent-CA can be measured on real surfaces (Marmur, 1986; Marmur and Cohen, 1997; Marmur, 2003; Czachor, 2006).

In determining which method is the most suitable one to describe the wettability, conclusions of authors like Grader (1986) should be taken into account. As previously mentioned in Chapter 4, this author affirmed that the dynamic CA (e.g. CRM) is the most important when the main objective is the characterization of the wetting process, as the value of the equilibrium CA does not provide any information in this sense. At the same time, different researches have been focused on finding methods approaching the intrinsic CA (Marmur, 2003; Czachor, 2006). Having this in mind, wetting behavior description should be focused on finding the most suitable experimental approach, according to the objectives of the research. When the objective is the determination of the intrinsic CA, the use of the standard bi-liquid CRM without the use of a correction factor regarding the geometry of the system should be avoided. This is especially important for samples with small hydrophobicity, considering the comparatively bad resolution of this method, and also for soil samples with significant amounts of silt and/or clay. In such cases, these materials proved to be sensitive to the geometrical arrangement of the particles, meaning that the packing procedure will be a critical factor (Siebold, 1997 and 2000). However, as already demonstrated in Chapter 5, CRM can render valuable information regarding the characterization of wetting behavior when the complete curves  $W = f(t)$  are considered. If the main objective is a fast characterization of the wetting behavior of a set of samples, WPM-ACA proved to be a very sensitive method for the whole range of hydrophobicity, and in combination



**Fig. 28** Evaluation of wettability for a DCDMS-treated sample of silt. A: Water Drop Penetration Time. B: Capillary Rise Method. C: Wilhelmy Plate Method.

with the receding CA allows to quantify the soil hysteresis (Morra and Della Volpe, 1998; Chibowski et al., 2002). In turn, when the objective is to estimate the intrinsic CA ( $\theta_1$ ), WPM-ECA should be preferred. Here, a crucial point is to determine the most correct measurement set-up for each case (e.g. preparation of the sample, immersion speed), a topic to be considered for future research. For example, in the present research, differences reaching up to  $40^\circ$  (WPM-ACA) were observed for the same sample, depending on the different pressure added to the particles on the adhesive tape. These considerations are also applicable when the objective is the assessment of the surface free energy components ( $\sigma$ ) of the Young equation. As already mentioned in Chapter 3, it must be considered that this relation assumes an equilibrium CA, resulting in errors in the estimation of  $\sigma$  if a dynamic CA is used (Morra and Della Volpe, 1998; Chibowski and Perea y Carpio (2002). At the same time, as previously mentioned in Chapter 4, when the objective is the modelling of the capillary process, limitations in the agreement between experimental and predicted values can be expected. In this sense, the Equivalent Capillary model, although valid, still is insufficient for the complete characterization of the entire process. Such



limitations can be expected according to authors like Stange (2003) and Fick and Borhan (2006). They demonstrated that the wetting process in microgravity conditions can be divided into three stages (inertial, convective loss of energy, and viscous regime). Siebold et al. (2000) divided it initially in two, inertial and viscous regime, where only for the second stage the linear relation between liquid uptake and time predicted by the LW equation is observed. According to the results of Chapter 4, an additional stage can be defined under gravity conditions, that means, where the capillary forces are considerably low, but still positive in relation to gravitation. During this stage, liquid uptake into the long columns was observed until the equilibrium is reached, near one week after the measurement started. The experimental test of the Equivalent Capillary model showed that this last stage can not be fitted with a satisfying correlation coefficient according to the already mentioned values suggested by Marmur and Cohen (1997).

As mentioned in Chapter 4, a significant factor to be considered for the accurate modelling of the capillary process is the geometry of the system (Czachor, 2006). Regarding the Equivalent Capillary model, this factor is related to the correct assessment of the factor C, which constituted a limitation to the results of the present thesis. The importance of C is demonstrated in Fig. 29, based on the same set of data already shown in Chapter 4 (silt, MW samples). Compared are the estimated values of the intrinsic CA ( $\theta_I$ ) using different values of C. As seen, starting from the dynamic CA ( $\theta_D$ ) estimated by applying the wetting model,  $\theta_I$  can range from  $0^\circ$  up to near  $45^\circ$  for the reference material, for values of C between 0.1 and 0.5. These results are in very good agreement with the theoretical conclusions of Marmur (2003).

Finally, according to Fick and Borhan (2006), a realistic model can only be expected when the whole wetting process can be predicted, something that is not yet possible. Future research on this topic should be focused on all possible sources of errors (ignored by the Lucas-Washburn equation) (Lavi et al., 2008), as also on the improvement of the description of geometry-related properties. As example, Shi and Gardner (2000) and Kalogianni et al. (2004) observed significant differences in the dynamic CA measured for swelling and non-swelling materials (silt and polymers, respectively), due to the fact that in the first materials the wetting process is usually more affected by the re-arrangement of the particles. This phenomenon was observed in the present research, in specific cases of the experiments with long columns, but not quantified. Shi and Gardner (2000) also demonstrated that the estimated CA can be significantly lower

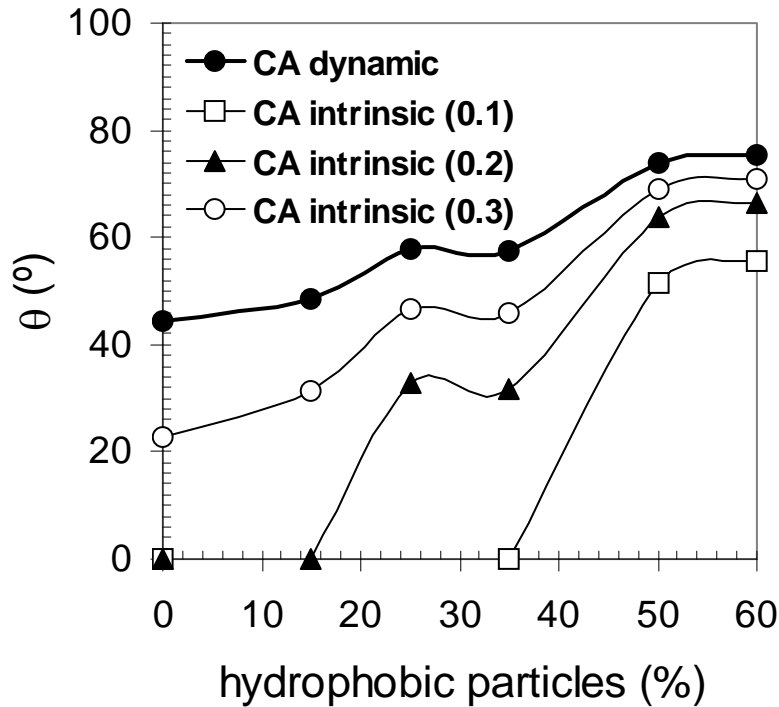


**Fig. 29** Intrinsic CA ( $\theta_i$ ) estimated from the dynamic CA ( $\theta_D$ ), according to the Equivalent Capillary Model, for different values of  $C$ . Example for silt (mixed wettability samples). The value of  $C$  is indicated in brackets.

when these processes are taken into account, which leads to the conclusion that the next stage in the modelling of wetting kinetics should necessarily include the concept of non-uniform porous-systems, as already investigated by authors like Erickson et al. (2002), who carried out numerical simulations of heterogeneous systems.

## 6.2. Evaluation of natural soils

In contrast to all other investigations, in Chapter 5 the wetting behavior of natural soil systems was evaluated with the standard CRM approach.

The main conclusions regarding this evaluation can be summarized as follows:

- *The CAs of aggregates were higher for grassland and forest in relation to arable lands. However, the homogenized aggregates showed similar CAs in all cases, meaning that different soils can have similar amounts of potentially hydrophobic components, demonstrating a significant dependence of the CA on the spatial distribution of the organic matter at the aggregates-scale.*

- *The evaluation of packings of intact soil aggregates and single aggregates showed good and consistent levels of reproducibility.*
- *The description of wetting behavior in soils with CRM should not be restricted to based homogenized samples and the coefficient  $k$  should be also included, especially to reveal differences in samples with small CA.*

The results for natural soils allow to answer, at least initially, given the restricted number analyzed ( $n = 12$ ), a major question arising from this thesis in relation to the validity of the experiments carried out with model materials and their relation with natural soil systems. In this context, the results of the MW model materials become more relevant, as they are supposed to represent the behavior of these real systems better than the HW materials, as previously suggested by theoretical models like those proposed by Ustohal et al. (1998) and McHale et al. (2005), in simulations based on systems of perfect spheres, with different spatial distribution of the hydrophobic particles. However, MW results in model materials should be also taken as approximations, as the systematic mixture of hydrophobic and hydrophilic particles could eventually correspond to a HW model of water repellent components distribution. As suggested by Goebel (2007), a logical extension of experiments should be focused on testing MW model materials with increasing heterogeneity regarding the distribution of the water repellent particles.

The results presented in Chapter 5 in general are in good agreement with those derived from model materials (Chapter 2), e.g. increasing CA with increasing amount of SOM, with values of  $\theta^{\text{CRM}} > 50^\circ$  for all homogenized samples, even for those top-soils with a low level of water repellency. The dependence of the CA on the spatial distribution of SOM is then confirmed by literature, demonstrating that the CRM is a suitable approach to reveal these differences in natural soils. Diverse authors, like Ellies et al. (1995 and 1996), Chenu et al. (2000) and Eynard et al. (2004), using experimental methods like SDM and WDPT, determined the importance of the spatial distribution of SOM (which is often more significant than its total amount on defining wetting properties). At the same time, Ellerbrock et al. (2005) concluded that the wetting behavior in natural soils should be rather interpreted in terms of the effectiveness of SOM than its total amount. However, although the results presented in this thesis regarding natural soils are in good agreement with these findings, other relevant aspects here were not directly investigated, like the qualitative properties of SOM (Doerr et al., 2000; Morley et al., 2005).

Regarding the experimental set-up, the good reproducibility of the packing of aggregates confirms the suitability of CRM to evaluate heterogeneous materials like natural soils. The main limitation evaluating the wetting curves is related to the accurate delimitation between the slope I (inter-aggregates space) and slope II (intra-aggregates space). Even when a good agreement was found between the slope II and the wetting behavior of single-aggregates (indicating that slope II reflects mainly the intra-pore system), the potentially very complex distribution of SOM in the aggregates (Hallett et al., 2001; Munkholm et al., 2002; Seguel and Horn, 2006) needs further research. Goebel (2007) concluded that SOM can show an extremely heterogeneous distribution into aggregates of different size. In this context, a method suitable to use together with the results of CRM for a more accurate definition of both slopes (I and II) can be the sieving of different size-fractions and ulterior peeling of aggregates (Ellies et al. 2002b), where the wetting behavior of the different aggregates-layers are individually evaluated (e.g. SDM).

A relevant result is the value  $\theta^{\text{CRM}} = 0^\circ$  obtained in some samples of aggregate packings and single aggregates (see Table 8), a value normally not achieved with the standard homogenized-material procedure, for model materials as well as for natural soils. It supports the necessity of using the factor  $k$  ( $k = \cos\theta$ ) together with the corresponding CA, especially to differentiate between samples located in the more wettable domain. This last aspect can be considered as a major conclusion regarding the characterization of natural soils samples with CRM, especially considering that this approach is the only one suitable to characterize the wettability of intact aggregates in terms of CA. In this context, two points already investigated in model materials, must be considered in order to improve the characterization via CAs for natural soils: (i) the necessity of comparison between the results between CRM and those from other experimental approaches and (ii) the correction of the overestimated  $\theta^{\text{CRM}}$ . Both points are shown in Fig. 30, by comparing CRM and WPM results for the same set of natural samples evaluated in Chapter 5. As WPM is not suitable for testing intact aggregates, only homogenized material is analyzed. Firstly are compared  $\theta^{\text{CRM}}$  versus  $\theta_A^{\text{WPM}}$  (Fig. 29A) and  $\theta^{\text{CRM}}$  versus  $\theta_E^{\text{WPM}}$  (Fig. 30B). Secondly are compared the dynamic  $\theta^{\text{CRM}}$  (equivalent to the dynamic CA from the Equivalent Capillary Model) and the corrected value (intrinsic CA or  $\theta_I$ ) by applying the C-geometry factor from the Kozeny-Carman equation (Marmur and Cohen, 1997; Marmur, 2003) (see Chapter 4). For C the value calculated for GB 40-70  $\mu\text{m}$  was used, considering the higher stability that this

material showed in the experiments with segmented columns, where effects like swelling of particles were not present (Shi and Gardner, 2000). It must also be mentioned that the data presented in Fig. 30 should be considered only as examples leading to future research on the topic, as the objectives of the present thesis were focused on testing primarily model materials (with well defined properties). In agreement with the results shown in Fig. 1, there are significant differences between both experimental methods, especially in the hydrophilic domain ( $CA < 60^\circ$ ) and between  $\theta^{CRM}$  and  $\theta_A^{WPM}$ . A better agreement is observed when the estimated  $\theta_I$  from CRM is compared with  $\theta_E^{WPM}$ . In this line, the correction by the factor C often leads to estimate  $\theta_I = 0^\circ$  in the more wettable samples, while the lowest value estimated for  $\theta_E^{WPM}$  is slightly higher than  $30^\circ$  (Fig. 30B). These observations reinforce the conclusion regarding to include the factor k in addition to  $\theta^{CRM}$ , especially when different experimental methods are used to describe the wetting properties of natural soils.

A significant factor regarding the characterization of wettability in natural soils is related to the stability of CA with time. Seasonal variation of wetting behavior has been reported in soils under different kinds of manure (Chan, 1992; Burcar et al., 1994; Buczko et al., 2005). A significant relation between wetting behavior and factors like water content (King, 1981; de Jonge et al., 1999; Doerr et al., 2000), temperature (Scott, 1997; Jaramillo, 2003) and vegetation (Doerr et al., 2000) has been reported. In the present thesis, as a preliminar evaluation needing further research, the stability of CA was tested in two natural soils. Table 10 shows general information and the CAs of the samples, measured before and after experiments of capillary rise in long segmented columns. Initially,  $\theta^{CRM}$  and  $\theta_A^{WPM}$  estimate repellency (CAs  $> 90^\circ$ ) for both samples, while  $\theta_E^{WPM}$  estimated values in the subcritical range. The experiments in segmented columns demonstrated that liquid uptake is possible (up to 18 cm). The re-measurement of CA (air-dried samples) also showed a significant increment of water repellency, especially for the sample A. These differences were also observed by measuring  $\sigma_{LV}$  before and after the experiments:  $\sigma_L$  decreased  $4.1 \text{ mN m}^{-1}$  from the initial value ( $72.8 \text{ mN m}^{-1}$ ) for sample A, and  $3.0 \text{ mN m}^{-1}$  for sample B after 1 week (normal variation for  $\sigma_L$  in model materials  $\pm 0.5 \text{ mN m}^{-1}$ ), which was possibly related to migration of SOM from the sample to the liquid into the reservoir. A significant observation was that in both samples, the liquid uptake into the segmented columns was almost absent during the first 72 hours ( $H < 2 \text{ cm}$ ), then increasing and reaching the

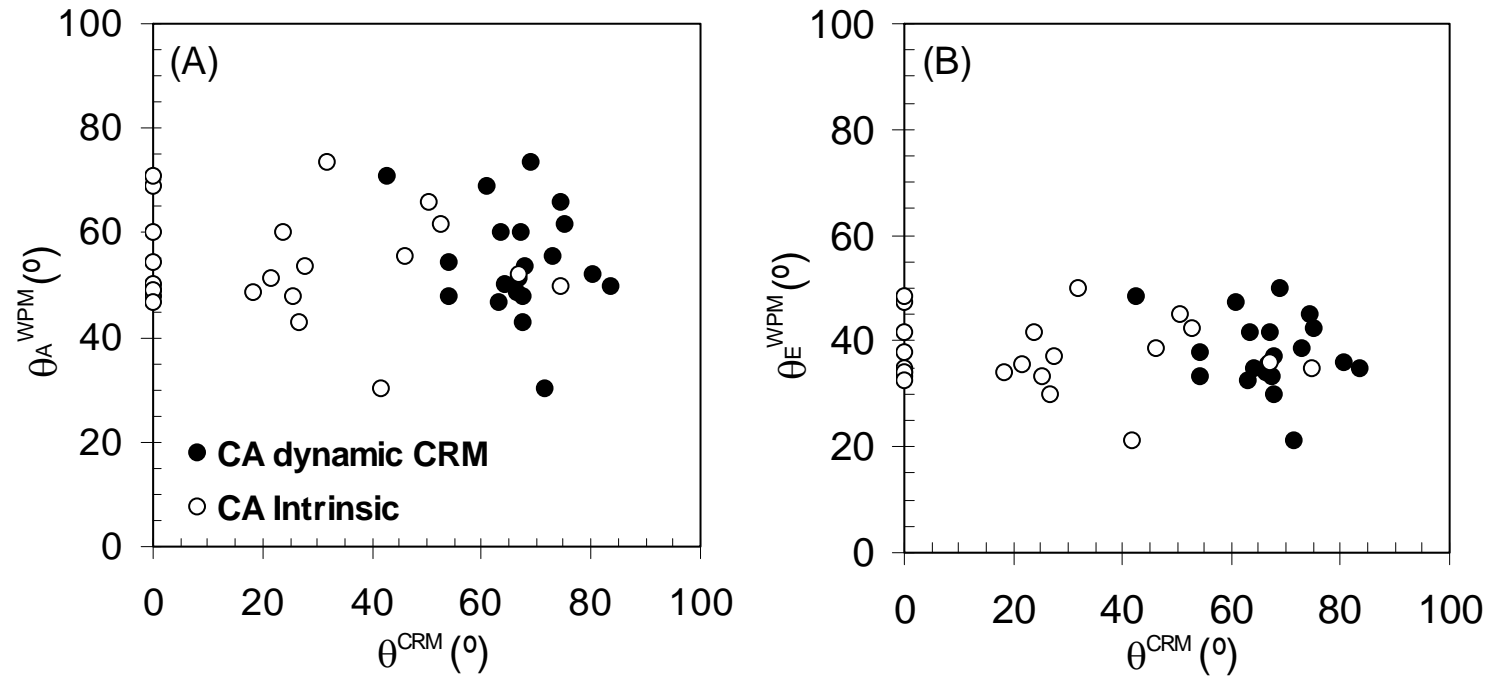


**Fig. 30** Example for a set of natural soil samples, of the estimation of the intrinsic CA ( $\theta_I$ ) by correcting the dynamic CA measured with the Capillary Rise Method ( $\theta^{\text{CRM}}$ ) with the estimated C geometry factor, in comparison with the values estimated with the Wilhelmy Plate Method ( $\theta_A^{\text{WPM}}$  and  $\theta_E^{\text{WPM}}$  approaches).

**Table 10:** Values of contact angle and equilibrium height of water ( $H_1$ ) of two natural soils evaluated in experiments with long segmented columns.

Sample	$\theta^{CRM}$		$\theta_A^{WPM}$		$\theta_E^{WPM}$		$H_1$ (cm)	Color and texture
	1	2	1	2	1	2		
A	>90	>90	114.1	127.8	72.8	100.5	16	7.5 YR 4/1 (Brownish gray) Sandy loam
B	>90	>90	121.3	128.2	86.1	94.4	18	10 YR 3/2 (Brownish black) Loam

1: Measurement carried out before the experiment.

2: Measurement carried out after the experiment (1 week).

equilibrium height after approximately one week. This result is in good agreement with the research of Hurrass and Schaumann (2006), who concluded that the wetting process of natural soils is eventually very slow, mainly due to the action of SOM. These findings are also supported by researches like Utomo and Dexter (1982), Woche et al. (2005) and Goebel (2007). Certainly, it has been demonstrated that the aspect of CA as a function of time should be also applied to the methods tested in the present thesis, in order to get accurate estimations of wetting behavior in natural soils.

### 6.3. Concluding remarks and perspectives

The results presented here allow to support both main hypotheses of this thesis: the characterization of the wetting properties by capillary rise (advancing dynamic CA) can lead to significant deviations from the Young-defined intrinsic CA ( $\theta_I$ ). These deviations apparently are related to the geometrical properties of the test medium (e.g. texture), although their effect was not completely described and quantified in this thesis, given the high complexity in modelling the wetting behavior of porous media. At the same time, WPM and also SDM are revealed as reasonable accurate methods for use on porous media and especially natural soils. A crucial fact regarding the assessment of  $\theta_I$  is that all the experimental approaches should be considered as approximations, due to the numerous assumptions of the Young equation. With this in mind, the “most suitable” method for describing the wetting-behavior, will be directly related to the objectives of the experiment.

For capillary rise, a next step regarding the Equivalent Capillary model should be the accurate assessment of the  $C$  factor, e.g. for a range of different textures, in order to improve the corrections leading to the estimation of  $\theta_l$ . However, it must be considered that even when easy-to-apply models constitute a significant improvement in this topic of research (Or and Tuller, 2005), the complexity of natural pore-systems is still far away to be completely described with a perfect straight-cylindrical system (Marmur, 2003). Further research should be focused on combining alternative models of the porous-system, e.g. the “111” plane of spheres proposed by Shirtcliffe et al. (2006), where the pores have a near triangular-section instead of a circular one and where different geometrical combinations are possible regarding the distance between the particles. Regarding WPM, future research should be initially focused on finding the best measurement set-up for each kind of sample, especially when soils with a highly time-dependent wetting behavior are tested. For the experiments carried out in segmented columns, a parameter not yet completely evaluated is the receding CA, corresponding to drainage conditions, as defined by Ustohal (1998). Initial measurements for this thesis were carried out as an additional result of the  $K_C$  evaluation in reference materials. These initial results, expressed as WRC, were in good agreement with the description of Shahidzadeh et al. (2003 and 2004) for highly wettable materials. However, the evaluation of samples with different degrees of water repellency and distribution of the water repellent components (e.g. HW vs. MW) is still missing. At the same time, the combination of both advancing and receding CAs will allow to complete the scope of results in order to improve the description of the wetting properties (e.g. WPM versus capillary rise under the impact of gravity).

Regarding the application of the experimental approaches on natural soils and given the limited set of samples here evaluated, the more logical next step is to extend the research focused on the CRM-WPM-SDM comparison to a wider scope of soils, considering aspects like the description of wettability in function of depth and kind of manure. This last topic is especially relevant considering that in countries like Chile, research about water repellency has been focused primarily on grassland soils than on forest soils. This last aspect is even more important by considering that the commercial plantations in this country (near  $2 \cdot 10^6$  ha) are constituted mainly by *Pinus spp.* and *E. globulus* R. Br. (Infor, 2008), which, as already mentioned in the introduction, are recognized for inducing significant water repellency (Doerr et al., 1996; Coelho et al, 2005; Keizer et al., 2005). The soils of south Chile suffer near four thousand events of fire



per year, mostly of anthropogenic origin in addition to those occurred in past years for clearfelling (Ellies, 1983; Gutiérrez et al., 2005), but their consequences on increasing the water repellency and/or erosion rates (De Bano, 1981 and 2000; Robichaud and Hungerford, 2000) are still vastly unknown. Finally, considering the high variability of soils, those derived from volcanic-ashes in Chile, which cover near half of the arable land (Donoso, 1981), still constitute a challenging task. For example, in the so-called Ñadis and Hualves (soils with very extreme annual wetting-regime) (Janssen et al., 2004), the effect of soil management (which usually consists of massive drainage and tillage) on the wetting behavior has not been completely described.

## References

- Adamson, A.W.** 1990. *Physical Chemistry of Surfaces*, 5th ed., John Wiley and Sons, New York. 808 p.
- Arye, G.; Bachmann, J.; Woche, S. K.; Chen, Y.** 2006. Applicability of interfacial theories of surface tension to water-repellent soils. *Soil Sci. Soc. Am. J.* 70: 1417-1429.
- Arye, G.; Nadav, I.; Chen, Y.** 2007. Short-term reestablishment of soil water repellency after wetting: Effect on capillary pressure-saturation relationship. *Soil Sci. Soc. Am. J.* 71: 692-702.
- Bachmann, J.; Ellies, A.; Hartge, K. H.** 2000. Sessile drop contact angle method. *J. Hydr.* 231: 66-75.
- Bachmann, J.; Woche, S.K.; Goebel, M.-O; Fischer, R. B.** 2001. Contact angle and surface charge of various mixtures of wettable and hydrophobic silt particles. *J. Soil Sci. Plant Nutr.* 2: 26-33.
- Bachmann, J.; Woche, S.K.; Goebel, M.-O; Kirkham, M. B.; Horton, R.** 2003. Extended methodology for determining wetting properties of porous media. *Water Resour. Res.* 39(12): 1353.
- Bachmann, J.; Arye, G.; Deurer, M.; Woche, S. K.; Hornton, R.; Hartge, K. H.; Chen, Y.** 2006. Universality of a surface tension-Contact angle relation for hydrophobic soils of different texture. *J. Plant Nutr. Soil Sci.* 169: 745-753.
- Balesdent, J.; Chenu, C.; Balabane, M.** 2000. Relationship of soil organic matter dynamics to physical protection and tillage. *Soil Till. Res.* 53: 215-230.
- Bear, J.** 1972. *Dynamics of fluids in porous media*. Dover, pp. 579-626.
- Becerra, J. C.** 2006. Efecto de la materia orgánica y el manejo sobre la hidrofobicidad de suelos volcánicos. *R. C. Suelo Nutr. Veg.* 6(2): 13-27.
- Bico, J.; Marzolin, C.; Quéré, D.** 1999. Pearl drops. *Europhys. Lett.* 47(2): 220-226.
- Binks, B.P.; Clint, J. H.; Fletcher, P.D.; Lees, T.J.; Taylor, P.** 2006. Particle film growth driven by foam bubble coalescence. *Chem. Commun. (Camb.)* (33): 3531-3533, DOI: 10.1039/b606308j.
- Brandon, S.; Marmur, A.** 1996. Simulation of contact angle hysteresis on chemically heterogeneous surfaces. *J. Colloid. Interface Sci.* 183: 351-355.
- Bond, R. D.** 1968. Water repellent sands. *Trans. 9<sup>th</sup> Int. Congr. Soil Sci.* 1: 339-347.
- Buczko, U.; Bens, O.; Hüttl, R. F.** 2005. Variability of soil water repellency in sandy forest soils with different stand structure under Scots pine (*Pinus silvestris*) and beech (*Fagus sylvatica*). *Geoderma* 126: 317-336.

- Burcar, S.; Miller, W. W.; Tyler, S. W.; Johnson, D. W.** 1994. Seasonal preferential flow in two Sierra Nevada soils under forested and meadow cover. *Soil Sci. Soc. Am. J.* 58: 1555-1561.
- Carman, P. C.** 1936. Fluid flow through granular beds. *Trans. Inst. Chem. Engs.* 15: 150-156.
- Carman, P. C.** 1938. The determination of the specific surface of powders I. *J. Soc. Chem. Indus.* 57: 225-234.
- Cassie, A. B. D.** 1948. Contact angles. *Discuss. Faraday Soc.* 3: 11-16.
- Chan, K. Y.** 1992. Development of seasonal water repellence under direct drilling. *Soil Sci. Soc. Am. J.* 56: 326-329.
- Chenu, C.; Le Bissonnais, Y.; Arrouays, D.** 2000. Organic matter influence on clay wettability and soil aggregate stability. *Soil Sci. Soc. Am. J.* 64: 1479-1486.
- Chibowski, E.; Ontiveros-Ortega, A.; Perea-Carpio, R.** 2002. On the interpretation of contact angle hysteresis. *J. Adhesion Sci. Technol.* 16(10): 1367-1404.
- Chibowski, E.; Perea-Carpio, R.** 2002. Problems of contact angle and solid surface free energy determination. *Adv. Colloid Interface Sci.* 98: 245-264.
- Clothier, B. E.** 2001. Infiltration. *In: Soil and environmental analysis, physical methods.* 2<sup>nd</sup> edition. K.A. Smith and C. E. Mullins (eds.). Marcel Dekker Inc., New York. 239-280 pp.
- Coelho, C. O. A.; Laouina, A.; Regaya, K.; Ferreira, A. J. D.; Carvalho, T. M. M.; Chaker, M.; Naafa, R.; Naciri, R.; Boulet, A. K.; Keizer, J. J.** 2005. The impact of soil water repellency on soil hydrological and evergreen *Quercus* forest in the Western Mediterranean. *Austr. J. Forest Res.* 43: 309-318.
- Craig, F. F.** 1971. The reservoir engineering aspects of water-flooding. *Soc. Pet. Eng., AIME Monograph*, 3. n.p.
- Crockford, S.; Topalidis, S.; Richardson, D. P.** 1991. Water repellency in a dry sclerophyll forest-measurements and processes. *Hydrol. Process.* 5: 405-420.
- Czachor, H.** 2006. Modelling the effect of pore structure and wetting angles on capillary rise in soils having different wettabilities. *J. Hydrol.* 328: 604-613.
- Dang-Vu, T.; Hupka, J.** 2005. Characterization of porous materials by capillary rise method. *Phys. Problems Min. Process.* 39: 47-65
- Darcy, H. 1856.** Les fontaines publiques de la Ville de Dijon. Victor Dalmont, Paris. n.p.
- DeBano, L. F.** 1981. Water repellent soils: a state-of-the-art. USDA. Forest service. Pacific southwest forest and range experiment station. General Technical Report PSW - 46. California. 21 p.

- DeBano, L. F.** 2000. Water repellency in soils: a historical overview. *J. Hydrol.* 231-232: 4-32
- Dekker, L.; Ritsema, C. J.** 1994. How water moves in a water repellent sandy soil. 1. Potential and actual water repellency. *Water Resour. Res.* 30: 2507-2517.
- Dekker, L.; Ritsema, C. J.** 2000. Wetting patterns and moisture variability in water repellent Dutch soils. *J. Hydrol.* 231-232: 148-164.
- Dekker, L. W.; Oostindie, K.; Ritsema, C. J.** 2005. Exponential increase of publications related to soil water repellency. *Aust. J. Soil Res.* 43: 403-441.
- Dekker, L. W.; Ritsema, C. J.; Oostindie, K.** 2000. Extent and significance of water repellency in dunes along the Dutch coast. *J. Hydr.* 231-232: 112-125.
- DiCarlo, D. A.; Bauters, T. W. J.; Damault, C. J. G.; Steenhuis, T. S.; Parlange, J. Y.** 1999. Rapid determination of constitutive relations with fingered flow. In: Proc. International Workshop on Characterization and Measurement of the Hydraulic Properties of Unsaturated Porous Media. Riverside, CA. October 22-24, 1997. pp. 433-440.
- Dmitriev, N. M.** 1996. Permeability coefficient tensor in the Kozeny-Carman capillary model. *Fluid dyn.* 31(4): 560-566.
- Doerr, S. H.** 1998. On standardizing the “Water Drop Penetration Time” and the “Molarity of an Ethanol Droplet” techniques to classify soil hydrophobicity: a case study using medium textured soils. *Earth. Surf. Process. Landforms* 23: 663-668.
- Doerr, S. H.; Shakesby, R. A.; Walsh, R. P. D.** 1996. Soil hydrophobicity variations with depth and particle size fraction in burned and unburned *Eucalyptus globulus* and *Pinus pinaster* forest terrain in the Agueda basin, Portugal. *Catena* 27: 25-47.
- Doerr, S. H.; Shakesby, R. A.; Walsh, R. P. D.** 2000. Soil water repellency: its causes, characteristics and hydro-geomorphological significance. *Earth Sci. Rev.* 51: 33-65.
- Doerr, S. H.; Dekker, L. W.; Ritsema, C. J.; Shakesby, R. A.; Bryant, R.** 2002. Water repellency of soils: The influence of ambient relative humidity. *Soil Sci. Am. J.* 66: 401-405.
- Doerr, S. H.; Shakesby, R. A.; Dekker, L. W.; Ritsema, C. J.** 2006. Occurrence, prediction and hydrological effects of water repellency amongst major soil and land-use types in a humid temperate climate. *Eur. J. of Soil Sci.* 57: 741-754.
- Donoso, C.** 1981. Ecología forestal, el bosque y su medio ambiente. Santiago (Chile), Universitaria. 369 p.
- Ellerbrock, R. H.; Gerke, H. H.; Bachmann, J.; Goebel, M. -O.** 2005. Composition of organic matter fractions for explaining wettability of three forest soils. *Soil Sci. Soc. Am. J.* 69: 57-66.

- Ellies, A.** 1983. Die Wirkungen von Bodenerhitzungen auf die Benetzungseigenschaften einiger Boden Suedchiles. *Geoderma*. 29: 129-138.
- Ellies, A.; Grez, R.; Ramirez, C.** 1995. Cambios en las propiedades humectantes de suelos sometidos a diferentes manejos. *Turrialba* 45(1-2): 42-48.
- Ellies, A.; Grez, R.; Ramírez, C.** 1996. Efecto de la materia orgánica sobre la capacidad de humectación y las propiedades estructurales de algunos Andisoles. *Agro Sur* 24(1): 48-58.
- Ellies, A.; Mac Donald, R.; Ramírez, C.** 2002a. Efecto de la resistencia a la humectación sobre la estabilidad al agua de los agregados del suelo. *Suelo y Nutrición Vegetal* 2: 1-9.
- Ellies, A.; Mac Donald, R.; Ramírez, C.; Campos, P.** 2002b. Manejo del suelo y capacidad de humectación en los agregados. *Bol. Soc. Chil. Ci. Suelo* 18: 47-51.
- Ellies, A.; Ramirez, C.; Mac Donald, R.** 2003. Wetting capacity distribution in aggregates from soils with different management. *Food Agr. Env.* 1(2): 2002-2022.
- Erickson, D.; Li, D.; Park, C. B.** 2002. Numerical simulations of capillary-driven flows in nonuniform cross-sectional capillaries. *J. Colloid Inter. Sci.* 250: 422-430.
- Eynard, A.; Schumacher, T. E.; Lindstrom, M.; Malo, D. D.; Kohl, R.** 2004. Wettability of soils aggregates from cultivated and uncultivated Ustolls and Usterts. *Aus. J. Soil Res.* 42: 163-170.
- El Ghzaoui, A.** 1999. Determination of contact angles: consistency between experiment and theory. *J. Appl. Phys.* 86(5): 2920-2922.
- Fick, A. D.; Borhan, A.** 2006. Numerical simulation of the spontaneous penetration of liquids into cylindrical capillaries. *Ann. N. Y. Acad. Sci.* 1077: 426-442.
- Girifalco, L. A.; Good, R. J.** 1957. A theory for the estimation of surface and interfacial energies. I. Derivation and Application to Interfacial Tension. *J. Phys. Chem.* 61: 904.
- Goebel, M. -O.** 2007. Impact of surface wetting properties on soil physical processes relevant for organic matter decomposition. PhD Thesis, Faculty of Natural Sciences, Leibniz University Hannover. Hannover, Germany. 132 p.
- Goebel, M. -O.; Bachmann, J.; Woche, S.; Fischer, W. R.; Horton, R.** 2004. Water potential and aggregate size effects on contact angle and surface energy. *Soil Sci. Soc. Am. J.* 68: 383-393.
- Goebel, M. -O.; Bachmann, J.; Woche, S. K.; Fischer, W. R.** 2005. Soil wettability, aggregate stability, and the decomposition of soil organic matter. *Geoderma*. 128: 80-93.
- Good, R. J.** 1993. Contact angle, wetting and adhesion: a critical review. *In: Contact angle, wettability and adhesion.* Mittal, K. L. (ed.). Festschrift in honor of Professor R. J. Good. VSO, Utrecht, The Netherlands. p: 3-36.

- Grader, L.** 1986. On the modelling of the dynamic contact angle. *Colloid Polymer Sci.* 264: 719-726.
- Grundke, K.** 2001. Wetting, spreading and penetration. in: *Handbook of Applied Surface and Colloid Chemistry*. Ed. Krister Holmberg. p. 119-142.
- Grundke, K.; Augsburg, A.** 2000. On the determination of the surface energetics of porous polymer materials. *J. Adhesion Sci. Tech.* 14: 765-775.
- Gutiérrez, M.; Pizarro, C.; Avendaño, K.; Galindo, G.; Escudey, M.** 2005. Efecto de la temperatura sobre la selectividad de intercambio K-Ca y Mg-Ca en una simulación de incendio forestal en andisoles. *Bol. Soc. Cs. Suelo* (21): 182.
- Hackett, F. E.** 1921. The rate of ascent of liquids through granular materials. *Trans. Faraday Soc.* 17: 260-267.
- Hallett, P. D.; Baumgartl, T.; Young, Y. M.** 2001. Subcritical water repellency of aggregates from a range of soil management practices. *Soil Sci. Soc. Am. J.* 65: 184-190.
- Hansen, D.** 2004. Discussion of “On the use of the Kozeny-Carman equation to predict the hydraulic conductivity of soils”. *Can. Geotech. J.* 41: 990-993.
- Hawkins, A. E.** 1993. *The shape of powder-particle outlines*. Research Studies Press Ltd., John Wiley & Sons. New York, NY. 150 p.
- Hillel, D.** 1998. *Environmental soil physics*. Academic Press. San Diego, CA. 771 p.
- Hoffman, R.** 1975. A study of the advancing interface. I. Interface shape in liquid-gas systems. *J. Colloid. Interface Sci.* 60: 11-38.
- Homma, H.; Lee, C.; Kuroyagi, T.; Izumi, K.** 2000. Evaluation of time variation of hydrophobicity of silicone rubber using dynamic contact angle measurement. *In: Proceedings of the 6<sup>th</sup> International Conference on Properties and Applications of Dielectric Materials*. Xi'an, China. p: 637-640.
- Hurrass, J.; Schaumann, G.** 2006. Hydration kinetics of wettable and water-repellent soils. *Soil Sci. Soc. Am. J.* 71: 280-288.
- Instituto Forestal (INFOR), CL.** 2008. Estadísticas forestales. Internet. Available in <http://www.infor.cl>
- Ishakoglu, A.; Filiz, A.** 2005. The influence of contact angle on capillary pressure-saturation relations in a porous medium including various liquids. *Inter. J. of Eng. Sci.* 43(8-9): 744-755.
- Jaramillo, J. D. F.** 2003. Efecto de la temperatura de secado del suelo sobre la repelencia al agua en Andisoles bajo cobertura de *Pinus patula*. Informe de investigación. Universidad Nacional de Colombia. Medellín. 36 p.

- Jackson, P. V.; Hunt, J. A.; Doherty, P. J.; Cannon, A.; Gilson, P.** 2004. Hydrophilicity of 3-D biomaterials: The Washburn equation. *J. Mater. Sci. Mater. Medicine*. 15: 507-511.
- Janssen, I.; Krueemmelbein, J.; Hora, R.; Ellies, A.** 2004. Physical and hydraulic properties of the ñadi-soils in south-chile: comparison between untilled and tilled soil. *Cs. Suelo Nutr. Veg.* 4(1): 14-28.
- Johnson, R. E.; Dettre, R. H.** 1964. Contact angle hysteresis. *In: Contact angle, wettability and adhesion.* *Adv. Chem.* 43: 112-143.
- de Jonge, L. W.; Jacobsen, O. H.; Moldrup, P.** 1999. Soil water repellency : effects of water content, temperature and particle size.
- Kalogianni, E. P.; Savopoulos, T.; Karapantsios, T. D.; Raphaelides, S. N.** 2004. A dynamic wicking technique for determining the effective pore radius of pregelatinized starch sheets. *Colloids Surf. B: Biointerfaces.* 35: 159-167.
- Karbowiak, T.; Debeaufort, F.; Voilley, A.** 2006. Importance of surface tension characterization for food, pharmaceutical and packaging products: a review. *Critical Rev. Food Sci. Nutr.* 46: 391-407.
- Keizer, J. J.; Ferreira, A. J. D.; Coelho, C. O. A.; Doerr, S. H.; Malvar, M. C.; Domingues, C. S. P.; Perez, I. M. B.; Ruiz, C.; Ferrari, K.** 2005. The role of tree stem proximity in the spatial variability of soil water repellency in a eucalypt plantation in coastal Portugal. *Aus. J. Soil Res.* 43: 251-259.
- King, P. M.** 1981 Comparison of methods for measuring severity of water repellence of sandy soils and assessment of some factors that affect its measurement. *Aust. J. Soil Res.* 19: 275-285.
- Kissa, E.** 1996. Wetting and wicking. *Textile Res. J.* 66(10): 660-668.
- Kozeny, J.** 1927. Über Kapillare Leitung des Wassers im Boden. *Sitzungsber. Akad. Wiss., Wien.* 136a: 271-306.
- Labajos-Broncano, L.; González-Martín, M. L.; Bruque, J. M.** 2002. Influence of effective porosity in the determination of contact angles in porous solids by imbibition techniques. *J. Adhesion Sci. Technol.* 16(11): 1515-1528.
- Lavi, B.; Marmur, A.; Bachmann, B.** 2008. Porous media characterization by the two-liquid method: effect of dynamic contact angle and inertia. *Langmuir* 24(5): 1918-1923.
- Letey, J.** 1969. Measurement of contact angle, water drop penetration time and critical surface tension. *Proceed. Symp. Wat. Rep. Soils.* pp. 43-47.
- Letey, J.; Carrillo, M. L. K.; Pang, X. P.** 1999. Approaches to characterize the degree of water repellency. *J. Hydrol.* 231-232: 61-65.

- Letey, L.; Osborn, J.; Pelishek, R. E.** 1962. Measurement of liquid-solid contact angle in soil and sand. *Soil Sci.* 93: 149-153.
- Lucas, R.** 1918. Über das Zeitgesetz des Kapillaren Aufstiegs von Flüssigkeiten. *Kolloid. Z.* 23: 15-22.
- MacMullin, R. B., Muccini, G. A.** 1956. Characteristics of porous beds and structures. *A. I. Ch. E. J.* 2(3): 393-403.
- Manthey, S.** 2006. Two-phase flow processes with dynamic effects in porous media – parameter estimation and simulation. Dr. Ing. Thesis, Institut für Wasserbau der Universität Stuttgart. 149 p.
- Marmur, A.** 1992. Penetration and displacement in capillary systems of limited size. *Adv. Colloid. Interface Sci.* 39: 13-33.
- Marmur, A.** 1993. Contact angle equilibrium: the intrinsic contact angle. In: Contact angle, wettability and adhesion. K.L. Mittal (ed). pp. 125-137.
- Marmur, A.** 2003. Kinetics of penetration into uniform porous media: Testing the equivalent-capillary concept. *Langmuir* 19: 5956-5959.
- Marmur, A.** 2006. Soft contact: measurement and interpretation of contact angles. *Soft Matt.* 2:12-17.
- Marmur, A.; Chenb, W.; Zograf, G.** 1986. Characterization of particle wettability by the measurement of floatability. *J. Colloid Interface Sci.* 113: 114-120.
- Marmur, A.; Cohen, R.** 1997. Characterization of porous media by the kinetics of liquid penetration: The vertical capillaries model. *J. Colloid Interface Sci.* 189: 299-304.
- Mauran, S.; Rigaud, L.; Coudeville, O.** 2001. Application of the Carman-Kozeny correlation to a high-porosity and anisotropic consolidated medium: The compressed expanded natural graphite. *Trans. in P. Media.* 43: 355-376.
- Meiron, T. S.; Marmur, A.; Saguy, I. S.** 2004. Contact angle measurement on rough surfaces. *J. Colloid. Interface Sci.* 274: 637-644.
- McGhie, D. A; Posner, A. M.** 1980. Water repellence of a heavy-textured Western Australian surface soil. *Austr. J. Soil Res.* 18: 309-323.
- McHale, G.; Newton, M. I.; Shirtcliffe, N. J.** 2005. Water-repellent soil and its relationship to granularity, surface roughness and hydrophobicity: a materials science review. *Eur. J. Soil Sci.* 56: 445-452.
- Miyama, M.; Yang, Y.; Yasuda, T.; Okuno, T.; Yasuda, H.** 1997. Static and dynamic contact angles of water on polymeric surfaces. *Langmuir.* 13: 5494-5503.



- Morley, C. P.; Mainwaring, K. A.; Doerr, S. H.; Douglas, P.; Llewellyn, C. T.; Dekker, L. W.** 2005. Organic compounds at different depths in a sandy soil and their role in water repellency. *Austr. J. Soil Res.* 43: 239-249.
- Morra, M.; Della Volpe, C.** 1998. Letter to the editor. *J. Biomedical Mat. Res.* 42: 473-474.
- Morrow, N. R.** 1976. Capillary pressure correlations for uniformly weeted porous media. *J. Can. Petr. Technol.* 15:49-69.
- Munkholm, L. J.; Schjønning, P.; Kay, B.** 2002. Tensile strength of soil cores in relation to aggregate strength, soil fragmentation and pore characteristics. *Soil Till. Res.* 64: 125-135.
- Narsilio, G.; Santamarina, J. C.** 2008. Clasificación de suelos: fundamento físico, prácticas actuales y recomendaciones. Available in <http://materias.fi.uba.ar/6408/santamarina.pdf>
- Naasz, R.; Michel, J. C.; Charpentier, S.** 2008. Water repellency of organic growing media related to hysteretic water retention properties. *Eur. J. of Soil Sci.* 59(2): 156-165.
- Oades, J.** 1993. The role of biology in the formation, stabilization and degradation of soil structure. *Geoderma* 56: 377-400.
- Pagliai, M.; Vignozzi, N.** 2003. Image analysis and microscopic techniques to characterize soil pore system. In: *Physical approach to methods in precision agriculture and quality*. J. Blahovec and M. Kutílek ed. pp. 13-38.
- Philip, J. R.** 1971. Limitations of scaling by the contact angle. *Soil Sci. Am. Proc.* 34: 507-509.
- Princen, H. M.** 1970. Advantages and limitations of the grooved Wilhelmy Plate. *Aus. J. Chem.* 23: 1789-1799.
- Prunty, L.; Casey, F. X. M.** 2002. Soil water retention curve description using a flexible smooth function. *Vad. Zone J.* 1: 179-185.
- Regalado, C. M.; García-Santos, G.; Hernández, J. M.; Pérez, A.; Socorro, A. R.** 2003. Caracterización de la zona no saturada de un bosque maduro de Laurisilva en el Parque Nacional de Garajonay: Hidrofobicidad e implicaciones hidrológicas. *Estudios de la Zona no Saturada del Suelo.* 6: 193-200.
- Reinson, J. R.; Fredlund, D. G.; Wilson, G. W.** 2004. Unsaturated flow in coarse porous media. *Can. Geotech. J.* 42: 252-262.
- Ritsema, C. J.; Dekker, L. W.** 2000. Preface. *Journal of Hydrology.* 231-232: 1-3.
- Ritsema, C. J.; Dekker, L. W.; HEIJES, W. J.** 1997. Three-dimensional fingered flow patterns in a water repellent sandy field soil. *Soil Sci.* 162: 79-90.
- Robichaud, P. R.; Hungerford, R. D.** 2000. Water repellency by laboratory burning of four northern Rocky Mountain forest soils. *J. Hydrol.* 231-232: 207-219.

- Rodriguez, E.; Giacomelli, F.; Vásquez, A.** 2004. Permeability-porosity relationship in RTM for different fiberglass and natural reinforcements. *J. Composite Mat.* 38(3): 259-268.
- Roura, P.; Fort, J.** 2004. Local thermodynamic derivation of Young's equation. *J. Colloid Interface Sci.* 272: 420-429.
- Salem, H.** 2001. Application of the Kozeny-Carman equation to permeability determination for a glacial outwash aquifer, using grain-size analysis. *Energy Sour.* 23: 461-473.
- Schneider, R.P., Chadwick, B. R., Jankowski, J., Acworth, I.** 1997. Modification of substratum physicochemistry by material adsorbed from groundwater - analysis by contact angles and relevance to microbial adhesion. *Geomicrobiology J.* 14: 151-172.
- Sedev, R.; Fabretto, M.; Ralston, J.** 2004. Wettability and surfaces energetics of rough fluopolymer surfaces. *J. Adh.* 80(6): 497-520.
- Seguel, O.; Horn, R.** 2006. Structure properties and pore dynamics in aggregate beds due to wetting-drying cycles. *J. Plant Nutr. Soil Sci.* 169: 221-232.
- Sciffer, S.** 2000. A phenomenological model of dynamic contact angle. *Chem. Eng. Sci.* 55: 5933-5936.
- Science Lab., US.** 2005. Material safety data sheet: Dichlorodimethylsilane. Internet. Available in <http://www.sciencelab.com/xMSDSDichlorodimethylsilane-9923727>
- Scott, D. F.** 1997. The contrasting effects of wildfire and clearfelling on the hydrology of a small catchment. *Hydr. Processes* 11: 543-555.
- Shahidzadeh, N.; Bertrand, E.; Dauplait, J.; Borgotti, J.; Vié, P.; Bonn, D.** 2003. Effect of wetting on gravity drainage in porous media. *Trans. Porous Med.* 52: 213-227.
- Shahidzadeh, N.; Tournié, A.; Bichon, S.; Vié, P.; Rodts, S.; Faure, P.; Bertrand, F.; Azouni, A.** 2004. Effect of wetting on the dynamics of drainage in porous media. *Trans. Porous Med.* 56: 209-224.
- Shedid, S. A.; Ghannam, M. T.** 2004. Factors affecting contact-angle measurement of reservoir-rocks. *J. Pet. Sci. Eng.* 44: 193-203.
- Shi, S. Q. ; Gardner, D. J.** 2000. A new model to determine contact angles on swelling polymer particles by the column wicking method. *J. Adhesion Sci. Technol.* 14(2): 301-314.
- Shirtcliffe, N. J.; McHale, G.; Newton, M.I.; Pyatt, F. B; Doerr, S.** 2006. Critical conditions for the wetting of soils. *Appl. Physics Lett.* 89: 094101.
- Siebold, A.; Walliser, A.; Nardin, M.; Oppliger, M.; Schultz, J.; Walliser, A.** 1997. Capillary rise for thermodynamic characterization of solid particle surface. *J. Colloid. Interface Sci.* 186: 60-70.

- Siebold, A.; Nardin, M.; Schultz, J.; Walliser, A.; Oppliger, M.** 2000. Effect of dynamic contact angle on capillary rise phenomena. *Physicochem. Eng. Asp.* 161: 81-87.
- Singh, U. B., Gupta S. C., Flerchinger G. N., Moncrief J. F., Lehmann, R. G., Endinger, N. J. F, Traina, S. J. Logan T. J.** 2000. Modeling Polydimethylsiloxane degradation based on soil water content. *Environ. Sci. Technol.* 34: 266-273.
- Singh, P. N, Wallender, W. W.** 2006. Modifying Kozeny-Carman equation for evaluating saturated hydraulic conductivity in clay with adsorbed water layers. American Society of Agricultural and Biological Engineers. St. Joseph, Michigan. Paper number 062224.
- Spelt, J. K.; Li, D.; Neumann, A. W.** 1992. The equation of state approach to interfacial tensions. In: *Modern approaches to wettability: theory and applications.* Schrader, M. E., Loeb, G. (eds.). Plenum Press, New York. pp. 101-142.
- Spohrer, K.; Herrmann, L.; Ingwersen, J.; Stahr, K.** 2006. Applicability of uni- and bimodal retention functions for water flow modeling in a tropical Acrisol. *Vad. Zone J.* 5: 48-58.
- Stange, M.; Dreyer, M.; Rath, H. J.** 2003. Capillary driven flow in circular cylindrical tubes. *Phys. Fluids* 15(9): 2587-2601.
- Stange, C. F.; Horn, R.** 2005. Modeling the soil water retention curve for conditions of variable porosity. *Vad. Zone J.* 4: 602-613.
- Steenhuis, T. S.; Hunt, A. G.; Parlange, J. Y.; Ewing, R. P.** 2005. Assessment of the application of percolation theory to a water repellent soil. *Aus. J. Soil Res.* 43: 357-360.
- Täumer, K.** 2007. Analyzing soil water repellency phenomena. Dr. Ing. Thesis. Fakultät VI, Technische Universität Berlin. Berlin, Germany. 68 p.
- Tschapek, M.** 1984. Criteria for determining the hydrophilicity-hydrophobicity of soils. *Zeitschrift für Pflanzenernährung und Bodenkunde.* 147: 137-149.
- Ustohal, P.; Stauffer, F.; Dracos, T.** 1998. Measurement and modeling of hydraulic characteristics of unsaturated porous media with mixed wettability. *J. Contam. Hydrol.* 33: 5-37.
- Utomo, W. H.; Dexter, A. R.** 1982. Changes in soil aggregates water stability induced by wetting and drying cycles in non-saturated soil. *J. Soil Sci.* 33: 623-637.
- van Genuchten, M. Th.** 1980. A closed-form equation for predicting the hydraulic conductivity of unsaturated soils. *Soil Sci. Soc. Am. J.* 44: 892-898.
- van Genuchten, M. Th.; Leij, F. J.; Yates, S. R.** 1991. The RETC code for quantifying the hydraulic functions of unsaturated soils, version 1.0. EPA Report 600/2-91/065, U.S. Salinity Laboratory, USDA, ARS. Riverside, California.
- van Mourik, S.; Veldman, A. E. P.; Dreyer, M. E.** 2005. Simulation of capillary flow with a dynamic contact angle. *Microgravity Sci. Technol.* 17(3): 91-98.

- Washburn, E. W.** 1921. The dynamics of capillary flow. *Phys. Rev.* 17: 273-283.
- Watson, C.L. and Letey, J.** 1970. Indices for characterizing soil-water repellency based upon contact angle-surface tension relationships. *Soil Sci. Soc. Am. Proc.* 34: 841-844.
- Wenzel, R. N.** 1936. Resistance of solid surfaces to wetting by water. *Ind. Eng. Chem.* 28: 988.
- Wilhelmy, L.** 1863. Über die Abhängigkeit der Capillaritäts-Konstanten des Alkohols von Substanz und Gestalt des Benetzten festen Körpers. *Ann. Phys.* 119: 177-217.
- Woche, S. K.; Goebel, M. O.; Kirkham, M. B.; Horton, R.; Van der Ploeg, R. R.; Bachmann, J.** 2005. Contact angle of soils as affected by depth, texture and land management. *Eur. J. Soil Sci.* 56: 236-251.
- Yang, Y.; Zografis, G.** 1986. J. Pharm. The use of the Washburn-Rideal Equation for studying capillary flow in porous media. *J. Pharm. Sci.* 75: 719-721.
- Yang, X. F.** 1995. Equilibrium contact angle and intrinsic wetting hysteresis. *Appl. Phys. Lett.* 67 (15): 2249-2251.
- Young, T.** 1805. Cohesion of Fluids. *Phil. Trans. Roy. Soc.* 95: 65.
- Zhong, W.; Ding, X.; Tang, Z. L.** 2001. Modeling and analyzing liquid wetting in fibrous assemblies. (online: 02-06-08). Available in:  
[http://findarticles.com/p/articles/mi\\_qa4025/is\\_200109/ai\\_n8972652/pg\\_1](http://findarticles.com/p/articles/mi_qa4025/is_200109/ai_n8972652/pg_1)
- Zisman, W. A.** 1964. Relation of equilibrium contact angle to liquid and solid constitution. *In: Contact angle, wettability and adhesion.* Adv. Chem. Ser. 43, Washington, D.C.: Am. Chem. Soc. 1. pp. 1-51.

# Appendix

## contents

**Fig. A1** Evaluation of the initial capillary effect (ICE)  $\theta_A^{\text{WPM}}$  and  $\theta_R^{\text{WPM}}$  for sand.  
A: Initial capillary rise effect (ICE) in WPM curves. Examples for samples with 0%, 10% (=  $5.0 \times 10^{-5}$  mL g<sup>-1</sup> DCDMS), 25% (=  $1.3 \times 10^{-4}$  mL g<sup>-1</sup> DCDMS) and 100% (=  $5.0 \times 10^{-4}$  mL g<sup>-1</sup> DCDMS) hydrophobic particles. B: Initial capillary rise effect in comparison with  $\theta_A^{\text{WPM}}$  and  $\theta_R^{\text{WPM}}$  (mixed wettability samples)..... iii



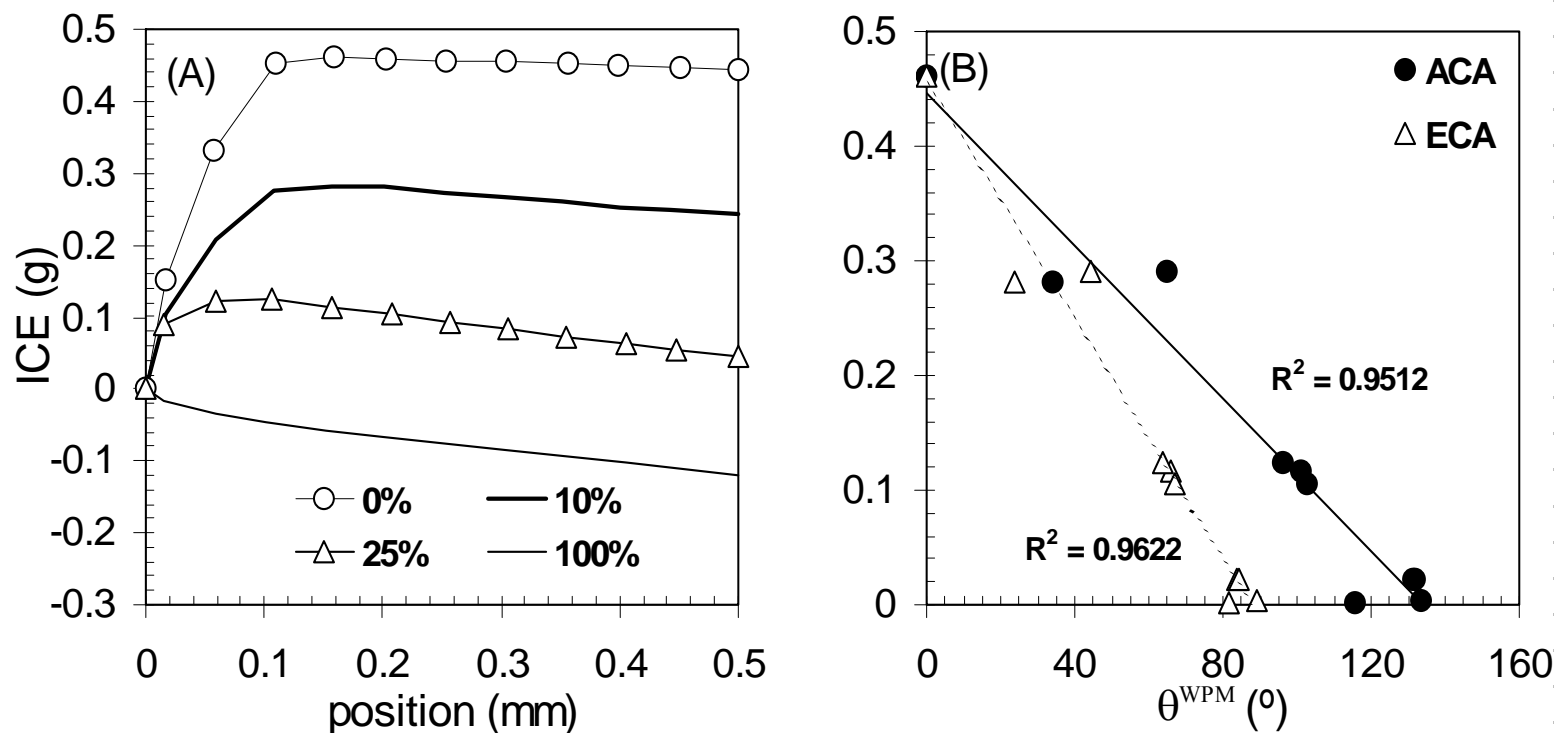


**Fig. A1** Evaluation of the initial capillary effect (ICE)  $\theta_A^{\text{WPM}}$  and  $\theta_R^{\text{WPM}}$  for sand. A: Initial capillary rise effect (ICE) in WPM curves. Examples for samples with 0%, 10% ( $= 5.0 \times 10^{-5} \text{ mL g}^{-1}$  DCDMS), 25% ( $= 1.3 \times 10^{-4} \text{ mL g}^{-1}$  DCDMS) and 100% ( $= 5.0 \times 10^{-4} \text{ mL g}^{-1}$  DCDMS) hydrophobic particles. B: Initial capillary rise effect in comparison with  $\theta_A^{\text{WPM}}$  and  $\theta_R^{\text{WPM}}$  (mixed wettability samples).





# Curriculum vitae

## PERSÖNLICHE DATEN

Name: Juan Carlos Ramírez-Flores  
Geburtsdatum / -ort: 26. Februar 1972 in Valdivia, Chile  
Staatsangehörigkeit: Chilenisch  
Familienstand: Ledig, keine Kinder

## SCHULBILDUNG

1978 - 1985 Escuela Superior D N° 1. Valdivia, Chile (Grundschule)  
1986 - 1989 Liceo de Hombres A N° 6. Valdivia, Chile (Gymnasium)  
Abitur

## STUDIUM

03/1990 - 08/1997 Licenciatura (Diplom)  
Instituto de Silvicultura, Universidad Austral de Chile  
Diplomarbeit: Determinación del área geográfica potencial para el establecimiento en Chile de *Acacia melanoxylon* R. Br.  
Abschluss: Diplom - Ingeniero Forestal (Forstingenieur)

03/2000 - 10/2002 Magister en ciencias  
Instituto de Silvicultura, Universidad Austral de Chile  
Dissertation: Caracterización de la presencia de termitas y su relación con variables de sitio, en focos ubicados en predios forestales de las provincias de Biobío, Malleco y Valdivia.  
Abschluss: Magister en Ciencias Mención Silvicultura (Waldbau)

03/2005 – 06/2009 Wissenschaftliche Hilfskraft und Doktorand am Institut für Bodenkunde der Gottfried Wilhelm Leibniz Universität Hannover

## MITGLIEDSCHAFTEN IN WISSENSCHAFTLICHEN VEREINIGUNGEN

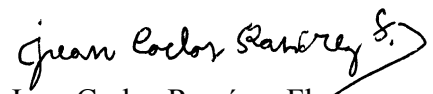
05/2005 - Deutsche Bodenkundliche Gesellschaft (DBG)



# Erklärung

Hiermit erkläre ich, dass diese Dissertation selbständig verfasst wurde und alle benutzten Hilfsmittel sowie evtl. zur Hilfestellung herangezogene Institutionen vollständig angegeben wurden.

Die Dissertation wurde nicht schon als Diplom- oder ähnliche Prüfungsarbeit verwendet.

  
Juan Carlos Ramírez-Flores

Hannover (Niedersachsen), den 19-06-2009

